

# Optical self-switching of unidirectional distributively coupled waves

A A Maier

## Contents

<b>1. Introduction</b>	<b>991</b>
<b>2. Equations and integrals for the amplitudes of single-frequency unidirectional distributively coupled waves in a cubically nonlinear medium</b>	<b>993</b>
2.1 Equations for the amplitudes of waves in tunnel-coupled optical waveguides; 2.2 Equations for a periodic structure; 2.3 Equations for unidirectional distributively coupled waves with different polarisations; 2.4 Equations for coupled modes; 2.5 General form of the equations for the amplitudes and their integrals, and the equation for the intensities; 2.6 Possible deviations of equations from the general form	
<b>3. Optical self-switching on arrival of one wave at the input of a system</b>	<b>999</b>
3.1 Optical self-switching in a system with identical unidirectional distributively coupled waves; 3.2 Self-phase-matching of waves; 3.3 Optical self-switching in a system with nonidentical unidirectional distributively coupled waves; 3.4 Influence of optical losses on optical self-switching; 3.5 Influence of the phase of a signal on its amplification	
<b>4. Optical self-switching in the presence of two waves at the input</b>	<b>1009</b>
4.1 Solution of the equations for identical unidirectional distributively coupled waves. 4.2 General solution of the equations; 4.3 Condition for and characteristic points, depth, and slope of optical self-switching; 4.4 Switching of a pump by a weak signal. Giant and linear signal amplification; 4.5 Optical transistor with an enhanced gain, stable against pump intensity instabilities; 4.6 Self-phase-matching of waves with similar input intensities; 4.7 Nonidentical unidirectional distributively coupled waves with $\Delta = 0$ ; 4.8 Self-locking of waves and limits of changes in the intensities; 4.9 Dependence of the intensities on the input phase difference; 4.10 Comparison with Winful's results; 4.11 Special features of self-switching of unidirectional distributively coupled waves with orthogonal polarisations	
<b>5. Optical switching in a cubically nonlinear system with unidirectional distributively coupled waves by a signal of different frequency or with different polarisation</b>	<b>1019</b>
5.1 Equations for the wave amplitudes; 5.2 Integrals of equations; 5.3 Numerical analysis of equations; 5.4 Elimination of the influence of the phase of a signal on its amplification in tunnel-coupled optical waveguides	
<b>6. Optical multivibrators based on unidirectional distributively coupled waves</b>	<b>1023</b>
6.1 Optical multivibrators unstable against a phase shift in a feedback loop; 6.2 Optical multivibrators stable against a signal phase shift	
<b>7. Optical self-switching in a system with three unidirectional distributively coupled waves</b>	<b>1025</b>
7.1 Equations and integrals; 7.2 Three identical tunnel-coupled optical waveguides distributed in one plane; 7.3 Coupling between all waveguides	
<b>8. Conclusions</b>	<b>1027</b>
<b>References</b>	<b>1027</b>
<b>Appendix I</b>	<b>1029</b>
<b>Appendix II</b>	<b>1029</b>

**Abstract.** Theoretical and experimental fundamentals of the phenomenon of optical self-switching of unidirectional distributively coupled waves are presented. These waves represent a whole class of waves in optics: waves in tunnel-

coupled optical waveguides, waves undergoing the Bragg diffraction, waves with different polarisations in an anisotropic (birefringent) waveguide or crystal, waves with different frequencies in a quadratically nonlinear medium, etc.

A A Maier Institute of General Physics, Russian Academy of Sciences, ul. Vavilova 38, 117942 Moscow  
Tel. (095) 135-83-91

Received 29 December 1994; revision received 24 March 1995  
*Uspekhi Fizicheskikh Nauk* 165 (9) 1037–1075 (1995)  
Translated by A Tybulewicz

## 1. Introduction

In the last 20 years we have seen increasing and continuing interest in ultrafast all-optical light switches. This is due to a number of reasons. First, there is the ever-increasing demand for ultrafast processing of large volumes of information in combination with the need to transmit

information along optical communication lines, and also the drive to develop supercomputers. Second, the rapid growth of integrated [1–7], fibre [8–10, 3] and non-linear [11–14, 6] optics is creating a demand for fundamentally new ultrafast all-optical instruments and devices (in particular, optical transistors); this growth also is providing a technological base needed for such devices. Third, the interest in optical switches arises from the fundamental limits on the response time of electric and electro-optical switches: the minimum switching time in these switches is limited by the charge–discharge processes in the electric circuit of a device (i.e. by the values of the circuit capacitance, resistance, and inductance), which is usually at least 0.1–1 ns [3].

The earliest work on optical switches by V N Lugovoi [15], H Seidel [16], and A Szoke et al. [17] was all published in 1969 and dealt with bistable Fabry–Perot cavities. M A Duguay and J W Hansen also published work in 1969 on Kerr switches [18]; there were also other communications [19–21]. I would like to mention here the paper of G A Askar'yan of 1968 [22] on self-reflection of light and self-isolation of objects. Although Askar'yan considered a slow nonlinearity, the analogy with the work of Kaplan [21] is readily apparent: Askar'yan speaks of induced total internal reflection [22] whereas later [21] Kaplan discusses frustrated total internal reflection.

By 1982 the published work on optical switches became voluminous and the optical bistable switches based on the Fabry–Perot cavity [23, 24] and other systems with oppositely directed coupled waves [25–31] have become the best known and popular. However, such switches suffer from a number of shortcomings. First, their response time is limited by the time needed to establish the field in a cavity. Second, a powerful reflected wave forms at the input to the system. Third, such switches are unsuitable for inclusion in integrated optical circuits. Information on these and other optical switches can be found in reviews [30, 31].

New extensive opportunities for the development of promising optical switching devices and optical transistors are provided, as I demonstrated for the first time in Refs [32–34],† by a different class of systems with unidirectional distributively coupled waves. These devices were investigated by our team [32–34, 36–72] and by other authors [35, 73–107]. The main flow of work in the West on the same subject began in 1986 and in the last 5–6 years the number of publications increased explosively and now there are hundreds of them. Therefore, without aiming to cover all the latest papers on this new topic, I shall try to present the theoretical and experimental fundamentals from a unified point of view.

Unidirectional distributively coupled waves (UDCW's) play an important role particularly in integrated [1–7, 108], fibre [8–10, 109], and nonlinear optics [11–14, 6], although their linear theory was first developed for x rays [110, 111] and microwaves [112]. We can divide UDCWs into *two groups: with the coupling coefficient independent of and dependent on the wave amplitudes*.‡

†Also in 1982 Jensen [35] put forward a similar switch based on one of the forms of unidirectional distributively coupled waves, namely the waves in tunnel-coupled optical waveguides (see below) in the special case when light is coupled into one of the identical waveguides.

‡The coupling coefficient is the quantity defined by the set of equations (2.5.1).

*The first (larger) group of UDCWs with the coupling coefficient independent of the wave amplitudes includes: waves in tunnel-coupled optical waveguides (TCOWs), i.e. in two parallel closely spaced (separated by a distance  $\sim 1-10 \mu\text{m}$ ) optical waveguides; waves with different polarisations in the same birefringent waveguide or in a birefringent crystal; transmitted and diffracted waves in a periodic structure; two modes in an inhomogeneous optical waveguide, etc. [1–7].*

In the linear regime when the wave intensities are low and the nonlinearity of the medium in which they are travelling can be ignored, periodic (sinusoidal) exchange of energy takes place between these waves as they propagate (Fig. 1). For example, if one of the waves (we shall call it the zeroth wave) is applied to the input of the system, then — at some distance from the input — energy is transferred to another wave (we shall call it the first wave); next, energy returns to the zeroth wave, goes back to the first wave, etc.

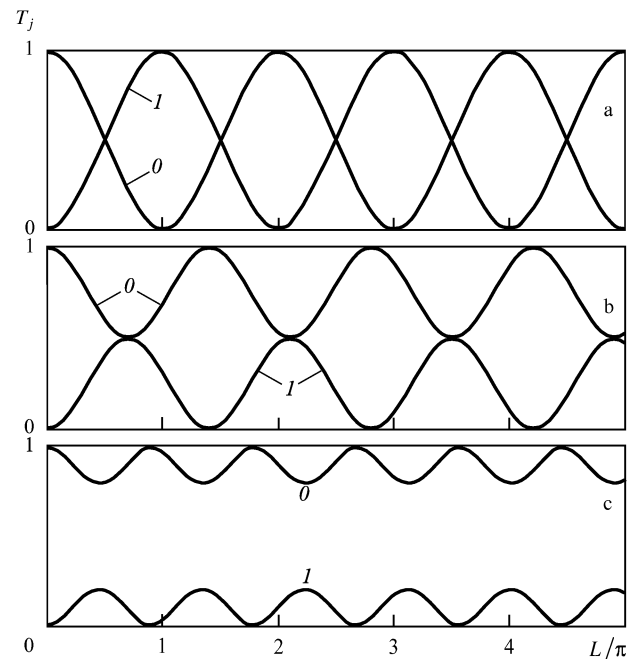


**Figure 1.** Dependence of the power (normalised to its initial value  $T_j = I_j/I_{00}$ , where  $j=0$  or  $1$ ) of two UDCWs (0 and 1) on the normalised coupling length  $L = 2\pi Kl/\lambda\beta$  in the linear regime;  $K$  is the wave coupling coefficient,  $l$  is the length of the system,  $\beta = (\beta_1 + \beta_0)/2$ ,  $\beta_j$  is the effective refractive index of the  $j$ th wave;  $\xi = 0$  (a),  $\xi = \alpha\beta/K = 1$  (b),  $\xi = 2$  (c);  $\alpha = \beta_1 - \beta_0$ . One of the waves (zeroth) is coupled into the system:  $I_{00} \neq 0$ ,  $I_{10} = 0$ .

If the waves are identical, i.e. if their effective refractive indices are the same, the transfer is complete; if the waves are not identical, i.e. if they have different effective refractive indices, the transfer is incomplete (see Fig. 1). Therefore, the power transfer coefficient of each wave depends on the difference between the effective refractive indices of the waves [1–7].

This suggests that in the nonlinear regime, when the refractive index depends on the wave intensity, the power transfer coefficient of each wave should depend on the initial intensity, i.e. *nonlinear power transfer or pumping over is possible*. These considerations stimulated my interest in the study of the nonlinear interaction between such waves.

We were able to detect a very interesting, hitherto unknown, phenomenon which we called self-switching of UDCWs. Under certain conditions a small change in the input intensity of one of the UDCWs causes a major change in the ratio of these waves at the output of the system. The change in the power of each wave at the output could be tens, hundreds, thousands, millions (!) or more times greater than the change in the input power. On the basis of this phenomenon, we proposed a novel class of optical transistors [32, 33].

At the time we started our work, the nonlinear interaction between the UDCWs belonging to the first group had been ignored almost completely. The exceptions were the few investigations of the ‘nonlinear girotopry’ (Akhmanov and Zharikov, reported in 1967 [113]), and some earlier work of Maker, Terhune, and Savage published in 1964 and 1965 [114, 115], who noted the influence of the cubic nonlinearity on the polarisation of the output waves. Almost simultaneously with our work [33], Stolen, Botineau, and Ashkin reported [116] nonlinear transfer between waves with different polarisations in a birefringent fibre waveguide and nonlinear power transfer in such a system; however, abrupt switching of light between waves with different polarisations and an optical transistor based on this were not mentioned in Ref. [116], in contrast to our work [32, 33].

Self-switching in the first group of UDCWs is dealt with in the present review.

*The second group of UDCWs includes waves with the coupling coefficient dependent on the wave amplitudes.* These are primarily the waves with two or three different frequencies in a medium with the quadratic nonlinearity; in particular, these are the waves with frequencies  $\omega$  and  $2\omega$ . This group includes also waves participating in concurrent (parallel) stimulated Raman scattering. The interaction of such waves is fundamentally nonlinear. Investigations of such waves, which began over 25 years ago, represent the birth of modern nonlinear optics [11, 12]. However, even in this field of optics there were some ‘blank spots’ at the time we began our work. Numerous investigations have been reported of the dependences of the wave intensities or of the frequency conversion coefficient on the longitudinal coordinate or on the length of a crystal. The aim of these investigations has been to ensure the maximum conversion within the length of a crystal. However, the changes in the ratio of the intensities of the waves of different frequencies (for example,  $\omega$  and  $2\omega$ ) at the output of a quadratically nonlinear medium, due to a change in the input intensity of one of the waves, have not been studied. The exception was the work of Jain and Pratt [117] who proposed to construct an optical transistor based on second-harmonic generation in a tellurium crystal, but on the basis of a principle different than that proposed in our papers relating to these topics [49, 50, 52, 53]. Although the solutions of the equations describing the interaction of waves at the frequencies  $\omega$  and  $2\omega$  in a quadratically nonlinear medium (plane waves in a field which could vary) were given in Bloembergen’s book [12], published back in 1965, these solutions had not been investigated analytically for a nonconstant field in the presence of both waves ( $\omega$  and  $2\omega$ ) at the entry to the medium under the conditions of a phase mismatch and an arbitrary relationship between the wave phases at the input.

Our investigations made it possible to predict and describe theoretically [49, 50, 52, 53] the hitherto unknown phenomenon of self-switching of such UDCWs, similar to self-switching of the waves belonging to the first group. On this basis we were the first to propose [49, 50, 52] a class of optical transistors and of all-optical light switches.

The phenomenon of self-switching of UDCWs is very complex and it has a large number of facets. There are various modes of this phenomenon, it can occur in a variety of ways, it can have a range of depths and directions, and its slope may vary by a factor of hundreds or thousands (for the same length of a system), depending on the initial conditions and on the parameters of the system. For example, complete self-switching of nonidentical waves is possible (although in the linear regime such complete switching of these waves is, in principle, impossible!—see Fig. 1); on the other hand, self-switching of identical waves may be incomplete (see Sections 3.6 and 3.11 below); various operational modes are possible: optical transistor, giant amplifier, double self-switch (Sections 2.3 and 3.4), and so on. We found simple analytic formulas for the description of self-switching: the conditions for the appearance of this phenomenon, its slope, depth, characteristic points, etc. The construction of any specific device (optical transistor, amplifier, limiter, multivibrator, logic element, etc.) requires selection of a suitable (for this device) self-switching mode. Self-switching of the UDCWs is accompanied by self-phase-matching. These and other topics are discussed below.

The first section provides a brief derivation of the equations for the three kinds of nonlinear systems involving the first group of UDCWs and the general form of equations for such waves. The second section demonstrates that self-switching of UDCWs is possible and this phenomenon is investigated for the case when one of the waves is applied to the input. The third section deals with the self-switching of UDCWs when both waves are delivered to the input. The fourth section provides an account of switching of a powerful pump by a signal whose frequency or polarisation differs from the frequency or polarisation of the pump. The fifth section describes optical multivibrators based on this phenomenon. The sixth section is devoted to the self-switching of three UDCWs.

## 2. Equations and integrals for the amplitudes of single-frequency unidirectional distributively coupled waves in a cubically nonlinear medium

The interaction of UDCWs in a cubically nonlinear medium is described in Ref. [33] by the method of slowly varying amplitudes, which has proved its worth in nonlinear [11–13] and integrated optics [3–6], as well as in the dynamic theory of x-ray diffraction [110, 111]. Let us begin with the familiar equation

$$\nabla^2 \mathbf{E} - \frac{\hat{\epsilon}}{c^2} \frac{\partial^2 \mathbf{E}}{\partial t^2} = \frac{1}{c^2} \frac{\partial^2 \mathbf{P}_{nl}}{\partial t^2}, \quad (2.1)$$

where the cubically nonlinear polarisation is  $\mathbf{P}_{nl} = \hat{\theta} : \mathbf{E} \mathbf{E} \mathbf{E}$  and  $\hat{\theta}(x, y)$  is the distribution of the cubic susceptibility tensor† over a transverse cross section of the system.

†The factor  $4\pi$ , missing from the right-hand side of Eqn (2.1), is included in the components of the tensor  $\hat{\theta}$ .

Under steady-state conditions, the field with a given frequency is

$$E(x, y, z, t) = E_\omega(x, y, z) \exp(i\omega t) + E_\omega^*(x, y, z) \exp(-i\omega t) \quad (2.2)$$

and, therefore, under steady-state conditions the equation for the field at this frequency  $\omega$  is

$$\nabla^2 E_\omega + \frac{\omega^2}{c^2} \hat{\epsilon} E_\omega = -\frac{\omega^2}{c^2} P_{nl,\omega} \quad (2.3)$$

and its nonlinear polarisation is

$$P_{nl,\omega} = \hat{\theta} : (E_\omega^* E_\omega E_\omega + E_\omega E_\omega^* E_\omega + E_\omega E_\omega E_\omega^*) . \quad (2.4)$$

## 2.1 Equations for the amplitudes of waves in tunnel-coupled optical waveguides

In tunnel-coupled optical waveguides (Figs 5a and 5d) the refractive index at each point is a linear function of the intensity. The field  $E_\omega$  is in its turn a superposition of two coupled (zeroth and first) waves propagating, respectively, in the zeroth and first waveguides:

$$E_\omega(x, y, z) = e_0 A_0(z) E_0(x, y) \exp\left(i \frac{\omega}{c} z \beta_0\right) + e_1 A_1(z) E_1(x, y) \exp\left(i \frac{\omega}{c} z \beta_1\right) , \quad (2.1.1)$$

where  $A_j(z)$  are the slowly varying (complex) wave amplitudes,  $e_j$  are the polarisation unit vectors of these waves,  $E_j(x, y)$  are the distributions of the fields over transverse cross sections of the waveguides (field profiles),  $\beta_j$  are the effective refractive indices of the waveguides, and  $j = 0$  or  $1$  are the serial numbers of the waves.

It will be assumed that the amplitudes  $A_j(z)$  have the meaning and dimensions of electric fields (effectively averaged over the cross section of the system with the coordinate  $z$ ), which leads to normalisation of the dimensionless field profiles so that the quantities  $c\beta_j |A_j|^2 / 2\pi$  correspond to the wave intensities, i.e. it is assumed that

$$\frac{c\beta_j}{2\pi} |A_j|^2 \iint |E_j(x, y)|^2 dx dy = P_j , \quad (2.1.2)$$

where  $P_j$  is the optical power carried by the  $j$ th wave. If the area of the effective cross section of the  $j$ th waveguide is  $S_j$ , it follows from our normalisation that

$$\iint |E_j|^2 dx dy = S_j .$$

The field profiles satisfy the following system of equations:

$$\nabla_\perp^2 E_j + \frac{\omega^2}{c^2} (n_j^2 - \beta_j^2) E_j = 0 , \quad (2.1.3)$$

i.e. they are the eigenfunctions of these equations.

Substituting expression (2.1.1) into expression (2.4) and bringing together similar terms, we obtain the general expression for the nonlinear polarisation at the frequency  $\omega$ :

$$P_{nl,\omega} = \hat{\theta} : \left\{ 3e_0 e_0 e_0 |E_0|^2 E_0 |A_0|^2 A_0 \exp\left(i \frac{\omega}{c} z \beta_0\right) + (e_0 e_1 e_0 + e_0 e_0 e_1 + e_1 e_0 e_0) 2|E_0|^2 E_1 |A_0|^2 A_1 \exp\left(i \frac{\omega}{c} z \beta_1\right) + (e_0 e_1 e_1 + e_1 e_0 e_1 + e_1 e_1 e_0) E_1^2 E_0^* A_1^2 A_0^* \exp\left[i(\beta_1 + \alpha) \frac{\omega}{c} z\right] \right\} ,$$

$$+ (e_1 e_0 e_0 + e_0 e_1 e_0 + e_0 e_0 e_1) E_0^2 E_1^* A_0^2 A_1^* \exp\left[i(\beta_0 - \alpha) \frac{\omega}{c} z\right] + (e_1 e_1 e_0 + e_1 e_0 e_1 + e_0 e_1 e_1) 2|E_1|^2 E_0 |A_1|^2 A_0 \exp\left(i \frac{\omega}{c} z \beta_0\right) + 3e_1 e_1 e_1 |E_1|^2 E_1 |A_1|^2 A_1 \exp\left(i \frac{\omega}{c} z \beta_1\right) \left. \right\} , \quad (2.1.4)$$

where  $\alpha \equiv \beta_1 - \beta_0$ .

Let the distribution of the refractive indices in a transverse section of each waveguide with a serial number  $j = 0$  or  $1$ , over the transverse coordinate  $x$  directed along the shortest distance joining the waveguide centres, be described by

$$n_0^2 = \begin{cases} n_l^2, & x < 0, \\ n_0^2(x, y), & 0 \leq x \leq t_0, \\ \bar{n}^2, & x > t_0, \end{cases} \quad (2.1.5)$$

$$n_1^2 = \begin{cases} \bar{n}^2, & x < d + t_0, \\ n_1^2(x, y), & d + t_0 \leq x \leq d + t_0 + t_1, \\ n_r^2, & x > d + t_0 + t_1, \end{cases}$$

where  $n_j(x, y)$  is the refractive index of the light-carrying core or layer in the  $j$ th waveguide,  $t_j$  is the size of this core or layer along the  $x$  axis,  $n_l$  and  $n_r$  are, respectively, the refractive indices of the material filling the space to the left and right of the edges of the light-carrying cores of layers in the zeroth and first waveguides,  $\bar{n}$  is the refractive index of the material filling the gap between the light-carrying cores, and  $d$  is the size of this gap (along the  $x$  axis).

The square of the refractive index  $n^2(x, y)$  of a system of two tunnel-coupled optical waveguides can be represented in the form [8]

$$n^2(x, y) = (n_0^2 - \bar{n}^2 - n_l^2) + (n_1^2 - \bar{n}^2 - n_r^2) + (n_l^2 + \bar{n}^2 + n_r^2) = (n_0^2 - \bar{n}^2) + (n_1^2 - \bar{n}^2) + \bar{n}^2 . \quad (2.1.6)$$

Let us substitute expression (2.1.1) into expression (2.3), drop the second derivatives of the amplitudes with respect to  $z$ , and take into account the set of equations (2.1.3)–(2.1.6). Let us multiply both sides of the resultant equation by  $E_0^*(x, y)$  and  $E_1^*(x, y)$  in turn, and integrate once over the transverse cross section. If the quantities of the second order of smallness are ignored, the result is [32, 33]

$$\begin{cases} 2i\beta \frac{c}{\omega} \frac{dA_0}{dz} + K_{01} A_1 \exp\left(i\alpha \frac{\omega}{c} z\right) = -\theta_0 |A_0|^2 A_0, \\ 2i\beta \frac{c}{\omega} \frac{dA_1}{dz} + K_{10} A_0 \exp\left(-i\alpha \frac{\omega}{c} z\right) = -\theta_1 |A_1|^2 A_1, \end{cases} \quad (2.1.7)$$

where  $\beta = (\beta_0 + \beta_1)/2$ ; the coupling coefficients are

$$K_{01} = \frac{(e_0 e_1) \iint (n_0^2 - \bar{n}^2) E_1(x, y) E_0^*(x, y) dx dy}{\iint |E_0(x, y)|^2 dx dy} ,$$

$$K_{10} = \frac{(e_0 e_1) \iint (n_1^2 - \bar{n}^2) E_0(x, y) E_1^*(x, y) dx dy}{\iint |E_1(x, y)|^2 dx dy} ,$$

which is the form used in linear integrated optics [3, 4, 8];

$$\theta_j = \frac{3 \iint \bar{\theta}_j |E_j(x, y)|^4 dx dy}{\iint |E_j|^2 dx dy} \quad (2.1.8)$$

are the nonlinear coefficients of the waveguides and the convolutions of the tensor  $\hat{\theta}$  have the form  $\hat{\theta}_j = e_j \hat{\theta} : e_j e_j e_j$ . The tensor  $\hat{\theta}$  can usually be assumed to have the value of  $\hat{\theta}$  for an isotropic medium [118] (see Appendix I); in this case we obtain  $\hat{\theta}_j = \theta_{xxx}^{(j)} = \theta_{yyy}^{(j)} = \theta_{zzz}^{(j)}$ .

Equations similar to the system of equations (2.1.7), but more cumbersome and ignoring a possible nonidentity of the waveguides, were derived by Jensen [35] simultaneously with publication of our work [33] (as judged by the dates of submission of the papers). Our priority in this matter was confirmed by a USSR patent [32].

## 2.2 Equations for a periodic structure

Let us derive equations for the wave amplitudes under the Bragg diffraction conditions in a periodic structure (Figs 5c and 5g). The linear and cubic-nonlinear susceptibilities will be expanded as Fourier series in terms of the reciprocal lattice vectors [110, 111]:

$$\hat{X} = \hat{\varepsilon} - 1 = \sum_m \hat{X}_{mh} \exp(im\mathbf{h} \cdot \mathbf{r}), \quad (2.2.1)$$

$$\hat{\theta} = \sum_m \hat{\theta}_{mh} \exp(im\mathbf{h} \cdot \mathbf{r})$$

(here,  $m = 0, \pm 1, \pm 2, \dots$ ), and the total electric field near the Bragg condition will be represented as the sum of the transmitted and diffracted waves, propagating along the directions '0' and 'h':

$$\mathbf{E}_\omega(\mathbf{r}) = e_0 A_0(\mathbf{r}) \exp(i\mathbf{k}_0 \cdot \mathbf{r}) + e_h A_h(\mathbf{r}) \exp(i\mathbf{k}_h \cdot \mathbf{r}), \quad (2.2.2)$$

where  $A_{0,h}(\mathbf{r})$  are the slowly varying amplitudes of the waves,  $k_0 = n_0 \omega / c$ ,  $n_0 = \sqrt{1 + X_0}$ ,  $\mathbf{k}_h = \mathbf{k}_0 + \mathbf{h}$ ,  $h = 2\pi/\tilde{d}$ ,  $\tilde{d}$  is the structure period, and  $e_{0,h}$  are the polarisation unit vectors.

Let us now substitute expressions (2.2.1) and (2.2.2) into expressions (2.3) and (2.4), and drop the second derivatives of the amplitudes. When similar terms are collected, the result is a general expression for the nonlinear polarisation at a frequency  $\omega$ , which is identical with expression (2.1.4). However, the profiles of the fields are now formally assumed to be unity, and the subscripts 0 and 1 are understood to mean 0 and h. If we drop the nonzero Fourier components of  $\hat{\theta}$ , because they are quantities of the second order of smallness, we obtain a system of reduced equations for the amplitudes [38]:

$$2in_0 \frac{c}{\omega} \left( \cos \vartheta_0 \frac{\partial A_0}{\partial z} + \sin \vartheta_0 \frac{\partial A_0}{\partial x} \right) = X_{-h} A_h + (\theta_0^{(0)} |A_0|^2 + \theta_0^{(0,h)} |A_h|^2) A_0, \quad (2.2.3)$$

$$2in_0 \frac{c}{\omega} \left( \pm \cos \vartheta_h \frac{\partial A_h}{\partial z} \mp \sin \vartheta_h \frac{\partial A_h}{\partial x} \right) = X_h A_0 - 2\alpha A_h + (\theta_0^{(h)} |A_h|^2 + \theta_0^{(h,0)} |A_0|^2) A_h,$$

where the upper signs apply to the Laue case ( $\mathbf{h} \perp \mathbf{n}$ ) and the lower signs to the Bragg case ( $\mathbf{h} \parallel \mathbf{n}$ ) [110, 111],  $\mathbf{n}$  is the normal to the surface of a sample,  $z = \mathbf{n} \cdot \mathbf{r}$ , the parameter  $\alpha = (k_h - k_0)c/\omega \approx n_0(\vartheta - \vartheta_B) \sin(2\vartheta_B)$  represents the deviation from the Bragg condition,  $\vartheta_0 = \mathbf{k}_0 \cdot \mathbf{n}$ ,  $\vartheta_h = \mathbf{k}_h \cdot \mathbf{n}$ ,  $\vartheta_B = \arcsin(hc/2\omega n_0)$  is the Bragg angle, and the convolu-

tions of the Fourier components of the tensors are

$$X_{\pm h} = e_0 \hat{X}_{\pm h} e_h, \quad \theta_0^{(0)} = e_0 \hat{\theta}_0 : e_0 e_0 e_0, \quad \theta_0^{(h)} = e_h \hat{\theta}_0 : e_h e_h e_h, \quad (2.2.4)$$

$$\theta_0^{(0,h)} = e_0 \hat{\theta} : (e_h e_h e_0 + e_h e_0 e_h + e_0 e_h e_h),$$

$$\theta_0^{(h,0)} = e_h \hat{\theta}_0 : (e_0 e_h e_0 + e_0 e_0 e_h + e_h e_0 e_0).$$

The set of equations (2.2.3) represents a generalisation of the Takagi equations [110, 111] to a nonlinear medium.

Let us consider the diffraction of a plane monochromatic wave in the symmetric Laue case:  $\partial A_{0,h} / \partial x = 0$  and  $\vartheta_0 = \vartheta_h = \vartheta$ . Let us also change the variables:  $z\omega/c / \cos \vartheta \Rightarrow z_L$ ,  $A_h \Rightarrow A_h \exp(i\alpha z_L)$ .

An isotropic medium is encountered frequently in practice (Appendix I) and we then have

$$\theta_0^{(0)} = \theta_0^{(h)} = \theta, \quad \theta_0^{(0,h)} = \theta_0^{(h,0)} = \theta[1 + C^2], \quad (2.2.5)$$

$$X_{-h} = \bar{X}_{-h} C, \quad X_h = \bar{X}_h C,$$

where the factor in the above expression is  $C = e_0 \cdot e_h$ ;  $C = 1$  if the unit vectors  $e_0$  and  $e_h$  are perpendicular to the plane of diffraction and  $C = \cos 2\vartheta$ , if  $e_0$  and  $e_h$  lie in the same plane;  $\bar{X}_{\pm h}$  are the Fourier components of the susceptibility  $X$  of the isotropic medium. Substitution of expression (2.2.5) into expression (2.2.3) gives [38]

$$\begin{cases} 2in_0 A_0' = \bar{X}_{-h} C A_h \exp(i\alpha z_L) + \theta(|A_0|^2 + (1 + C^2)|A_h|^2) A_0, \\ 2in_0 A_h' = \bar{X}_h C A_0 \exp(-i\alpha z_L) + \theta(|A_h|^2 + (1 + C^2)|A_0|^2) A_h, \end{cases} \quad (2.2.6)$$

where the prime denotes the derivative with respect to  $z_L$ .

## 2.3 Equations for unidirectional distributively coupled waves with different polarisations

Waves with the orthogonal polarisations propagating in a birefringent crystal or in an optical waveguide (in integrated optics, it is usual to speak of TE and TM waves) represent one of the examples of UDCWs (Figs 5b and 5f).

The coordinates in the principal system will be  $x'$  and  $y'$ . As usual, let us start with the wave equation which, for the field with a given frequency  $\omega$  under steady-state conditions, has the form of Eqn (2.3) with its nonlinear polarisation given by expression (2.4).

Let us consider this equation in a coordinate system  $x, y$  rotated relative to the principal system  $x'$  and  $y'$  by an angle  $\varphi$ . The matrix  $\hat{\varepsilon}$  in expression (2.4) is described in the rotated coordinate system by

$$\hat{\varepsilon}' = \begin{pmatrix} \varepsilon_1 & 0 \\ 0 & \varepsilon_2 \end{pmatrix} \quad (2.3.1)$$

and in the principal system it is represented with the aid of the rotation matrix

$$\hat{A} = \begin{pmatrix} \cos \varphi & \sin \varphi \\ -\sin \varphi & \cos \varphi \end{pmatrix} \quad (2.3.2)$$

(with the elements  $a_{ij}$ ) in a familiar way:  $\varepsilon_{ij} = a_{ii'} a_{jj'} \varepsilon_{i'j'}$ , i.e.

$$\begin{aligned} \varepsilon_{11} &= \varepsilon_1 \cos^2 \varphi + \varepsilon_2 \sin^2 \varphi, \\ \varepsilon_{12} &= \frac{1}{2} (\varepsilon_2 - \varepsilon_1) \sin(2\varphi) = \varepsilon_{21}, \\ \varepsilon_{22} &= \varepsilon_1 \sin^2 \varphi + \varepsilon_2 \cos^2 \varphi. \end{aligned} \quad (2.3.3)$$

The field in the coordinate system of interest to us,  $x$  and  $y$ , can be represented by a superposition of two orthogonally polarised waves:

$$\begin{aligned} E_\omega(x, y, z) = & e_x A_x(z) E_x(x, y) \exp\left(i\beta_x \frac{\omega}{c} z\right) \\ & + e_y A_y(z) E_y(x, y) \exp\left(i\beta_y \frac{\omega}{c} z\right), \end{aligned} \quad (2.3.4)$$

where  $A_x(z)$  and  $A_y(z)$  are the amplitudes of the waves polarised along the  $x$  and  $y$  axes, and varying slowly along the longitudinal coordinate  $z$ ;  $e_x$  and  $e_y$  are the polarisation unit vectors of these waves;  $E_x(x, y)$  and  $E_y(x, y)$  are the field profiles satisfying, like Eqns (2.1) and (2.2), the normalisation condition  $\iint |E_x|^2 dx dy = \iint |E_y|^2 dx dy = S$  (where  $S$  is the area of the waveguide or beam cross section), when  $A_x$  and  $A_y$  have the meaning and dimensions of electric fields.

If we consider waves with the orthogonal polarisations in an optical waveguide (TE and TM waves), then  $E_x$ ,  $E_y$ , and  $\beta_x$ ,  $\beta_y$  satisfy the following equations:

$$\begin{aligned} \nabla_\perp^2 E_x + \frac{\omega^2}{c^2} (\epsilon_{11} - \beta_x^2) E_x &= 0, \\ \nabla_\perp^2 E_y + \frac{\omega^2}{c^2} (\epsilon_{22} - \beta_y^2) E_y &= 0, \end{aligned} \quad (2.3.5)$$

i.e. they are eigenfunctions and the eigenvalues of these equations. However, if the waves have the orthogonal polarisations in a bulk anisotropic crystal, then  $\Delta_\perp E_x = \Delta_\perp E_y = 0$  can be substituted in the set of equations (2.3.5) and then

$$\begin{aligned} \beta_x = n_x = \sqrt{\epsilon_{11}} &= \sqrt{\epsilon_1 \cos^2 \varphi + \epsilon_2 \sin^2 \varphi} \\ &\approx n'_x \cos^2 \varphi + n'_y \sin^2 \varphi, \\ \beta_y = n_y = \sqrt{\epsilon_{22}} &= \sqrt{\epsilon_1 \sin^2 \varphi + \epsilon_2 \cos^2 \varphi} \\ &\approx n'_x \sin^2 \varphi + n'_y \cos^2 \varphi, \end{aligned} \quad (2.3.6)$$

where  $n'_x = \sqrt{\epsilon_1}$ ,  $n'_y = \sqrt{\epsilon_2}$  are the refractive indices of the waves polarised along the  $x'$  and  $y'$  axes.

Let us now substitute expression (2.3.4) into Eqns (2.3) and (2.4), and drop the second derivatives of the amplitudes. In the case of the nonlinear polarisation  $P_{nl,\omega}$  we obtain an expression which is fully identical with expression (2.1.4), if the subscripts in expression (2.1.4) are modified: 0 is replaced with  $x$  and 1 with  $y$ .

Let us multiply both parts of the resultant equation in turn by  $e_x E_x^*(x, y)$  and  $e_y E_y^*(x, y)$ , integrate each time over the transverse cross section, and use the system of equations (2.3.5). Moreover, let us bear in mind that in the case of an isotropic medium the components of the tensor  $\hat{\theta}$  with three identical subscripts and one different subscript ( $\theta_{xyyy}$ ,  $\theta_{yyxy}$ ,  $\theta_{xyyx}$ , etc.) all vanish, but for a medium with a weak anisotropy these components are quantities of the second order of smallness (Appendix I). Ignoring quantities of the second order of smallness, we then obtain

$$\begin{cases} 2i\beta \frac{c}{\omega} \frac{dA_x}{dz} + K_{xy} A_y \exp\left(i\alpha \frac{\omega}{c} z\right) \\ = -\theta_x |A_x|^2 A_x - \theta_{xy} |A_y|^2 A_x - \tilde{\theta}_{xy} A_y^2 A_x^* \exp\left(2i\alpha \frac{\omega}{c} z\right), \\ 2i\beta \frac{c}{\omega} \frac{dA_y}{dz} + K_{yx} A_x \exp\left(-i\alpha \frac{\omega}{c} z\right) \\ = -\theta_y |A_y|^2 A_y - \theta_{yx} |A_x|^2 A_y - \tilde{\theta}_{yx} A_x^2 A_y^* \exp\left(-2i\alpha \frac{\omega}{c} z\right), \end{cases} \quad (2.3.7)$$

where  $\alpha = \beta_y - \beta_x$ , but if a sample is an anisotropic crystal, then  $\alpha = (\sqrt{\epsilon_2} - \sqrt{\epsilon_1}) \cos(2\varphi)$ ;  $\beta = (\beta_x + \beta_y)/2$ , and the coupling coefficients are

$$\begin{aligned} K_{xy} &= \frac{\iint \epsilon_{12} E_y(x, y) E_x^*(x, y) dx dy}{\iint |E_x(x, y)|^2 dx dy}, \\ K_{yx} &= \frac{\iint \epsilon_{21} E_x(x, y) E_y^*(x, y) dx dy}{\iint |E_y(x, y)|^2 dx dy}, \end{aligned} \quad (2.3.8)$$

where  $\epsilon_{12} = \epsilon_{21}$  are described by the set of expressions (2.3.3); the nonlinear coefficients are [57]

$$\begin{aligned} \theta_x &= \frac{3 \iint \theta_{xxxx} |E_x|^4 dx dy}{\iint |E_x|^2 dx dy}, \\ \theta_{xy} &= \frac{2 \iint (\theta_{xyyx} + \theta_{xyxy} + \theta_{xxyy}) |E_x|^2 |E_y|^2 dx dy}{\iint |E_x|^2 dx dy}, \\ \tilde{\theta}_{xy} &= \frac{\iint (\theta_{xxyy} + \theta_{xyxy} + \theta_{yyxx}) E_x^* E_y^2 dx dy}{\iint |E_x|^2 dx dy}. \end{aligned} \quad (2.3.9)$$

The quantities  $\theta_y$ ,  $\theta_{yx}$ ,  $\tilde{\theta}_{yx}$  are obtained from the above expressions by the simple substitution:  $x \Rightarrow y$ ,  $y \Rightarrow x$ .

It is usually permissible to ignore the dependences of the components of the tensor  $\hat{\theta}$  on the transverse coordinates.

The components of the tensor  $\hat{\theta}$  are represented by the set of expressions (2.3.9) in the coordinate system  $x, y$ . When the principal coordinate system  $x'$  and  $y'$  is adopted, these components are transformed in accordance with the familiar formulas

$$\theta_{mnlk} = a_{mm'} a_{nn'} a_{kk'} a_{ll'} \theta_{m'n'k'l'},$$

where  $m = x, y$ ;  $n = x, y$ , and so on.

Since the anisotropy of the medium is assumed to be weak, the corresponding components of the tensor  $\hat{\theta}$  can be regarded as the same in both systems; we then have (Appendix I)

$$\begin{aligned} \theta_{xxxx} = \theta_{x't'x't'} = \theta_{y'y'y'y'} = \theta_{yyyy} &= \theta, \\ \theta_{xyyx} + \theta_{xyxy} + \theta_{xxyy} = \theta_{yxxy} + \theta_{yxxy} + \theta_{yyxx} &= \theta. \end{aligned}$$

Bearing in mind this weak anisotropy of the sample, ( $|\epsilon_{12}| \ll \epsilon_{11} \approx \epsilon_{22}$ ), let us assume that rotation of the coordinate axes does not alter (in the first order of perturbation theory) the field profiles, i.e. the eigenfunctions of the system of equations (2.3.5), and changes only their eigenvalues.

In contrast to the case of TCOWs, the system of equations (2.3.7) generally contains a term with  $\theta_{xy}$ , which contains the complex-conjugate phase. It should be stressed that since  $K \propto \epsilon_{12}$ , it follows that  $K/\alpha \propto \tan(2\varphi)$ .

If the frequencies of the waves  $A_y$  and  $A_x$  are identical, it follows from the set of expressions (2.3.9) that

$$\theta_x = \theta_y = \theta, \quad \theta_{xy} = \theta_{yx} = \frac{2\theta}{3}, \quad \tilde{\theta}_{xy} = \tilde{\theta}_{yx} = \frac{\theta}{3}. \quad (2.3.10)$$

In this case, if  $\alpha = 0$ , it is convenient to adopt the circular polarisations

$$A_x = \frac{A_+ + A_-}{\sqrt{2}}, \quad A_y = \frac{A_+ - A_-}{\sqrt{2}i}, \quad (2.3.11)$$

when, subject to the set of expressions (2.3.10), the system of equations (2.3.7) becomes [78]

$$\begin{cases} 2i\beta \frac{c}{\omega} \frac{dA_+}{dz} + iK_{xy}A_- = P_+, \\ 2i\beta \frac{c}{\omega} \frac{dA_-}{dz} - iK_{xy}A_+ = P_-, \end{cases} \quad (2.3.12)$$

where

$$P_- = -\frac{2}{3}\theta A_-(2|A_+|^2 + |A_-|^2),$$

$$P_+ = -\frac{2}{3}\theta A_+(2|A_-|^2 + |A_+|^2).$$

If  $\alpha \neq 0$ , we must begin with the substitution [119]

$$A_x = a_x \exp\left(\frac{i\alpha z\omega}{2c\beta}\right), \quad A_y = a_y \exp\left(-\frac{i\alpha z\omega}{2c\beta}\right), \quad (2.3.13)$$

and consider the amplitudes  $a_x$  and  $a_y$ , and then use the amplitudes  $a_x$  and  $a_y$  to find the circular polarisations described by expression (2.3.11). In this case, both  $A_+$  and  $A_-$  also correspond to the system of equations (2.3.12), but instead of  $K_{xy}$ , the first of them contains the complex coupling coefficient  $K_{xy} + i\alpha$ , and the second equation has the Hermitian-conjugate coefficient  $K_{xy} - i\alpha$ .

The term  $\tilde{\theta}_{xy}$  in the system of equations (2.3.7) can be removed by employing fibre waveguides [84] in which the optic axis undergoes rotational periodic oscillations with increase in  $z$ . These oscillations occur along the longitudinal axis of the fibre and their amplitude is small. The spatial amplitude of the oscillations is  $\beta_0 \gg K$ . The coupling coefficient then depends sinusoidally on  $z$  and the inequality  $|\alpha| \gg K$  is obeyed. Substitution of the variables in accordance with Ref. [84] (which means adoption of new amplitudes  $\tilde{a}_x$  and  $\tilde{a}_y$ ) leads to equations for  $\tilde{a}_x$  and  $\tilde{a}_y$  which are fully identical with the system of equations (2.1.7) where  $\alpha$  is replaced with  $\alpha_{\text{eff}} = \alpha - \beta_0$  (the role of this parameter is described in Section 3.3) and the nonlinear coefficients are now  $\theta_0 = \theta_1 = \theta/3$ . Selection of the wavelength [84] ensures the exact or at least approximate equality  $\alpha_{\text{eff}} = \alpha(\lambda) - \beta_0$  (physically this means that the difference between the wave vectors of the waves is compensated by the reciprocal lattice vector of the periodic structure).

#### 2.4 Equations for coupled modes

The equations for the amplitudes of two unidirectional coupled optical modes in a cubically nonlinear inhomogeneous single optical waveguide are also described by the system of equations (2.1.7), but the coefficients in these equations are calculated in accordance with somewhat different formulas. The linear coupling is due to the inhomogeneity of the waveguide which is the result of, for example, corrugations, bending, or thickness variations. The coupling coefficient is described by formulas given in Refs [3, 4], which we shall not reproduce here. The nonlinear coefficient is given by expression (2.1.8), but now  $E_j(x, y)$  is the profile of the  $j$ th optical mode in a single waveguide. The cross coefficients  $\theta_{01}$  can usually be ignored, as in the case of TCOWs, since the overlap integrals of the profiles of optical modes of different orders

are small compared with the overlap integrals of the profiles of modes of the same order.

#### 2.5 General form of the equations for the amplitudes and their integrals, and the equation for the intensities

The system of equations for the amplitudes of UDCWs in a cubically nonlinear medium when the coupling coefficient  $K$  is constant can be represented in their general form quite satisfactorily by the following approximation:

$$\begin{cases} i\beta \frac{\lambda}{\pi} \frac{d\tilde{A}_0}{dz} + K\tilde{A}_1 \exp\left(\frac{i\tilde{\alpha}z2\pi}{\lambda}\right) = -\tilde{\theta}_0|\tilde{A}_0|^2\tilde{A}_0 - \theta_{01}|\tilde{A}_1|^2\tilde{A}_0, \\ i\beta \frac{\lambda}{\pi} \frac{d\tilde{A}_1}{dz} + K\tilde{A}_0 \exp\left(-\frac{i\tilde{\alpha}z2\pi}{\lambda}\right) = -\tilde{\theta}_1|\tilde{A}_1|^2\tilde{A}_1 - \theta_{10}|\tilde{A}_0|^2\tilde{A}_1, \end{cases} \quad (2.5.1)$$

where the nonlinear coefficients are determined by the characteristics of the specific system: in the case of TCOWs and coupled optical modes of different orders in the same waveguide, we can assume that  $\theta_{01} = \theta_{10} = 0$ ; for UDCWs in a periodic structure and the corresponding waves with the circular polarisations these coefficients are given by expressions (2.2.5), (2.3.12), and (2.3.10).

In either case, the simple substitution

$$\theta_0 = \tilde{\theta}_0 - \theta_{01}, \quad \theta_1 = \tilde{\theta}_1 - \theta_{10}, \quad \alpha = \tilde{\alpha} - \frac{I(\theta_{01} - \theta_{10})}{2\beta}, \quad (2.5.2)$$

$$A_0 = \tilde{A}_0 \exp\left(-\frac{i\theta_{01}Iz\pi}{\lambda\beta}\right), \quad A_1 = \tilde{A}_1 \exp\left(-\frac{i\theta_{10}Iz\pi}{\lambda\beta}\right),$$

where  $I \equiv |A_0|^2 + |A_1|^2$ , reduces the system of equations (2.5.1) to [33]:

$$\begin{cases} i\beta \frac{\lambda}{\pi} \frac{dA_0}{dz} + KA_1 \exp\left(\frac{i\alpha z2\pi}{\lambda}\right) = -\theta_0|A_0|^2A_0, \\ i\beta \frac{\lambda}{\pi} \frac{dA_1}{dz} + KA_0 \exp\left(-\frac{i\alpha z2\pi}{\lambda}\right) = -\theta_1|A_1|^2A_1, \end{cases} \quad (2.5.3)$$

which are fully identical with the system of equations (2.1.7) for tunnel-coupled optical waveguides.

It therefore follows that the solution of the system of equations (2.5.1) reduces in fact to the solution of equations for TCOWs. In other words, as stressed in Ref. [33] and in our subsequent work [36, 38, 41], a slight difference between the right-hand sides of Eqns (2.5.1) and (2.5.3) does not affect the dependences of the output on the input intensities, and the theory of UDCWs in a cubically nonlinear system, usually applied in our work to the specific case of tunnel-coupled waveguides, does in fact apply generally to cubically nonlinear systems carrying UDCWs (naturally, if  $K$  and  $\theta$  are independent of the wave amplitudes). We shall therefore consider the systems of equations (2.5.3).

We shall introduce the moduli ( $\rho_j$ ) and phases ( $\varphi_j$ ) of the amplitudes  $A_j = \rho_j \exp(i\varphi_j)$ , as well as the quantities  $I_j = \rho_j^2$  proportional to the wave intensities. Then, the system of equations (2.5.3) becomes [34]

$$\begin{aligned} \beta I_0' &= -K\sqrt{I_0 I_1} \sin \psi, \\ \beta I_1' &= K\sqrt{I_0 I_1} \sin \psi, \\ 2\beta(\psi' - \alpha) &= K \frac{I_0 - I_1}{\sqrt{I_0 I_1}} \cos \psi + (\theta_1 I_1 - \theta_0 I_0), \end{aligned} \quad (2.5.4)$$

where  $\psi = \alpha z2\pi/\lambda + \varphi_1 - \varphi_0$ ; the prime denotes the derivative with respect to  $2\pi z/\lambda$ .

The systems of equations (2.5.3) and (2.5.4) have two integrals [32, 33].

$$I = I_0 + I_1, \tag{2.5.5}$$

which represent the law of conservation of energy in the system; we also have

$$G = K\sqrt{I_0 I_1} \cos \psi - \alpha\beta I_0 + \frac{\theta_0 I_0^2}{4} + \frac{\theta_1 I_1^2}{4}. \tag{2.5.6}$$

We shall now use dimensionless ‘intensities’  $J_j \equiv I_j/I_{0M}$  obtained by normalisation of  $I_j$  to what is known as the critical (full self-switching) value  $I_{0M} = 8K/|\theta_0 + \theta_1|$ , the meaning of which will be discussed in Section 2.

We shall denote the initial (at the input of the system) and final (at the output) values of the quantities as follows:

$$\begin{aligned} I_j(z=0) &\equiv I_{j0}, & J_j(z=0) &\equiv R_j \equiv \frac{I_{j0}}{I_{0M}}, & \psi(z=0) &\equiv \psi_0, \\ I_j(z=l) &\equiv I_{jl}, & J_j(z=l) &\equiv J_{jl} \equiv \frac{I_{jl}}{I_{0M}}, & \psi(z=l) &\equiv \psi_l, \end{aligned} \tag{2.5.7}$$

and we shall introduce the coefficient representing the transfer of the optical power through the system by the  $j$ th wave:

$$T_j \equiv \frac{I_{jl}}{I_{00} + I_{10}} \equiv \frac{J_{jl}}{R_0 + R_1},$$

if we define it as the fraction which is the ratio of the power in the  $j$ th wave at the output of the system to the total power introduced into the system. In calculations it is useful to introduce the coefficients

$$\theta_s \equiv \frac{\theta_0 + \theta_1}{2}, \quad \theta_d \equiv \frac{\theta_1 - \theta_0}{2}. \tag{2.5.8}$$

The integrals defined by expressions (2.5.5) and (2.5.6) lead to [62]

$$\cos \psi = \frac{\text{sign } \theta_s}{\sqrt{J_0 J_1}} \left[ \sqrt{R_0 R_1} \text{sign } \theta_s \cos \psi_0 + 2(J_1 - R_1) \left( R_0 - \frac{\Delta}{2} - J_1 \right) \right], \tag{2.5.9}$$

where

$$A = \xi + 2 \frac{\theta_d}{\theta_s} (R_0 + R_1) \tag{2.5.10}$$

and  $\xi \equiv \alpha\beta/K \text{sign } \theta_s$ .

In turn, it follows from relationship (2.5.9) that

$$\sin \psi = 2m \left[ \frac{f(J)}{J_0 J_1} \right]^{1/2}, \tag{2.5.11}$$

where  $J \equiv J_1$ ,  $m = \pm 1$ , and the value of  $m$  is governed by the sign of  $\sin \psi_0$ ,

$$\begin{aligned} f(J) &\equiv -(J - R_1)^2 \left( R_0 - \frac{\Delta}{2} - J \right)^2 \\ &\quad - (J - R_1) \left( R_0 - \frac{\Delta}{2} - J \right) \sqrt{R_0 R_1} \text{sign } \theta_s \cos \psi_0 \\ &\quad + \frac{R_0 (J - R_1 \cos^2 \psi_0)}{4} - \frac{(J - R_1) J}{4} \\ &\equiv - \left[ (J - R_1) \left( R_0 - \frac{\Delta}{2} - J \right) + \frac{\sqrt{R_0 R_1} \cos \psi_0}{2} \right]^2 \\ &\quad + \frac{(R_0 + R_1 - J) J}{4} \equiv -J^4 + aJ^3 + bJ^2 + \tilde{c}J + d, \end{aligned} \tag{2.5.12}$$

and

$$\begin{aligned} a &= 2R_0 + 2R_1 - \Delta, \\ b &= -R_0^2 - R_1^2 - \frac{1}{4} - 4R_0 R_1 + 2\Delta R_1 - \frac{\Delta^2}{4} \\ &\quad + \sqrt{R_0 R_1} \text{sign } \theta_s \cos \psi_0, \\ \tilde{c} &= \frac{R_0 + R_1}{4} + \left( R_0 + R_1 - \frac{\Delta}{2} \right) \sqrt{R_1} \left[ 2 \left( R_0 - \frac{\Delta}{2} \right) \right. \\ &\quad \left. \times \sqrt{R_1} - \sqrt{R_0} \text{sign } \theta_s \cos \psi_0 \right], \\ d &= -R_1 \left[ \left( R_0 - \frac{\Delta}{2} \right) \sqrt{R_1} - \sqrt{R_0} \text{sign } \theta_s \frac{\cos \psi_0}{2} \right]^2. \end{aligned}$$

Substitution of expression (2.5.11) into the last equation in the system (2.5.4) and integration gives [51, 56, 62]

$$2L = m \int_{R_1}^{J_{1l}} \frac{dJ}{\sqrt{f(J)}}, \tag{2.5.13}$$

where  $L = 2\pi Kl/\lambda\beta$ .

The problem of integration of Eqn (2.5.13) and, consequently, of finding the solution of the initial system of differential equations (2.5.3) thus reduces to determination of the roots of the algebraic equation [54, 51, 62]:

$$f(J) = 0. \tag{2.5.14}$$

If we know the roots of this equation, we can use a handbook of integrals etc. [120] to write down the solution. We shall use  $J_a, J_b, J_c, J_d$  to denote the roots of Eqn (2.5.14), where  $J_a$  and  $J_d$  are the real roots satisfying  $J_a > J_d$ , and the roots  $J_b$  and  $J_c$  are generally complex-conjugate. Eqn  $f(J) = 0$  has at least two real roots. One of the roots lies in the interval from zero to  $R_1$  and for  $\cos^2 \psi_0 = 1$ , this root is equal to  $R_1$ .

### 2.6 Possible deviations of equations from the general form

The system of equations (2.5.1) can be regarded as general subject only to the caution which applies to UDCWs with the orthogonal polarisations when the system of equations (2.3.7) may contain terms  $\tilde{\theta}_{xy} A_y^2 A_x^*$  and  $\tilde{\theta}_{yx} A_x^2 A_y^*$ , which can sometimes be eliminated (Section 2.3). If this is not possible, we can then employ the substitution described by the set of expressions (2.3.13) and relationships (2.3.10) to go over to the amplitudes with the circular polarisations which can be described by the general system of equations (2.5.1). Then, having solved these equations, we can go back to the amplitudes with the orthogonal polarisations. However, this procedure, involving the subsequent going to the intensities with the orthogonal polarisations, is not free of problems, particularly those resulting from fairly cumbersome transformations. A different approach [71] will be put forward below: it involves direct solution of the system of equations (2.3.7), which — on going over to the intensities and phases — assume the following general form:

$$\begin{aligned} \beta I_x' &= -K\sqrt{I_x I_y} \sin \psi - \tilde{\theta}_{I_x} I_y \sin(2\psi), \\ \beta I_y' &= K\sqrt{I_x I_y} \sin \psi + \tilde{\theta}_{I_y} I_x \sin(2\psi), \\ 2\beta(\psi' - \alpha) &= K \frac{I_x - I_y}{\sqrt{I_x I_y}} \cos \psi + \tilde{\theta}(I_x - I_y) \cos(2\psi) \\ &\quad + \theta_y I_y - \theta_x I_x + \theta_{yx} I_x - \theta_{xy} I_y, \end{aligned} \tag{2.6.1}$$

where  $\tilde{\theta} \equiv \tilde{\theta}_{xy} = \tilde{\theta}_{yx}$ .

The integrals of Eqns (2.3.7) and (2.6.1) are [71]

$$I = I_x + I_y, \quad (2.6.2)$$

$$G = K\sqrt{I_x I_y} \cos \psi - \alpha I_x + \frac{\tilde{\theta} I_x I_y \cos(2\psi)}{2} + \frac{\theta_{xy} I_x I_y}{2} + \frac{\theta_x I_x^2}{4} + \frac{\theta_y I_y^2}{4}. \quad (2.6.3)$$

Wabnitz, Trillo, et al. [77, 80] describe the nonlinear interaction of UDCWs in terms of the Stokes parameters. In our opinion [71], it is preferable to use two normalised Stokes parameters  $\varkappa = (I_x - I_y)/I$ ,  $\eta = 2 \cos \psi \sqrt{I_x I_y}/I = \cos \psi \sqrt{1 - \varkappa^2}$ . The system of equations (2.6.1) then becomes

$$\begin{cases} \varkappa' = (K + \tilde{\theta} I \eta) \sqrt{1 - \varkappa^2 - \eta^2}, \\ \eta' = -\left[\frac{(\theta_s + \tilde{\theta}) I \varkappa}{2} + \tilde{\alpha}\right] \sqrt{1 - \varkappa^2 - \eta^2}, \end{cases} \quad (2.6.4)$$

where  $\tilde{\alpha} = \alpha + I\theta_d/2$ ,  $\theta_s = (\theta_x + \theta_y - \theta_{xy} - \theta_{yx})/2$ ,  $\theta_d = (\theta_y - \theta_x + \theta_{yx} - \theta_{xy})/2$ . In terms of these variables, the integral  $G$  becomes  $\Gamma = I_n(\varkappa^2 + \eta^2) + 2\alpha\varkappa + 2K\eta$ .

The initial and final values of the various quantities will be designated as follows:

$$\begin{aligned} I_x(z=0) &\equiv I_{x0}, & I_y(z=0) &\equiv I_{y0}, \\ I_x(z=l) &\equiv I_{xl}, & I_y(z=l) &\equiv I_{yl}, \\ \varkappa(z=0) &\equiv \varkappa_0, & \varkappa(z=l) &\equiv \varkappa_l, \\ \eta(z=0) &\equiv \eta_0, & \eta(z=l) &\equiv \eta_l; \end{aligned} \quad (2.6.5)$$

the normalised input intensities [see expressions (2.5.7)] are

$$R_x \equiv \frac{|\theta| I_{x0}}{4\gamma}, \quad R_y \equiv \frac{|\theta| I_{y0}}{4\gamma}, \quad (2.6.6)$$

and the transfer coefficients are

$$T_x \equiv \frac{I_{xl}}{I} \equiv \frac{1 + \varkappa_l}{2}, \quad T_y \equiv \frac{I_{yl}}{I} \equiv \frac{1 - \varkappa_l}{2}. \quad (2.6.7)$$

The systems of equations (2.6.1) and (2.6.4) are analysed in Ref. [71] and in Section 3.11 below. Sections 2 and 3 of this review deal mainly with an analysis of the system of equations (2.5.4), which is equivalent to the system (2.5.3).

### 3. Optical self-switching on arrival of one wave at the input of a system

Let us consider a relatively simple case, when only one of the waves is applied to the input of a system with single-frequency UDCWs propagating in a cubically nonlinear medium. Let us assume that this is the zeroth wave:  $I_{00} \neq 0$ ,  $R_0 \neq 0$ ,  $I_{10} = R_1 = 0$ . Our task is to find the values of  $I_j$  and  $J_j$  in each transverse cross section of the system and at its output (i.e. the values of  $I_{jl}$  and  $J_{jl}$ ) and to analyse the resultant formulas.

#### 3.1 Optical self-switching in a system with identical unidirectional distributively coupled waves

Let us assume that the UDCWs are identical:  $\alpha = 0$ ,  $\theta_0 = \theta_1 = \theta$ . Then the roots of Eqn (2.5.14) are very simple:

$$\begin{aligned} J_d = 0, \quad J_a = R_0, \\ J_b = \frac{R_0 + \sqrt{R_0^2 - 1}}{2}, \quad J_c = \frac{R_0 - \sqrt{R_0^2 - 1}}{2}, \end{aligned} \quad (3.1.1)$$

and the critical intensity, described by the set of expressions (2.5.7), is  $I_{0M} = 4K/|\theta|$  [34, 35].

The function (2.5.12) can be described in two different ways. Depending on the way which is adopted, the integral in Eqn (2.5.13) reduces to one of the tabulated integrals. However, the resultant two forms of the solution can be reduced to one by identity transformations [62]. For brevity, we shall consider one solution method when  $f(J) = J(R_0 - J)[(J - R_0/2)^2 - (R_0^2 - 1)/4]$ . Calculation of the integral in Eqn (2.5.13) by means of tables [120] gives

$$L = mF(\mu, r), \quad (3.1.2)$$

where  $F(\mu, r)$  is an incomplete elliptic integral of the first kind with the modulus  $r = R_0$ , an additional modulus  $r_1 = (1 - r^2)^{1/2} = (1 - R_0^2)^{1/2}$ , and an amplitude  $\mu = 2 \arctan [(R_0 - J_{1l})/J_{1l}]^{1/2}$ .

Relationship (3.1.2) is equivalent to  $\cos \mu = \text{cn}(L, r)$ . Transformations yield [34, 35]

$$J_{jl} = \frac{R_0}{2} [1 + (-1)^j \text{cn}(L, r)], \quad (3.1.3)$$

where  $j = 0$  or  $1$  is the serial number of the wave. Another solution method is described in Ref. [34]. The solution described by formula (3.1.3) is valid both for  $I_{00} \leq I_{0M}$  ( $r = R_0 \leq 1$ ) and for  $I_{00} \geq I_{0M}$  ( $r = R_0 \geq 1$ ). If  $q = R_0^{-1} \equiv I_{0M}/I_{00} \leq 1$ , this solution can be transformed conveniently to

$$J_{jl} = \frac{R_0}{2} \left[ 1 + (-1)^j \text{dn}\left(\frac{L}{q}, q\right) \right]. \quad (3.1.4)$$

This is the intensity of each wave at the output of the system expressed in terms of the intensity of the input (zeroth) wave. The intensity of light in an arbitrary cross section of the system with a coordinate  $z$  can be found simply by replacing  $l$  and  $z$  in expressions (3.1.3) and (3.1.4).

The solution described by expression (3.1.3) determines also the coefficients representing the linear transfer of light  $T_j = I_{jl}/I_{00}$  ( $T_0 + T_1 = 1$ ), which are functions of two quantities:  $L$  and  $R_0$ . Therefore, if  $K$ ,  $l$ ,  $\lambda$ ,  $\theta$ , and  $I_{00}$  are varied and the quantities  $L$  and  $R_0$  remain unchanged, then  $T_j$  does not change either. The functions  $T_j(R_0)$  are not altered for a given value of  $L$  and the functions  $T_j(L)$  for a given value of  $R_0$ . We shall now analyse the solution given by expression (3.1.3).

(1) Let us first consider the case when  $r^2 = R_0^2 \equiv I_{00}^2/I_{0M}^2 \ll 1$  ( $r_1^2 \approx 1$ ). In this near-linear case the elliptic functions can be expressed in terms of the trigonometric functions [121], accurate apart from terms proportional to  $r^2$ , which we find from expression (3.1.3) [34]

$$J_{0l} \approx R_0 \cos^2 \frac{L}{2} + \frac{1}{8} R_0 R_0^2 \left[ L - \frac{1}{2} \sin(2L) \right] \sin L, \quad (3.1.5)$$

$$J_{1l} \approx R_0 \sin^2 \frac{L}{2} - \frac{1}{8} R_0 R_0^2 \left[ L - \frac{1}{2} \sin(2L) \right] \sin L.$$

In the purely linear case ( $\theta = 0$ ,  $r = 0$ ), we obtain the familiar linear-theory solutions [1–10]:

$$I_{0l} = I_{00} \cos^2 \frac{L}{2}, \quad I_{1l} = I_{00} \sin^2 \frac{L}{2}, \quad (3.1.6)$$

where the parameter  $L/\pi = 2IK/\lambda\beta$  shows, roughly speaking, how many times the waves exchange energy.

(2) The range of values of the parameters where

$$r = R_0 \equiv \frac{I_{00}}{I_{0M}} \simeq 1, \quad |r_1^2| = |1 - R_0^2| \ll 1, \quad \exp L \gg 1, \quad (3.1.7)$$

is the most interesting. The elliptic functions are approximated by the hyperbolic functions [121]. The effect under investigation can be described, as reported by us in Ref. [34, 36, 37], by compact and fairly accurate—up to within terms proportional to  $[r_1^2 \exp(L/16)]^2$ —approximations for the elliptic functions  $\text{cn}(L, r)$ ,  $\text{dn}(L, r)$ ,  $\text{sn}(L, r)$  for this range. These approximations are given in Appendix II. Application of these approximations modifies the solution described by expression (3.1.3) to [34]

$$J_{jl} \approx \frac{R_0}{2} \frac{(-1)^j \text{sech } L + [1 - (-1)^j (r_1^2/16) \exp L]^2}{1 + (r_1^4/256) \exp(2L)} \approx \frac{R_0}{2} - (-1)^j \frac{R_0}{2} \frac{(r_1^2/8) \exp L}{1 + (r_1^4/256) \exp(2L)}, \quad (3.1.8)$$

where  $r_1^2 \equiv 1 - R_0^2 \approx -q_1^2$ , i.e.  $r_1^2$  in the above expression is understood to be  $1 - R_0^2$ . If  $R_0 \geq 1$  and if we make the substitutions  $r_1^2 \equiv 1 - R_0^2 \Rightarrow -q_1^2 = 1 - R_0^2$  and  $L \Rightarrow L/q = LR_0 \approx L$ , we can approximate expression (3.1.4) by a formula obtained from expression (3.1.8) i.e. the result is practically identical with that given by expression (3.1.8). Therefore, the approximation represented by expression (3.1.8) is valid both for  $R_0 \leq 1$  (where  $r_1^2 \geq 0$ ,  $q_1^2 \leq 0$ ), and for  $R_0 \geq 1$  (where  $r_1^2 \leq 0$ ,  $q_1^2 \geq 0$ ).

We can rewrite expression (3.1.8) also as follows [34]:

$$T_j \approx \frac{1}{2} \frac{(-1)^j \text{sech } L + [1 - (-1)^j (r_1^2/16) \exp L]^2}{1 + (r_1^4/256) \exp(2L)}. \quad (3.1.8a)$$

Differentiation of expression (3.1.8) with respect to  $I_{00}$  and the assumption that  $\exp L \gg 1$  yield

$$\frac{\partial J_{jl}}{\partial I_{00}} = \frac{\partial J_{jl}}{\partial R_0} \approx \frac{\exp L}{8} \frac{1 - (r_1^4/256) \exp(2L)}{[1 + (r_1^4/256) \exp(2L)]^2} (-1)^j R_0^2. \quad (3.1.9)$$

It follows from expressions (3.1.8) and (3.1.9) that if

$$\frac{r_1^2}{16} \exp L = (-1)^j, \quad (3.1.10)$$

i.e. if the input intensity is [34]

$$I_{00} = I_M^{(j)} \equiv I_{0M} R_M^{(j)} \approx I_{0M} [1 + (-1)^j 8 \exp(-L)], \quad (3.1.11)$$

the power of the  $j$ th wave at the output is maximal and almost all the output radiation power is concentrated in the  $j$ th wave:  $I_{jl} \approx I_{00}$ ,  $J_{jl} \approx R_0$ ,  $T_j \approx 1$ . The power of the other wave is then negligible:

$$R_0 - J_{jl} \approx 1 - T_j \approx \frac{\text{sech } L}{4} \approx 2 \exp(-L) \ll 1. \quad (3.1.12)$$

An analysis of the solution of the system of equations (2.5.3) thus reveals an unexpected and interesting physical phenomenon. It is found that, irrespective of the length of the system, near the ‘critical’ value ( $I_{0M}$ ) of the input intensity a definite relationship is observed [34]: if the radiation intensity at the input is slightly less than the critical value, namely if  $I_{00} = I_M^{(1)} \approx I_{0M} [1 - 8 \exp(-L)]$ , then almost all the radiation leaves the system in the form of the first wave (Fig. 2a, point  $M_1$ ) but if the input intensity is slightly greater than the critical value, namely if  $I_{00} = I_M^{(0)} \approx I_{0M} [1 + 8 \exp(-L)]$ , then almost all the radia-

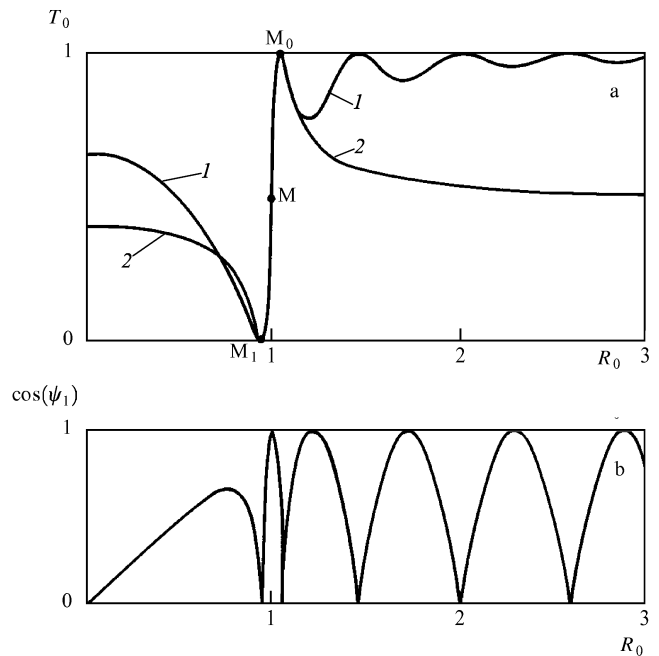


**Figure 2.** Dependences of  $T_0 = I_0/I_{00}$  (a) and  $\cos \psi_l$  (b) on  $R_0 \equiv I_{00}/I_{0M}$ , plotted on the assumption that  $L = 2\pi Kl/\lambda\beta = 1.6\pi$ : (1) exact solution (3.1.3); (2) approximation (3.1.8). In the self-switching region, curves 1 and 2 merge;  $\alpha = 0$ ,  $\theta_0 = \theta_1 = \theta$ .

tion leaves the system in the form of the zeroth wave (Fig. 2a, point  $M_0$ ). The change in the input intensity sufficient to switch completely the output radiation from one wave to the other,

$$\Delta I = I_M^{(0)} - I_M^{(1)} \approx 16I_{0M} \exp(-L) \ll I_{0M}, \quad (3.1.13)$$

is very small compared to  $I_{00}$ .

This abrupt switching of the radiation was called by us *radiation or light self-switching*, because it occurs as a result of a change in the input radiation intensity. The phenomenon of self-switching can be defined as a major change in the ratio of the wave intensities at the output of a system with UDCWs caused by a small change in the intensity of one of the input waves. Although in this section we shall concentrate on the simplest self-switching case where only one of the waves enters a system with identical UDCWs, this definition is valid also (as shown later) as a general definition of the phenomenon of radiation self-switching. It can also be called the *self-switching of unidirectional distributively coupled waves*.

We shall call the self-switching point  $M_j$  ( $j = 0$  or  $1$ ) the state of a system in which (under self-switching conditions) the intensity of the  $j$ th wave is maximal at the output ( $T_j = \text{max}$ ). In the case of identical UDCWs considered here, this state is reached when the input intensity is given by the set of expressions (3.1.11) when almost all the output radiation is concentrated in the  $j$ th wave ( $T_j \approx 1$ ).

For a given value of  $R_0$ , the point  $M_1$  corresponds to the parameter

$$L \approx \ln \left( \frac{16}{1 - R_0^2} \right) \approx \ln \left( \frac{8}{1 - R_0} \right), \quad (3.1.14)$$

and the point  $M_0$  corresponds to

$$L \approx \ln \left( \frac{16R_0^2}{R_0^2 - 1} \right) \approx \ln \left( \frac{8}{R_0 - 1} \right). \quad (3.1.15)$$

If  $I_{00} = I_M$  ( $r_1 = 0$ ), it follows from expression (3.1.8) that [34]

$$J_{jl} \approx \frac{R_0}{2} \left[ 1 + (-1)^j \frac{2 \exp(-L)}{1 + \exp(-2L)} \right], \quad (3.1.16)$$

i.e. the intensity of the zeroth wave is slightly higher and that of the first wave slightly lower than half the wave intensity at the input, but if  $\exp L \gg 1$ , the wave intensities become almost equal (Figs 2–4). More exactly, such equalisation occurs at the value [34]

$$I_{00} \approx I_{0M} [1 - 8 \exp(-2L)], \quad (3.1.17)$$

which is almost equal to  $I_{0M}$  for  $\exp L \gg 1$ .

For  $I_{00}$  so close to  $I_{0M}$  that [34]

$$\left[ \exp L \frac{r_1^2}{16} \right] \ll 1, \quad (3.1.18)$$

or, which is equivalent [34], if

$$\left[ \frac{I_{00} - I_{0M}}{I_{0M}} \right]^2 \ll 64 \exp(-2L), \quad (3.1.19)$$

we find from expression (2.1.16) that

$$I_{jl} \approx \frac{I_{00}}{2} \left[ 1 - (-1)^j \frac{1}{8} r_1^2 \exp L + 2(-1)^j \exp L \right]. \quad (3.1.20)$$

The slope or steepness of self-switching in the direct vicinity of  $I_{00}$  to  $I_{0M}$ , i.e. when condition (3.1.19) is obeyed, can be found from expression (3.1.9) or (3.1.10) in accordance with the formula given in Ref. [34]:

$$k_j = \frac{\partial I_{jl}}{\partial I_{00}} = \frac{\partial J_{jl}}{\partial R_0} \approx (-1)^j \frac{\exp L}{8}. \quad (3.1.21)$$

This reveals another interesting result. Near a certain value of the input intensity  $I_{00} = I_{0M}$  (called the critical or self-switching intensity) there is a linear section of the characteristic  $I_{jl}(I_{00})$  and the width of this section can be estimated from condition (3.1.19) and the slope is given by formula (3.1.21). The slope of this section can be very high ( $k \equiv |k_j| \gg 1$ ). In other words, if  $k \gg 1$ , a small change in the input power near the critical value produces a large ( $k$  times larger) change in the output power. This effect can be used to develop an optical small-signal amplifier or an optical transistor [32, 33] (Figs 5a–5c). This can be done if we inject, as one of the waves, radiation of constant intensity  $I_p \approx I_{0M}$  (which will be called the pump radiation) and at the same time (in this case in the form of the same wave) we also inject a weak alternating signal of intensity  $I_s$  (in the case under discussion the signal has the same frequency†), which is incoherent with the pump. The intensity (amplitude) of the signal lies within the limits of the linear section of the characteristic we are discussing here. The amplitude of the change in the power of each wave  $I_{jl}$  at the output will then be  $|k_s|$  greater than the amplitude of the signal power and the nature of the time dependence  $I_{jl}(t)$ , i.e. the profile of the amplified signal, will be the same as the profile of the initial signal, implying that the amplification will occur without distortions. The profile  $I_{0l}(t)$  repeats the profile of  $I_s(t)$  and  $I_{1l}(t)$  is an inverted image of  $I_s(t)$  (Fig. 5h).

Formula (3.1.21) thus defines the gain of an optical transistor and condition (3.1.19) determines the width of

the linear part of the transistor characteristic. The greater the number of times that energy is switched between the UCDWs in the length  $l$  of the investigated system under linear conditions, the more easy is the self-switching of the radiation in the nonlinear regime and the greater the optical transistor gain, which increases exponentially with increase in  $L$ . For example, if in the linear regime the switching occurs twice between the waves, we then have  $L = 2\pi$  and it follows from formula (3.1.21) that  $|k_s| \approx 67$ . If in the linear regime the switching between the waves occurs three times, i.e. if  $L = 3\pi$ , then  $|k_s| \approx 1550$ . Since in integrated optics we usually have  $K \sim 10^{-4} - 10^{-2}$ ,  $l \sim 0.1 - 1$  cm, and  $\lambda \sim 1 \mu\text{m}$ , it follows from formula (3.1.21) that the optical transistor gain can be very large.

We shall refer to the set of parameters of the system corresponding to the condition  $r_1 = 0$  and  $r = 1$  as the middle point M of radiation self-switching. In the present case this condition is equivalent to  $I_{00} = I_{0M}$  and the point M on the  $T_0(R_0)$  curve (see Figs 2a and 3) has the coordinates  $R_0 = 1$  and  $T_0 \approx 1/2$ ; at this point the slope of the curve is maximal. The index M is selected to denote the ‘middle’ point M and the intensity corresponding to M is the critical intensity  $I_M$  (Fig. 2). In the present case we have  $I_M = I_{0M} = 4K/|\theta|$  [34, 35]. In general,  $I_M$  may differ from the specific value  $I_{0M}$  (Section 3.3).

(3) In the range  $q^2 = r^{-2} = R_0^{-2} = I_M^2/I_{00}^2 \ll 1$  ( $q_1^2 \approx -r_1^2 \approx 1$ ) the elliptic functions can again be approximated by the trigonometric functions [121]. Substituting such approximations into expression (3.1.4), we obtain [34]:

$$T_1 \approx \frac{1}{4R_0^2} [\sin^2(LR_0) + R_0^{-2} \cos^2(LR_0)] \approx \frac{1}{4R_0^2} \sin^2(LR_0),$$

$$T_0 \approx 1 - \frac{1}{4R_0^2} \sin^2(LR_0). \quad (3.1.22)$$

The bulk of the radiation power is concentrated in the zeroth wave and it oscillates weakly with variation of  $LR_0$ . The period of the power oscillations along the  $L$  axis is  $2\pi/R_0$ , but along the  $R_0$  axis it is  $2\pi/L$ .

Evolution of the dependence  $T_0(R_0)$  as a result of changes in the parameter  $L$  is shown in Fig. 3 and

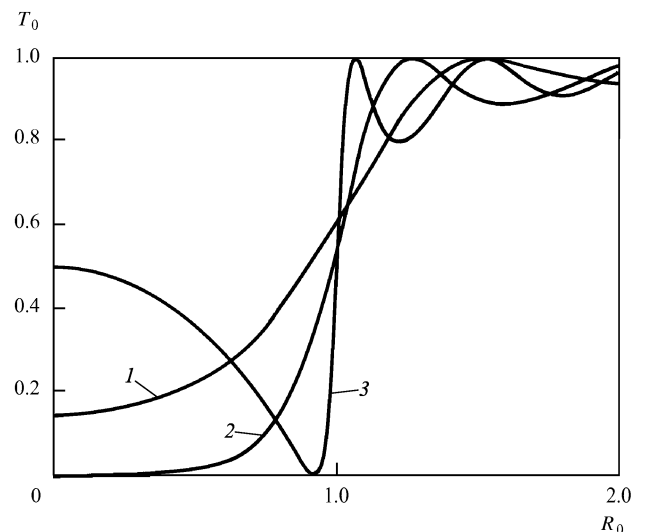


**Figure 3.** Evolution of the dependence of  $T_0$  on  $R_0$  as a result of changes in  $L$ : (1)  $L/\pi = 0.75$ , (2) 1, (3) 1.5;  $\alpha = 0$ ,  $\theta_0 = \theta_1 = \theta$ .

†The case when the signal frequency differs from the pump frequency is discussed in Section 5.

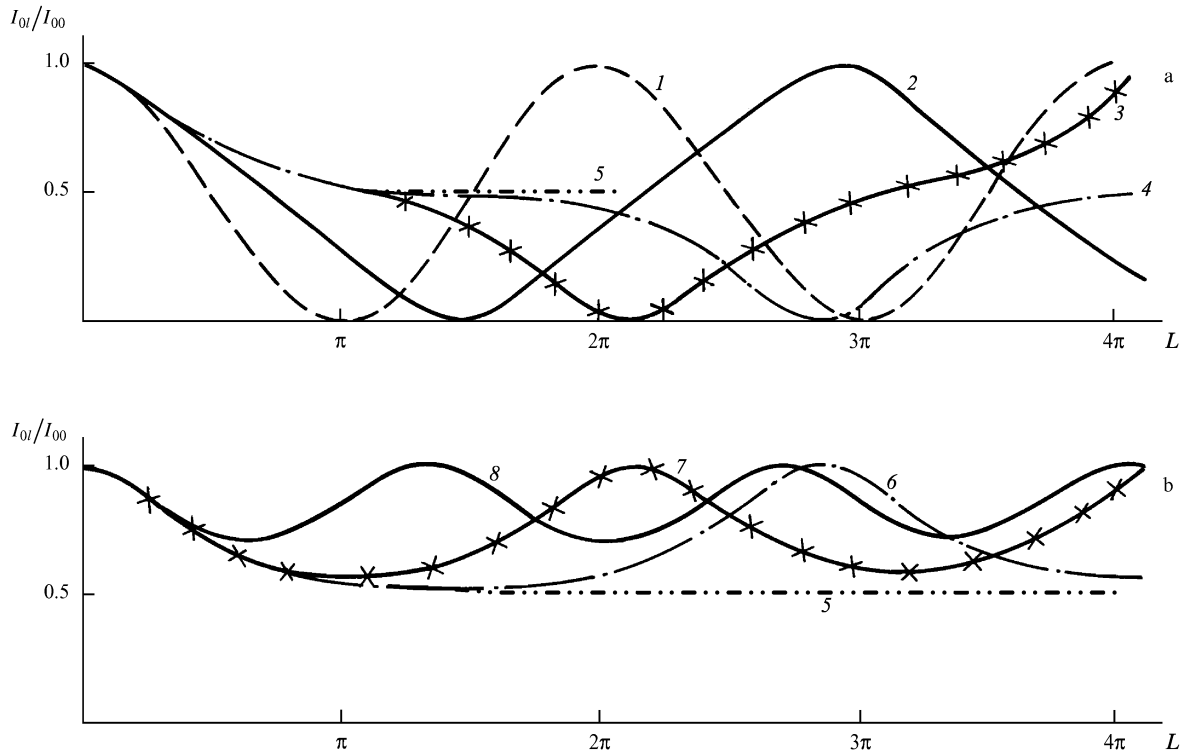


**Figure 4.** Dependences of  $T_0$  on  $L$  for  $R_0 \leq 1$  (a) and  $R_0 \geq 1$  (b): (1)  $R_0 = 0.1$ , (2) 0.9, (3) 0.99, (4) 0.999, (5) 1, (6) 1.001, (7) 1.01, (8) 1.1;  $\alpha = 0$ ,  $\theta_0 = \theta_1 = \theta$  (figure taken from Ref. [34]).

evolution of the dependence  $T_0(L)$  as a result of changes in the parameter  $R_0$  is demonstrated in Fig. 4. Analytic results and physical conclusions stated above are confirmed and illustrated by the results of a computer solution of the system of equations (2.5.3), presented in these two figures. It is interesting to see how the dependence  $T_0 = \sin^2(L/2)$ , well known from the linear theory [1–10], transforms as the parameter  $R_0^2 \equiv I_{0M}^2/I_{00}^2$  gradually increases from a value  $\ll 1$  to 1 and 4 (Fig. 4). In the limit  $I_{00} \rightarrow I_M$  ( $R_0 \rightarrow 1$ ), the effective length of the energy beats along the  $L$  axis tends to infinity and energy exchange between UDCWs ceases (line 5 in Fig. 4).

This radiation self-switching can also be used to limit the intensities of the pulses or to select pulses in accordance with their intensity [34]. For example, for  $L = 2\pi$ , a rectangular pulse with  $R_0 = 0.985$  appears at the output as the first wave and a pulse with  $R_0 = 1.015$  emerges as the zeroth wave [34].

We shall now consider a couple of examples of the realisation of self-switching.

*Example 1* (taken from Ref. [34]). Radiation enters one of the coupled strip waveguides, fabricated by a familiar method — of the kind described in Refs [1–10] — in a GaAs crystal for which we have the experimental value  $\theta \approx 2.3 \times 10^{-8}$  esu at  $\lambda = 1.06 \mu\text{m}$  [122]. Let us assume that  $l = 1$  cm,  $K = 5 \times 10^{-4}$ ,  $\beta = 3.5$ . In this case we have  $I_M = 4K|\theta| \approx 8.5 \times 10^4$  erg  $\text{cm}^{-3}$  and the pump wave intensity is  $\sim c\beta I_M/2\pi \approx 140$  MW  $\text{cm}^{-2}$ ; if the cross-sectional area of the waveguides is  $\sim 10^{-7}$   $\text{cm}^2$ , the pump power is  $P \approx 14$  W. The power gain of an optical transistor (Fig. 5a), given by expression (3.1.21) is then  $\partial I_{0l}/\partial I_{00} \approx 500$ ; according to condition (3.1.19), the relative width of the linear part of the characteristic is less than  $10^{-3}$

i.e. power differences (at the input of the zeroth waveguide) smaller than  $10^{-2}$  W can be amplified without distortion.

It is pointed out in Ref. [34] that in the case of InSb waveguides (with  $\theta$  approximately four orders of magnitude greater than for GaAs), the values of  $I_M$  and of the pump intensity can be considerably lower for the same value of  $|\partial I_{0l}/\partial I_{00}|$ . It was also mentioned in Ref. [34] that  $I_M$  can be reduced by several orders of magnitude if use is made of exciton resonances in III-V semiconductors (and, according to Ref. [123] there should be an increase in  $\theta$ ).

Attention was drawn in Ref. [36] that such self-switches can be made relatively readily from fibre waveguides. Their relatively weak nonlinearity may be compensated by a considerable length and also by a relatively low refractive index and selection of a short radiation wavelength  $\lambda \sim 0.5 \mu\text{m}$ . This can reduce  $K$  and thus the self-switching intensity  $I_M$  and yet retain a high gain in an optical transistor, because this gain is governed by the parameter  $L$ . Moreover, high-intensity radiation can be injected into an optical fibre and the maximum value of this intensity is usually limited by breakdown at the fibre end.

*Example 2* (taken from Ref. [36]). In this case light with  $\lambda = 0.53 \mu\text{m}$  is injected through the input of one of two tunnel-coupled optical waveguides which form a dual-core fibre. It is assumed that  $\theta \sim 10^{-12}$  esu,  $\beta = 1.46$ , and the distance in which light is transferred from one core to the other under linear conditions is  $l_b = 1$  m, i.e.  $K = \beta\lambda/2l_b \approx 3.6 \times 10^{-7}$ . In this case the critical intensity is  $c\beta I_M/2\pi \sim 10^9$  W  $\text{cm}^{-2}$  and for a core of cross-sectional area  $S \sim 10^{-7}$   $\text{cm}^2$ , the switching power is  $P_M \sim 100$  W. If the length of the tunnel-coupled waveguide system is  $l = 3l_b = 3$  m, the relevant parameter is  $L = 3\pi$  and an increase in the input power near the value of  $P_M$  by

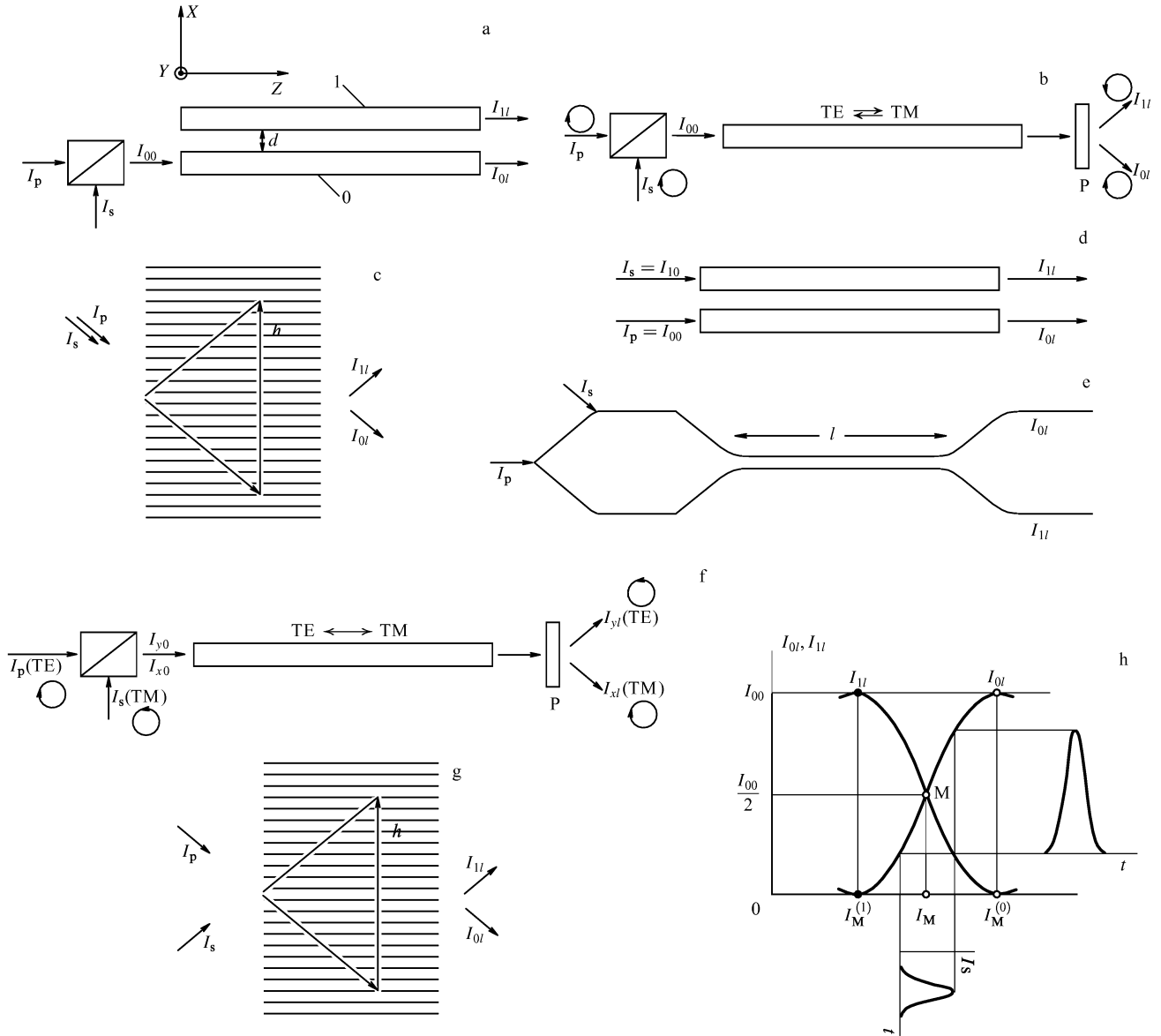


**Figure 5.** Examples of optical transistor, switch, and amplifier configurations based on nonlinear systems with UDCWs: (a, d, e) tunnel-coupled optical waveguides; (b, f) waveguides with UDCWs of different polarisations; (c, g) periodic structures; (h) operating principle of the configurations shown in Figs 5a–5c [36]. Here,  $I_p$  and  $I_s$  are the pump and signal intensities, such that

$I_p \gg I_s$  (the figure is taken from Refs [32, 33]). In the configurations a–d and g, and in the configuration f with the circular polarisations, the pump intensity is  $I_p \approx I_M$ , where  $I_M$  is the critical intensity; in the case of the configuration e, the pump intensity is  $I_p > I_M/2$ ; for the configuration f with the TE and TM polarisations and with  $K = 0$ , the pump intensity is  $I_p > 3|\alpha|/|\theta|$ .

$\delta P \sim 2S(I_M^{(0)} - I_M^{(1)}) \sim 16P_M \exp(-L) \sim 0.2 \text{ W}$  results in complete self-switching of light (from waveguide 1 to waveguide 0) at the output. Within the linear section of the characteristic ( $\delta P \leq 0.1 \text{ W}$ ) the gain, described by expression (3.1.21) is  $\partial I_0 / \partial I_{00} \approx 1600$ .

### 3.2 Self-phase-matching of waves

Let us see what happens to the phases of the waves in the course of their self-switching. Let us consider specifically the phases of UDCWs described by the system of equations (2.5.3), for example waves in TCOWs; the phases of other such waves are found by making the substitutions described by the set of expressions (2.5.2).

As in Section 2.1, we shall assume that UDCWs are identical ( $\alpha = 0$ ,  $\theta_0 = \theta_1 = \theta$ ). It follows from expres-

sion (2.5.9) that [34, 37]

$$\cos \psi = 2 \operatorname{sign} \theta \sqrt{J_0 J_1} = 2 \operatorname{sign} \theta \sqrt{(R_0 - J)J}. \quad (3.2.1)$$

Hence, we find directly that if  $R_0 > 1$  (i.e. if  $I_{00} > I_{0M}$ ), then

$$\begin{aligned} J_0 &> J_b = \frac{1}{2} \left( R_0 + \sqrt{R_0^2 - 1} \right), \\ J_1 &< J_c = \frac{1}{2} \left( R_0 - \sqrt{R_0^2 - 1} \right), \end{aligned} \quad (3.2.2)$$

i.e. if  $I_{00} > I_M$  there is a range of forbidden radiation intensities for each wave [34]!

Substitution of the solution described by expression (3.1.3) into expression (3.2.1) gives  $\cos\psi$  in a cross section of the system whose coordinate is  $z = l$  [37]:

$$\cos\psi_l = \text{sign}\theta r |\text{sn}(L, r)|. \quad (3.2.3)$$

If  $r = R_0 = q^{-1} > 1$ , i.e. if  $I_{00} > I_M$ , then formula (3.2.3) can be rewritten as follows [37]:

$$\cos\psi_l = \text{sign}\theta \left| \text{sn}\left(\frac{L}{q}, q\right) \right|. \quad (3.2.4)$$

Let us now analyse formulas (3.2.3) and (3.2.4).

(1) In the near-linear regime when  $r^2 = R_0^2 \ll 1$ , we find that

$$\begin{aligned} \cos\psi_l &\approx \text{sign}\theta r \left| \sin L - \frac{r^2}{4} \left[ L - \frac{\text{sign}(2L)}{2} \right] \cos L \right| \\ &\approx \text{sign}\theta r |\sin L|. \end{aligned} \quad (3.2.5)$$

In the purely linear case characterised by  $r = R_0 = 0$  we have  $\cos\psi_l = 0$  and  $\psi_l = \pi/2$ , i.e. the wave phases are shifted by  $\pi/2$ .

(2) In the radiation self-switching region ( $r = R_0 \approx 1$  and  $\exp L \gg 1$ ), if we adopt the approximation for the function  $\text{sn}(L, r)$ , derived in Appendix II and described by expression (II.3), we find that [37]

$$\cos\psi_l \approx \text{sign}\theta \frac{1 - (r_1^4/256) \exp(2L)}{1 + (r_1^4/256) \exp(2L)} \tanh L, \quad (3.2.6)$$

whereas in Section 3.1, we have  $r_1^2 \equiv 1 - R_0^2$ .

Approximations to formula (3.2.4) yield results which are almost fully identical with formula (3.2.6). In other words, the approximation represented by formula (3.2.6) is valid in the radiation self-switching region both for  $r = R_0 \leq 1$  (where  $r_1^2 = -q_1^2 = 1 - R_0^2 \geq 0$ ) as well as for  $r = R_0 \geq 1$  (where  $r_1^2 = -q_1^2 = 1 - R_0^2 \leq 0$ ).

In the immediate vicinity of the point M, where inequality (3.1.19) is obeyed, we obtain  $\cos\psi_l \approx \text{sign}\theta R_0 \tanh L$  and, sufficiently far from the input ( $\exp L \gg 1$ ,  $\tanh L \approx 1$ ), we have  $\cos\psi_l \approx R_0 \text{sign}\theta$ , i.e. if  $\theta > 0$  and  $I_{00} = I_M$  the zeroth and first waves are in phase (Fig. 2b)!

As pointed out earlier, we are speaking here of the phases of the waves described by the system of equations (2.5.3). In the case of the waves described by the system (2.5.1), the phases are found by the simple substitution described by the set of expressions (2.5.2). Thus, for identical UDCWs and the Bragg diffraction in an isotropic periodic structure we have  $\theta_j = \theta$ ,  $\theta_{01} = \theta_{10} = 2\theta$ ; therefore, we have  $\tilde{\theta}_0 = \theta_0 - \theta_{01} = -\theta$ ,  $\tilde{\theta}_1 = \theta_1 - \theta_{10} = -\theta$  and, if  $\theta > 0$ , we obtain  $\cos\psi_l = -1$ ,  $\psi = \pi$ , i.e. the waves at the middle point M are in antiphase. In any case, we can speak here of automatic phase matching at some specific input intensity equal to the critical value.

This automatic phase matching of the waves at the middle point M (Fig. 2b) will be called self-phase-matching [37]. It should be stressed that self-phase-matching of waves occurs already at a very short distance beyond the input (where  $\exp L \gg 1$ ) and continues over the rest of the length of the system. At the middle point M the sign of  $M \sin\psi_l$  is reversed. At distances from the input much less than the linear transfer length ( $L \ll 1$ ,  $\tanh L \ll 1$ ) it follows from formula (3.2.6) that the phases of the waves not yet equalised become opposite even for  $I_{00} = I_M$  ( $R_0 = 1$ ) and we have  $\cos\psi_l \approx 0$ . If  $0 \leq (r_1^4/256) \exp 2L \leq 1$ , then an

increase in the deviation of  $I_{00}$  from  $I_M$  (for a fixed value of  $L$ ) or with increase in  $L$  (for a fixed  $R_0$ ), we find that  $|\cos\psi_l|$  decreases from  $R_0$  to zero. The values  $R_0$  and  $L$  at which we have  $\cos\psi_l = 0$  can be found from expression (3.1.11) and they correspond to the self-switching points  $M_j$ .

It follows from formula (3.2.6) that as  $I_{00}$  approaches  $I_M$  (i.e. on approach to the middle point M), there is an increase in the length of the part of the system where the phases of the waves are matched and where the degree of their matching increases.

(3) At high intensities ( $q^2 = R_0^{-2} \ll 1$ ), we find from formula (3.2.4) that [37]

$$\begin{aligned} \cos\psi_l &\approx \text{sign}\theta \left| \sin(LR_0) - \frac{1}{4R_0^2} \left[ LR_0 - \frac{\sin(2LR_0)}{2} \right] \cos(LR_0) \right| \\ &\approx \text{sign}\theta |\sin(LR_0)|. \end{aligned} \quad (3.2.7)$$

The cosine of the phase difference oscillates along the  $L$  axis with a period  $\pi I_M/I_{00}$  and along the  $R_0$  axis with a period  $\pi/L$ , and also along the coordinate  $z$  of the system with a period  $2\beta\lambda/|\theta|I_{00}$ . The zeroth and first waves are in phase (for  $\theta > 0$ ) or in antiphase (for  $\theta < 0$ ) only over short parts of the system near the values  $z = l = (2m+1)\beta\lambda/|\theta|I_{00}$ ,  $m = 0, 1, 2, \dots$

Fig. 2b shows the dependence of the cosine of the difference between the wave phases on  $R_0$  for  $L = 1.6\pi$ . This dependence for other parameters  $L$  and also the dependence of  $\cos\psi_l$  on  $L$  for different  $R_0$  are all given in Ref. [37].

The results of this section supplement those given in Section 3.1. We can see that the radiation self-switching effect is related organically to self-phase-matching of the waves and to an abrupt change in the wave phases from zero to  $\pi/2$  (or from  $\pi$  to  $\pi/2$ ) as a result of a small change in the input intensity near its critical value.

### 3.3 Optical self-switching in a system with nonidentical unidirectional distributively coupled waves

We shall now consider the case of nonidentical UDCWs:  $\alpha \neq 0$ ,  $\theta_0 \neq \theta_1$ . We shall assume, as before, that radiation is coupled into the system in the form of just one wave:  $R_0 \neq 0$ ,  $R_1 = 0$ . Then, one of the roots of Eqn (2.5.14) is  $J_d = 0$  and the solution is [41]

$$J_{1l} = J_a \frac{1 - \text{cn}(s, r)}{(p/q + 1) + (p/q - 1) \text{cn}(s, r)}, \quad J_{0l} = R_0 - J_{1l}, \quad (3.3.1)$$

where  $s = 2L\sqrt{pq}$ ,  $p^2 = (J_a - J_b)(J_a - J_c)$ ,  $q^2 = J_b J_c$ ,  $r^2 = [J_a^2 - (p - q)^2]/(4pq)$ ,  $r_1^2 = 1 - r^2 = [(p + q)^2 - J_a^2]/(4pq)$ . We can easily show that  $p^2 > 0$ ,  $q^2 > 0$ .

It follows from the solution described by expression (3.3.1) that the maximum value of  $J_{1l}$  is  $J_{1l} = J_a \leq R_0$ . In other words, if  $J_a < R_0$ , energy is not transferred completely from the zeroth to the first wave and the ratio  $J_a/R_0 = (\Delta T)_{\max}$  determines the depth of possible energy transfer of the self-switching. This depth of transfer in self-switching is understood to be the difference between the maximum and minimum values of  $T_j$ :  $(\Delta T)_{\max} \equiv T_{j,\max} - T_{j,\min}$ ;  $0 \leq (\Delta T)_{\max} \leq 1$ .

**3.3.1 Complete transfer and complete self-switching.** It really follows from expression (3.3.1) that if

$$\alpha = \frac{\theta_0 - \theta_1}{4\beta} I_{00} \equiv \alpha_0, \quad (3.3.2)$$

then  $\Delta = 0$ ,  $I_a = I_{00}$ ,  $(\Delta T)_{\max} = 1$ , i.e. complete transfer of energy from the zeroth to the first wave is possible [41]. In this case we have  $p = q = \frac{1}{2}$  and  $I_M = I_{0M} = 8K/|\theta_0 + \theta_1|$ ; expression (3.3.1) then reduces to the solution described by expression (3.1.3) obtained for identical UDCWs. Consequently, in this case we can use the results of an analysis given in Section 3.1 and in Ref. [34], i.e. we can use formulas (3.1.11) and (3.1.21) if we bear in mind that the value of the critical intensity  $I_M$  now generally differs from the value  $I_{0M} = 4K/|\theta|$  which applies in the case of identical UDCWs.

**3.3.2 Incomplete self-switching when  $\alpha = \alpha_0 + \Delta\alpha$ .** A deviation of  $\alpha$  from  $\alpha_0$  should obviously reduce the value of  $I_a$  and, consequently, the self-switching depth (Fig. 6). If  $\Delta\alpha$  is small ( $|\Delta\alpha| \ll K$ ), then [41]

$$(\Delta T)_{\max} \approx 1 - (\Delta\xi)^2 + 4(\Delta\xi)^3, \quad (3.3.3)$$

where  $\Delta\xi = (\Delta\alpha) \text{sign}(\theta_0 + \theta_1)\beta/K$ . Therefore, in the first approximation in  $\Delta\alpha/K$ , the self-switching remains complete (Fig. 6a) and the solution described by expression (3.3.1) becomes [41]

$$I_{jl} \approx \frac{I_{00}}{2} [1 + (-1)^j \text{cn}(s, r)] + (-1)^j \frac{I_{00}^2}{2I_M} (\Delta\xi) \text{sn}^2(s, r), \quad (3.3.4)$$

where  $r \approx R_0[1 - R_0(\Delta\xi)]$ ,  $s \approx L[1 + R_0(\Delta\xi)]$  and, as usual,  $j = 0$  or  $1$ .

The self-switching or critical intensity  $I_M$  (corresponding to the middle point M), is defined, in accordance with Ref. [41] and Section 3.1, on the basis of the condition  $r = 1$ :

$$I_M \approx I_{0M}(1 + \Delta\xi), \quad (3.3.5)$$

where  $I_{0M} \equiv I_M(\alpha = 0) = 8K/|\theta_0 + \theta_1|$ .

If  $\exp L \approx \exp s \gg 1$ , then for

$$I_{00} = I_M^{(j)} \approx I_{0M} \{1 + (-1)^j 8 \exp[-L(1 + \Delta\xi)] + \Delta\xi\} \quad (3.3.6)$$

the output radiation is concentrated entirely in the  $j$ th wave [41], represented by points  $M_j$  of the system, in accordance with expression (3.1.11). We can see that characteristic switching self-switching points M and  $M_j$  may shift, depending on the sign of  $\Delta\xi$ , to the right or left relative to the points corresponding to the case when  $\alpha = \alpha_0$  (Fig. 6).

At the middle point M (i.e. when  $I_{00} = I_M$ ), we have [41]

$$\frac{\partial I_{jl}}{\partial I_{00}} \approx (-1)^j \frac{1 - \Delta\xi}{8} \exp[L(1 + \Delta\xi)], \quad (3.3.7)$$

$$I_{jl} \approx \frac{I_{00}}{2} [1 + (-1)^j (\Delta\xi)]. \quad (3.3.8)$$

It is evident from expression (3.3.7) that the gain of an optical transistor depends on  $\Delta\xi$ : it increases for  $\Delta\xi > 0$  and decreases for  $\Delta\xi < 0$  (see Fig. 6). The changes in the gain can be very considerable. For example, doubling of the gain corresponds to  $\Delta\xi = \ln 2/(1 + L)$ .

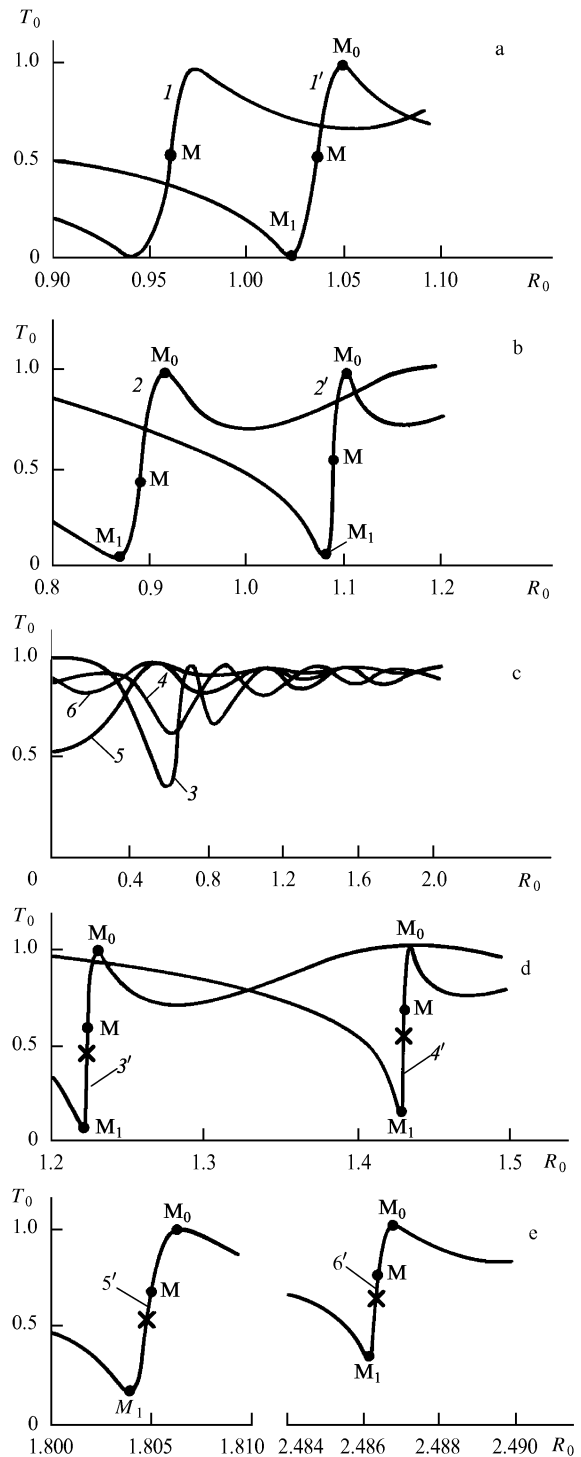


**Figure 6.** Dependences of  $T_0 = I_{0l}/I_{00}$  on the normalised input intensity  $R_0 = |\theta|I_{00}/4K$  of the zeroth wave, plotted for  $\theta_0 = \theta_1 = \theta$ ,  $L = 2\pi Kl/\lambda\beta = 2\pi$ , and the following values of  $\xi$ : (1)  $-0.04$ , (1')  $0.04$ , (2)  $-0.1$ , (2')  $0.1$ , (3)  $-0.25$ , (3')  $0.25$ , (4)  $-0.5$ , (4')  $0.5$ , (5)  $-1$ , (5')  $1$ , (6)  $-2$ , (6')  $2$ . The middle self-switching points are labelled M and the crosses are used to identify the points with the maximum slope (figure taken from Ref. [41]).

**3.3.3 Equal nonlinear coefficients.** When the nonlinear coefficients are equal ( $\theta_0 = \theta_1 = \theta$ ,  $\alpha \neq 0$ ) we have  $\alpha_0 = 0$ ,  $\Delta\alpha = \alpha$  and  $\Delta\xi = \xi \equiv (\alpha\beta/K) \text{sign} \theta$ . This important and most frequent case is realised, for example, in the case of tunnel-coupled optical waveguides made of the

same material in which the mismatch is due to the different waveguide thicknesses. Then,  $|\theta_1 - \theta_0|I_{00} \sim \alpha\theta_j I_{00}$  is a quantity of the second order of smallness and can be ignored, since in the derivation of the system of equations (2.5.3) only quantities of the order of  $K$ ,  $\alpha$ , and  $\theta_j I_{00}$  (i.e. of the first order of smallness) are included.

**3.3.4 Complete self-switching when  $\alpha = \alpha_M$ .** Relationship (3.3.2) implies that for each instantaneous value of the total intensity  $I_{00}$  there is a corresponding value  $\alpha = \alpha_0$ . This requirement is difficult to satisfy, but — in principle — this is possible. In the case of tunnel-coupled optical waveguides made of electro-optical materials it is necessary to apply an electric voltage proportional to  $I_{00}$  selected in such a way as to satisfy relationship (3.3.2). True, we can no longer speak of self-switching of the radiation, because in this case there is a contribution of the electro-optical effect.

The case when  $\alpha$  is fixed is of greater practical interest. The condition for radiation self-switching is  $I_{00} = I_{0M}$ . Therefore, complete self-switching can occur at a fixed value of  $\alpha$ , selected in advance, if this parameter is [41]

$$\alpha_M = \frac{\theta_0 - \theta_1}{4\beta} I_{0M} = \frac{2K(\theta_0 - \theta_1)}{\beta|\theta_0 + \theta_1|}. \quad (3.3.9)$$

The parameter  $\xi$  then becomes

$$\xi_M = 2 \frac{\theta_0 - \theta_1}{\theta_0 + \theta_1}. \quad (3.3.10)$$

If  $\xi = \xi_M$  is selected, then complete radiation self-switching, corresponding to  $(\Delta T)_{\max} \approx 1$ , can be expected (Fig. 7a) when  $I_{00}$  is varied near the critical value  $I_{0M}$ , which is true even in the case of nonidentical tunnel-coupled optical waveguides or a system with other nonidentical UDCWs! Therefore, we shall call  $I_{0M}$  the ‘critical complete self-switching intensity’ or simply the ‘complete self-switching intensity’ [41].

However, selection of  $\alpha = \alpha_M$  leads to a deviation of the solution from the form given by expression (3.1.3), which is valid only if  $\alpha = \alpha_0$  and, in spite of proximity of the values of  $I_{0M}$  and  $I_{00}$  (and, consequently, of  $\alpha_M$  and  $\alpha_0$ ), the nature of self-switching may change considerably compared with the case when  $\alpha = \alpha_0$ . The slope and direction (sign) of such complete self-switching is given by a formula taken from Ref. [41]:

$$\frac{\partial I_{jl}}{\partial I_{00}} \approx (-1)^j \frac{3\theta_0 - \theta_1}{\theta_0 + \theta_1} \frac{\exp L}{8}, \quad (3.3.11)$$

and if

$$R_M^{(j)} \approx 1 + (-1)^j 8 \frac{\theta_0 + \theta_1}{3\theta_0 - \theta_1} \exp L, \quad (3.3.12)$$

the radiation emerges from the system entirely in the form of the  $j$ th wave (corresponding to the points  $M_j$ ).

It follows from formulas (3.3.11) and (3.3.12) that if  $(3\theta_0 - \theta_1)/(\theta_0 + \theta_1) > 0$ , an increase in  $I_{00}$  near the value  $I_{0M}$  switches the radiation at the output from the first to the zeroth wave, but if  $(3\theta_0 - \theta_1)/(\theta_0 + \theta_1) < 0$ , the switching is in the opposite direction. The slope of the characteristic described by expression (3.3.11) depends on the relationship between  $\theta_0$  and  $\theta_1$ . For example, if  $\theta_0 = \theta \neq 0$ ,  $\theta_1 = 0$ , the slope is three times as high as for the case of identical UDCWs ( $\theta_0 = \theta_1 = \theta$ ) with the same value of  $L$ , and if  $\theta_0 = 0$ ,  $\theta_1 = \theta \neq 0$ , it has exactly the same absolute value as in the case when  $\theta_0 = \theta_1 = \theta$ , but the sign is now opposite

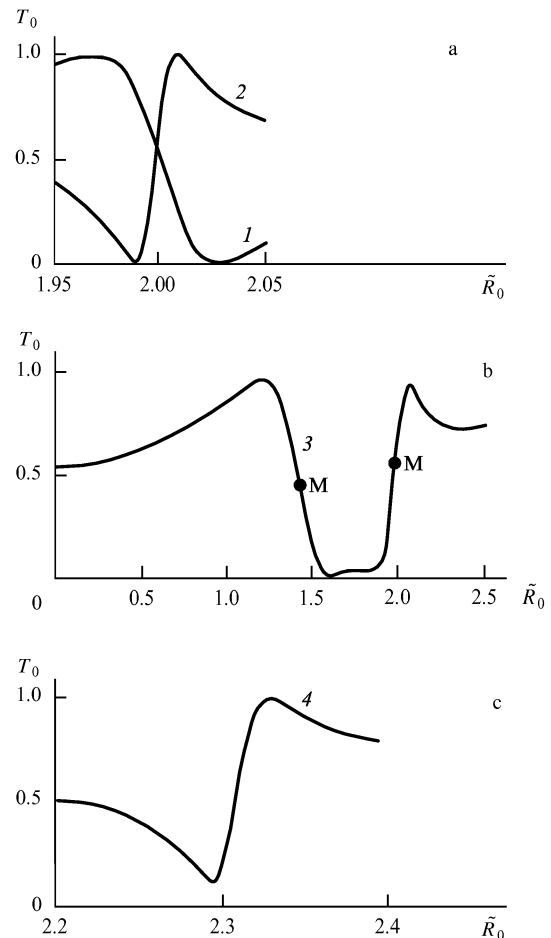


**Figure 7.** Dependences of  $T_0$  on  $\tilde{R}_0 \equiv \theta_{\max} I_{00}/4K$ , plotted for  $\theta_0 \neq \theta_1$  and  $L = 2\pi$ : (1)  $\theta_0 = 0$ ,  $\theta_1 = \theta \neq 0$  ( $\theta_{dn} = 0.5$ ),  $\xi = \xi_M = -2$ ; (2)  $\theta_0 = \theta \neq 0$ ,  $\theta_1 = 0$  ( $\theta_{dn} = -0.5$ ),  $\xi = \xi_M = 2$ ; (3)  $\theta_0 = 0.3\theta_1$  ( $\theta_{dn} = 0.35$ ),  $\Delta\xi = 0.01$ ; (4)  $\theta_0 = \theta_1/3$  ( $\theta_{dn} = 1/3$ ),  $\Delta\xi = 0.1$ . Here,  $\theta_{dn} \equiv (\theta_1 - \theta_0) \text{sign}(\theta_0 + \theta_1)/2\theta_{\max}$  is the normalised difference between the nonlinear coefficients;  $\theta_{\max} \equiv \max(|\theta_0|, |\theta_1|)$  (figure taken from Ref. [41]).

(Fig. 7a). If  $\theta_1 = 3\theta_0$  and  $\alpha = \alpha_M$ , self-switching does not occur;  $\partial I_{jl}/\partial I_{00} = 0$  and the points  $R_{0M}^{(j)}$  move away from unity to infinity.

**3.3.5 Incomplete self-switching when  $\alpha = \alpha_M + \Delta\alpha$ .** In practice, in view of the technological difficulties encountered in the fabrication of tunnel-coupled optical waveguides and of other systems in which UDCWs are used, it is unavoidable that there may be a deviation (though small) of the value of  $\alpha$  from  $\alpha_M$ , which reduces the self-switching depth (Fig. 7c) [41]:

$$(\Delta T)_{\max} \equiv \frac{I_a}{I_M} \approx 1 - \left( \frac{\theta_0 + \theta_1}{3\theta_0 - \theta_1} \right)^2 (\Delta\xi)^2 \times \left[ 1 - 2 \frac{(5\theta_0 - \theta_1)(\theta_0 + \theta_1)}{(3\theta_0 - \theta_1)^2} (\Delta\xi) \right], \quad (3.3.13)$$

where  $\Delta\xi = (\Delta\alpha)\beta \text{sign}(\theta_0 + \theta_1)/K = \xi - \xi_M$ ,  $\Delta\alpha = \alpha - \alpha_M$ ,  $|\Delta\xi| \ll 1$ . If  $(5\theta_0 - \theta_1)\Delta\alpha > 0$ , then an increase in  $|\Delta\alpha|$  reduces the self-switching depth much more than for  $(5\theta_0 - \theta_1)\Delta\alpha < 0$ . If  $\theta_0 = \theta_1$ , expression (3.3.13) reduces to expression (3.3.3).

The self-switching slope corresponding to  $\alpha = \alpha_M + \Delta\alpha$  is [41]

$$\frac{\partial I_{jl}}{\partial I_{00}} \approx (-1)^j \left[ \frac{3\theta_0 - \theta_1}{\theta_0 + \theta_1} - \frac{7\theta_0 - 5\theta_1}{3\theta_0 - \theta_1} (\Delta\xi) \right] \frac{\exp s}{8}, \quad (3.3.14)$$

where

$$s \approx L \left( 1 + \frac{\theta_0 + \theta_1}{3\theta_0 - \theta_1} \Delta\xi \right).$$

If  $\theta_0 = \theta_1$ , expression (3.3.14) reduces to expression (3.3.7).

The shift of the points M, M<sub>0</sub>, and M<sub>1</sub> along the R<sub>0</sub> axis, due to the mismatch  $\Delta\xi$ , is described by formulas given in Ref. [41].

At the moment of radiation self-switching ( $I_{00} = I_M$ ), it follows from expression (3.3.1) that

$$J_{II} \approx J_b - 2 \exp(-s)(J_a - 3J_b) \approx J_b \leq \frac{R_0}{2} = \frac{1}{2}, \quad (3.3.15)$$

and the equality sign in the above expression is satisfied in the case of complete self-switching ( $\Delta\xi = 0$ ,  $I_M = I_{0M}$ ), and at the moment of partial self-switching ( $\Delta\xi \neq 0$ ,  $J_b < R_0/2$ ) less than half of the input radiation is switched to the first wave.

### 3.3.6 Self-switching in the case of arbitrary values of $\alpha$ and $\theta_d$ .

For arbitrary values of  $\alpha$  and  $\theta_d$ , the critical value of R<sub>0</sub> can be found from the condition  $0 < J_b = J_c < J_a$  (which is equivalent to the condition  $r = 1$ ). This condition means that if  $J = J_b = J_c$ , then the  $f(J)$  curve touches the abscissa, i.e. we have simultaneously both  $f(J_b) = 0$ , in accordance with expression (2.5.14), and  $f'(J_b) = 0$ ; eliminating  $J_b$ , we obtain the following equation:

$$R_M^2 - 1 + 2\Delta R_M(4R_M^2 - 5) - 2\Delta^2(6R_M^2 + 1) + 6\Delta^3 R_M - \Delta^4 = 0, \quad (3.3.16)$$

which gives the exact value  $R_0 = R_M \equiv I_M/I_{0M}$  at the point M (only the values characterised by  $0 < J_b < J_a$  are physically meaningful). At low values of  $|\Delta|$ , Eqn (3.3.16) reduces to Eqn (3.3.5).

At the point M the value of T<sub>0</sub> is governed by the root J<sub>b</sub>:

$$T_{0M} \approx 1 - \frac{J_b}{R_M} = 1 + \frac{\Delta^3 - 6\Delta^2 R_M + \Delta(12R_M^2 + 1) - R_M(8R_M^2 - 7)}{(\Delta^2 - 2\Delta R_M + 4R_M^2 - 3)2R_M}. \quad (3.3.17)$$

The self-switching depth is described by

$$(\Delta T)_{\max} = \frac{1}{4J_b^2} = \left[ \frac{\Delta^2 - 2\Delta R_M + 4R_M^2 - 3}{\Delta^3 - 6\Delta^2 R_M + \Delta(12R_M^2 + 1) - R_M(8R_M^2 - 7)} \right]^2, \quad (3.3.18)$$

where R<sub>M</sub> is found from Eqn (3.3.16).

Eqns (3.3.16) and (3.3.18) provide useful information on I<sub>M</sub> and on  $(\Delta T)_{\max}$ , presented in Fig. 8.

If  $\theta_{dn} = \frac{1}{3} [\theta_{dn} \equiv (\theta_1 - \theta_0) \text{sign}(\theta_0 + \theta_1)]/2\theta_{\max}$ , where  $\theta_{\max} \equiv \max(|\theta_0|, |\theta_1|)$ , the tangent to the I<sub>M</sub>( $\xi$ ) curve is vertical at the point of complete self-switching. If  $\theta_{dn} > \frac{1}{3}$ , there is a range of values of  $\xi$  where one value of  $\xi$  corresponds to two values of I<sub>M</sub> and  $(\Delta T)_{\max}$ , i.e. there are two values of the total intensity (Fig. 8) near which we can expect radiation self-switching. Therefore, if  $\theta_{dn} > \frac{1}{3}$ , then

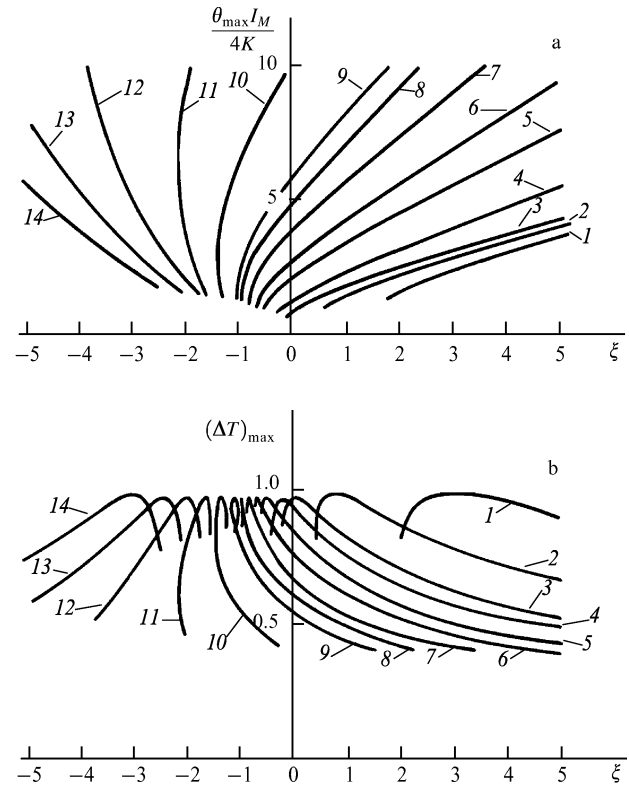


**Figure 8.** Normalised intensity  $\theta_{\max} I_M/4K$  (a) and depth  $(\Delta T)_{\max}$  (b) of radiation self-switching, plotted as a function of  $\xi$  for different values of  $\theta_{dn}$ : (1) -0.6, (2) -0.3, (3) 0, (4) 0.1, (5) 0.2, (6) 0.25, (7) 0.3, (8) 1/3, (9) 0.35, (10) 0.4, (11) 0.45, (12) 0.5, (13) 0.55, (14) 0.6 (figure taken from Ref. [41]).

for specific values of  $\alpha$  and  $K$  we can speak of *double radiation self-switching* (Fig. 7b). The depths of self-switching events are usually different, but in the range  $\theta_{dn} \geq \frac{1}{3}$  (for example, if  $\theta_{dn} = 0.35$ ) the  $(\Delta T)_{\max}(\xi)$  curve in Fig. 8 intersects itself. This means that both self-switching depths are the same (Fig. 7b).

Eqns (3.3.16)–(3.3.18) give  $R_M$ ,  $T_{0M}$ , and  $(\Delta T)_{\max}$  even for large values of  $|\Delta|$  and  $|\xi|$ . For example, if  $\theta_d = 0$ ,  $\Delta = \xi = 1$ , we readily find  $R_M = 1.8054$ ,  $T_{0M} = 0.6983$ , and  $(\Delta T)_{\max} = 0.8427$  (Fig. 6e); if  $\Delta = \xi = 2$ , we find that  $R_M = 2.4864$ ,  $T_{0M} = 0.7634$ , and  $(\Delta T)_{\max} = 0.7225$ . For  $\Delta = \xi < -0.1909$ , there is no  $R_M$ .

At high values of  $\xi$  the point M (Figs 6d and 6e) lies above the point identified by a cross ( $\times$ ), where the slope has its maximum. At the point M (i.e. for  $R_0 = R_M$  and  $T_0 = T_{0M}$ ), we have  $\cos \psi_l = 1$  and the sign of  $\sin \psi_l$  is reversed as a result of variation of R<sub>0</sub> [41], i.e. the process is similar to self-phase-matching of identical UDCWs (Section 3.2).

The results of numerical solutions of the system of equations (2.5.3) [41] are in agreement with formulas (3.3.3)–(3.3.18) and are illustrated in Figs 6 and 7. In the case of low values of  $|\xi|$  we indeed observe an almost complete transfer of energy from one wave to another, but at high values of  $|\xi|$ , as demonstrated by the general solution described by expression (3.3.1) the transfer of energy is incomplete. However, for negative values of  $\xi$  and for  $|\xi| \approx 1$  (Fig. 6c) the transferred power does not reach even half of the input power, but for positive values of  $\xi$  (Figs 6d and 6e) up to  $\xi = 1$  we can still speak of

radiation self-switching. For example, if  $\xi = 1$ , then  $\sim 84\%$  of the input power is transferred to the first wave. It should be stressed that an increase in  $\xi$  increases considerably the gain. On the other hand, in the case of identical UDCWs ( $\xi = 0$ ) when  $L = 2\pi$  at the point M we have, in accordance with expression (3.1.21), the slope  $\partial I_{0l}/\partial I_{00} \approx 67$ ; for non-identical UDCWs if  $\xi = 1$  and the value of  $L$  is as before, the maximum slope is  $\partial I_{0l}/\partial I_{00} \approx 1136$ . It follows that the selection of  $\xi = 1$  increases the slope by more than one order of magnitude and at the same time increases the critical intensity by 80% and reduces the switching depth by 16% (curve 5' in Fig. 6e).

Fig. 7a illustrates formulas (3.3.11) and (3.3.12); if  $\theta_0 = 0$ ,  $\theta_1 \neq 0$  an increase in  $I_{00}$  near  $I_{0M}$  switches completely the radiation at the output, and not from the first to the zeroth wave (as in the case of identical UDCWs) but vice versa.

Fig. 7b demonstrates double self-switching. The first occurs at  $I_M \approx 5.6K/\theta_{\max}$  and its slope is in agreement with formula (3.3.16). The second self-switching occurs at  $I_M \approx 7.9K/\theta_{\max}$  and it is much steeper than the first. When  $I_{00}$  is increased, the first self-switching takes place from the zeroth to the first wave and the second in the opposite direction.

Fig. 7c shows that radiation self-switching occurs also for  $\theta_0 = \theta_1/3$ , but only if  $(\Delta\xi) \neq 0$  [41].

It follows that nonidentity of tunnel-coupled optical waveguides may not only reduce the self-switching slope and thus reduce also the critical intensity, but it can also increase considerably (by one or two orders of magnitude) the self-switching slope and at the same time increase, but to a much lesser degree, the value of  $I_M$ . This nonidentity reduces also the self-switching depth, but this can be seen only in the second approximation. The influence of the sign of  $\Delta\xi$  on the self-switching slope appears already in the first order in  $\Delta\xi$ , but the self-switching depth is affected by this sign only in the third order in  $\Delta\xi$ .

It is known (Fig. 1) that complete energy exchange is not possible for nonidentical waves in the linear regime. However, in the nonlinear regime, complete radiation self-switching is possible even if the refractive indices of the waves are far from identical. It appears when condition (3.3.9) is satisfied: the meaning of this condition is that the nonidentity of the refractive indices is compensated by the nonidentity of the nonlinear coefficients. The slope and direction of such complete self-switching are given by formula (3.3.11).

Double radiation self-switching can occur for certain values of the parameters, i.e. switching may be observed near two values of the input intensity, each a critical value.

Trillo and Wabnitz published a paper [80] on the same subject, soon after Ref. [41], but they did not investigate analytically the solution described by expression (3.3.1).

Double radiation self-switching is possible not only in the case of nonidentical but also in the case of identical tunnel-coupled optical waveguides if two waves are injected (Sections 3.4 and 4.3) or even if one wave is injected, provided the nonlinearity saturation is considerable [98].

### 3.4 Influence of optical losses on optical self-switching

It is desirable to consider the influence of the optical losses on radiation self-switching because many systems with UDCWs not based on optical fibres may suffer from considerable losses. For example, in the case of GaAs tunnel-coupled optical waveguides the losses are usually up

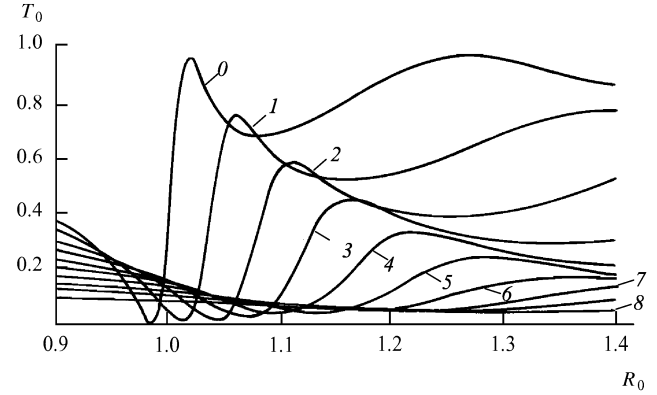


**Figure 9.** Radiation self-switching effect plotted for different losses in the distance equal to the coupling length  $l$  of UDCWs; the  $n$ th curve corresponds to the losses amounting to  $n$  dB;  $L = 2\pi$ ;  $\alpha = 0$ ;  $\theta_0 = \theta_1 = \theta$  (figure taken from Ref. [42]).

to  $5 \text{ dB cm}^{-1}$  [3–5]. Moreover, it is important to take the optical losses into account also because it is then possible to estimate, in the first approximation, the influence of secondary nonlinear effects (such as stimulated Raman scattering, stimulated Brillouin scattering, and generation of the second and higher harmonics) on radiation self-switching.

When the losses are taken into account, the system of equations (2.5.3) corrected for the losses becomes [42]

$$\begin{cases} i\beta \frac{\lambda}{\pi} \frac{dA_0}{dz} + KA_1 \exp\left(-\frac{i\alpha 2\pi z}{\lambda}\right) + i \frac{\lambda}{\pi} \beta \delta'_0 A_0 = -\theta_0 |A_0|^2 A_0, \\ i\beta \frac{\lambda}{\pi} \frac{dA_1}{dz} + KA_0 \exp\left(\frac{i\alpha 2\pi z}{\lambda}\right) + i \frac{\lambda}{\pi} \beta \delta'_1 A_1 = -\theta_1 |A_1|^2 A_1, \end{cases} \quad (3.4.1)$$

where  $\delta'_j$  is the loss factor.

The system of equations (3.4.1) can only be solved numerically. The results of numerical experiments carried out for a system with identical UDCWs ( $\alpha = 0$ ,  $\theta_0 = \theta_1 = \theta$ ,  $\delta'_0 = \delta'_1 = \delta$ ) when only one wave ( $R_1 = 0$ ) is injected into the system demonstrate (Fig. 9) that the losses of 1–5 dB in a distance equal to the wave coupling length  $l$  do not destroy radiation self-switching, although they weaken this effect: the self-switching depth and slope decrease. The larger the parameter  $L$ , the higher the level of losses at which radiation self-switching is still possible.

### 3.5 Influence of the phase of a signal on its amplification

If a signal and a pump, coherent with the signal, are applied to the input of one (for example, zeroth) tunnel-coupled optical waveguide or, more exactly, if a signal and a pump reach the input of a mixer in front of the waveguide, then the two waves interfere before entering the waveguide. Let the signal amplitude at the input to the mixer be  $A_{s0} = \sqrt{I_{s0}} \exp(i\varphi_{s0})$  and the pump amplitude be  $A_{p0} = \sqrt{I_{p0}} \exp(i\varphi_{p0})$ . Let us also assume that  $I_{p0} \approx I_M$  and that the power transfer coefficients of the mixer are  $T$  and  $R$  for the pump and signal, respectively [33]. Then the intensity at the mixer output of the radiation entering the zeroth waveguide is  $I_{00} = RI_{s0} + TI_{p0} + 2\sqrt{RT} \sqrt{I_{p0}I_{s0}} \times \cos(\varphi_{p0} - \varphi_{s0})$  and, according to expression (3.1.21) the small-signal gain is [66]

$$k_s = \frac{\partial I_{0l}}{\partial I_{s0}} = -\frac{\partial I_{1l}}{\partial I_{s0}} \approx \left( \sqrt{TR} \frac{\text{sign } \theta \cos \psi_0}{\sqrt{R_{s0}}} + R \right) \frac{\exp L}{8} \quad (3.5.1)$$

(where  $R_{s0} = I_{s0}/I_{0M}$ ,  $\psi_0 = \varphi_{p0} - \varphi_{s0}$ ), which is similar to formula (4.4.13).

If  $R_{s0} \rightarrow 0$ , we find that  $|k_s| \rightarrow \infty$ , i.e. a small signal experiences giant amplification (this is discussed in Ref. [36] and in Section 4.4) when a signal and a pump are applied to the inputs of different waveguides.

An optical transistor with an enhanced gain, discussed in Section 4.5 and in Refs [51, 54–56, 62] for the case when a signal and a pump reach the inputs of different waveguides, can also operate when a signal and a pump are applied to the input of one waveguide [66]. This is a consequence of formula (3.1.21) and of interference of the signal and pump at the input. This transistor is described by the same formulas as in the case when the signal and pump are injected into the inputs of different waveguides (Section 4.5). In particular, the signal gain in such an optical transistor is given by formula (4.5.3). Such operation of an optical transistor is possible when in the absence of a signal the system is at one of the points  $M_0$  or  $M_1$ , i.e. when the pump intensity satisfies formulas (3.1.11) and (3.3.6).

A strong influence of the interference of the phase difference at the input has both positive and negative consequences.

On the one hand, it makes it possible to increase greatly the signal gain, compared with the pump gain, and to control the distribution of the output wave intensities by altering the input phase of the signal. Another important factor is that the strong dependence of the small signal gain  $k_s$  on the difference between the signal and pump phases has the effect that the signal characterised by a certain (close to zero or to  $\pi$ ) phase shift relative to the pump should be amplified more strongly than the noise. Moreover, since the noise phase varies at random with time, time averaging of  $\cos \psi_0$  in formula (3.5.1) causes it to vanish, i.e. there is no giant amplification of the noise. Therefore, the giant amplification effect can be used to increase the signal/noise ratio.

On the other hand, in the development of optical computers it is usual to postulate the requirement that the phase of the signal arriving at a switching element should not influence the output power or the signal gain of this element. This requirement is quite natural and it arises from the desire that the transmission characteristics of the elements should be stable and independent of the optical path of the signal between the output of one element to the input of another. This phase independence of the output characteristics of the input signal is desirable also in the development of optical multivibrators, described in Section 6 and in Refs [56, 66]. Naturally, this influence of the signal phase can be avoided in a trivial manner by making the signal and pump incoherent relative to one another. However, this is not the optimal method. Other methods are discussed in Section 5.4.

#### 4. Optical self-switching in the presence of two waves at the input

The presence of a second wave at the input of a cubically nonlinear system with UDCWs complicates the process of interaction of these waves and introduces qualitatively new features. An analysis of this interaction shows that the radiation self-switching effect is not only possible, but it is more abrupt and more complex and appears in a much

greater variety of ways than when only one wave reaches the input. Let us therefore assume that both waves,  $R_0 \neq 0$ ,  $R_1 \neq 0$ , reach the input of a nonlinear system with two UDCWs. The task is to find  $I_j$  and  $\psi$  at the output of the system, i.e. the values of  $I_j$ ,  $J_{jl}$ , and  $\psi_l$ .

#### 4.1 Solution of the equations for identical unidirectional distributively coupled waves

If UDCWs are identical,

$$\beta_0 = \beta_1 = \beta, \quad \alpha = 0, \quad \theta_0 = \theta_1 = \theta, \quad \theta_{01} = \theta_{10}, \quad (4.1.1)$$

then the roots of Eqn (2.5.14) are

$$J_{a,d} = \frac{R_0 + R_1}{2} \pm \sqrt{D_+}, \quad (4.1.2)$$

$$J_{b,c} = \frac{R_0 + R_1}{2} \pm \sqrt{D_-},$$

where

$$D_{\pm} = \frac{1}{4} \left[ \frac{4\sqrt{R_0 R_1} \operatorname{sign} \theta \cos \psi_0 - 1 \pm \sqrt{D}}{2} + (R_0 - R_1)^2 \right]$$

$$\equiv \frac{1}{4} \left[ (R_0 + R_1)^2 - \frac{(1 \mp \sqrt{D})^2}{4} \right],$$

$$D = 16R_0 R_1 - 8\sqrt{R_0 R_1} \operatorname{sign} \theta \cos \psi_0 + 1.$$

The function described by expression (2.5.12) can be written in two different ways. Depending on the method used to write it down, the integral in expression (2.5.13) can be reduced to two different tabulated integrals. However, the two forms of the solution obtained in this way reduce to one another by identity transformations [62]. We then obtain [36]

$$J_{jl} = \frac{R_0 + R_1}{2} + (-1)^j \sqrt{D_+} \operatorname{cn}(S, r), \quad (4.1.3)$$

where  $S = s + F(\mu, r)m$ ,  $r^2 = D_+/(D_+ - D_-) \equiv 4D_+/\sqrt{D}$ ,  $s = L(D)^{1/4}$ ,  $r_1^2 = 1 - r^2 = -D_-/(D_+ - D_-) = -4D_-/\sqrt{D}$ ,  $\mu = \arccos[(R_0 - R_1)/2\sqrt{D_+}]$ .

The solution represented by expression (4.1.3) is valid for all real values of  $r$ . However, it is convenient to analyse this solution only in the range  $r \leq 1$ , i.e. for  $D_- \leq 0$ . However in the range  $r \geq 1$ , i.e. for  $D_- \geq 0$ , this solution can be represented conveniently by a suitable transformation [120] in the form

$$J_{jl} = \frac{R_0 + R_1}{2} + (-1)^j \sqrt{D_+} \operatorname{dn}\left(\frac{S}{q}, q\right), \quad (4.1.4)$$

where  $S = s + mF(\mu', q)q$ ,  $S/q = 2L\sqrt{D_+} + mF(\mu', q)$ ,  $\mu' = \arcsin(r \sin \mu) = \arcsin(q^{-1} \sin \mu)$ .

The solution described by expression (4.1.3) was obtained later by Winful [78] for the special case when  $R_0 = R_1 = R$  (Section 4.10).

#### 4.2 General solution of the equations

We can represent expression (2.5.12) in the form

$$f(J) = (J_a - J)(J - J_d) \left[ \left( J - \frac{J_b + J_c}{2} \right)^2 - \frac{(J_b - J_c)^2}{4} \right], \quad (4.2.1)$$

and thus reduce the integral in expression (2.5.13) to one which is tabulated in Ref. [120]. Integration of expression (2.5.13) gives

$$s = 2L\sqrt{PQ} = \{F(\mu_l, r) - F(\mu, r)\}m, \quad (4.2.2)$$

where

$$\begin{aligned}\mu_l &= 2 \arctan \left[ \frac{Q(J_a - J_{1l})}{P(J_{1l} - J_d)} \right]^{1/2}, \\ \mu &= 2 \arctan \left[ \frac{Q(J_a - R_1)}{P(R_1 - J_d)} \right]^{1/2}, \\ r^2 &= \frac{(J_a - J_d)^2 - (P - Q)^2}{4PQ}, \\ r_1^2 &= 1 - r^2 = \frac{(P + Q)^2 - (J_a - J_d)^2}{4PQ},\end{aligned}$$

$$P^2 = (J_a - J_b)(J_a - J_c), \quad Q^2 = (J_d - J_b)(J_d - J_c).$$

Transformations yield [51, 54–56, 62]

$$J_{1l} = \frac{(J_a + J_d P/Q) + (J_d P/Q - J_a) \operatorname{cn}(S, r)}{1 + P/Q + (P/Q - 1) \operatorname{cn}(S, r)}, \quad (4.2.3)$$

where  $S = s + F(\mu, r)m$ .

According to expression (4.2.3),  $J_{1l}$  reduces its maximum value, equal to  $J_a$ , when  $\operatorname{cn}(S, r) = -1$ ; the value of  $J_{0l}$  is then maximal and equal to  $R_0 + R_1 - J_a$ . If  $\operatorname{cn}(S, r) = 1$ ,  $J_{1l} = J_d$  is minimal and  $J_{0l} = R_0 + R_1 - J_d$  is maximal. The quantity  $(\Delta T)_{\max} = (J_a - J_d)/(R_0 + R_1)$  is the difference between the maximum and minimum values of the power transfer coefficient of the first wave and represents the depth of energy exchange between the waves;  $0 \leq (\Delta T)_{\max} \leq 1$ .

In the case of identical UDCWs the solution described by expression (4.2.3) reduces to that given by expression (4.1.3) and we then have  $(\Delta T)_{\max} = 2\sqrt{D_-}/(R_0 + R_1)$ . If  $R_1 = 0$ , we find that  $J_d = 0$ ,  $P = p$ ,  $Q = q$ ,  $\mu = 0$ ,  $F(\mu, r) = 0$ ,  $S = s$  and then the solution described by expression (4.2.3) reduces to that described by expression (3.3.1). If  $\Delta = 0$ ,  $R_1 = 0$ , the solution described by expression (4.2.3) is reduced to that described by expression (3.1.3).

In the range  $r \geq 1$  we can analyse expression (4.2.3) by introducing usefully parameters  $q = r^{-1}$ ,  $q_1^2 = 1 - q^2$  and applying the identity  $\operatorname{cn}(S, r) = \operatorname{dn}(S/q, q)$ , where  $S/q = s/q + F(\mu', q)m$ ,  $\mu' = \arcsin(q^{-1} \sin \mu)$ .

### 4.3 Condition for and characteristic points, depth, and slope of optical self-switching

The radiation self-switching effect generally appears when, first,

$$\exp S \gg 1 \quad (4.3.1)$$

and, second,

$$r \approx 1, \quad \text{i.e.} \quad |r_1|^2 \ll 1, \quad (4.3.2)$$

or more exactly

$$|r_1|^2 \exp S \lesssim 16. \quad (4.3.3)$$

Inequality (4.3.3) gives the estimate of the boundary of the self-switching region.

The *middle self-switching point* M will be defined as the set of parameters  $(R_0, R_1, \psi_0)$ , which is found from the condition  $r_1 = 0$  equivalent to  $J_b = J_c$ , i.e.

$$D_- = \frac{(J_b - J_c)^2}{4} = \frac{(a - J_a - J_d)^2}{4} - \frac{d}{J_a J_d} = 0. \quad (4.3.4)$$

If  $D_- < 0$ , then the roots  $J_b$  and  $J_c$  are complex conjugate. If  $D_- > 0$ , the roots  $J_b$  and  $J_c$  are real. Therefore, if the real

roots  $J_a$  and  $J_d$  are known (and they exist always), Eqn (4.3.4) gives the relationship between the parameters  $R_0, R_1, \psi_0$ , and  $\Delta$  at the middle point M. The condition  $J_d < J_b = J_c < J_a$  implies that two equalities are obeyed simultaneously:  $f(J_b) = 0$ , which is a form of Eqn (2.5.14), and  $f'(J_b) = 0$ . Elimination of  $J_b$  from these three equalities leads to an equation, similar to Eqn (3.3.16), which describes the relationship between  $R_0, R_1, \psi_0$ , and  $\Delta$  at the point M. However, we shall not give this equation because it is very cumbersome.

Near the middle point M, we have  $|J_b - J_c|^2 \ll |J_b + J_c|^2$  and

$$r_1^2 \approx -q_1^2 \approx - \left[ \frac{(J_b - J_c)(J_a - J_d)}{4(J_a - J_s)(J_s - J_d)} \right]^2, \quad (4.3.5)$$

where  $J_s = (J_b + J_c)/2$ .

In the self-switching region, i.e. when conditions (4.3.1)–(4.3.3) are obeyed, the solution described by expression (4.2.3) can be approximated by means of formulas given in Appendix II [54, 62]:

$$\begin{aligned}J_{1l} &\approx \left\{ J_a \left[ -\operatorname{sech} S + \left( 1 + \frac{r_1^2}{16} \exp S \right)^2 \right] \right. \\ &\quad \left. + J_d \frac{P}{Q} \left[ \operatorname{sech} S + \left( 1 - \frac{r_1^2}{16} \exp S \right)^2 \right] \right\} \\ &\quad \times \left\{ -\operatorname{sech} S + \left( 1 + \frac{r_1^2}{16} \exp S \right)^2 \right. \\ &\quad \left. + \frac{P}{Q} \left[ \operatorname{sech} S + \left( 1 - \frac{r_1^2}{16} \exp S \right)^2 \right] \right\}^{-1}, \quad (4.3.6)\end{aligned}$$

where  $J_{0l} = R_0 + R_1 - J_{1l}$  and the values of  $\operatorname{sech} S$  can be ignored.

The approximation represented by expression (4.3.6) can be used when  $r \leq 1$  and also when  $r \geq 1$ . Since in the self-switching region we have  $r_1^2 \approx -q_1^2$ ,  $S/q \approx S$ , it follows that in expression (4.3.6) we can replace  $r_1^2$  with  $-q_1^2$  and vice versa. If  $r \geq 1$ , the quantity  $r_1$  is imaginary and  $q_1$  is real.

The *self-switching points*  $M_j$  are the sets of the parameters  $R_0, R_1$ , and  $\psi_0$  for which the intensities  $J_{jl}$  are maximal in the self-switching region. According to expression (4.3.6), if [51, 54]

$$r_1^2 \exp S = 16, \quad (4.3.7)$$

then  $J_{1l} = J_a = \max$  and  $J_{0l} = R_0 + R_1 - J_a = \min$ . This defines the point  $M_1$ . If [51, 54]

$$r_1^2 \exp S = -16, \quad (4.3.8)$$

then  $J_{1l} = J_d = \min$  and  $J_{0l} = R_0 + R_1 - J_d = \max$ . This is the point  $M_0$ .

The difference between the maximum and minimum values of  $J_{jl}$  is  $J_a - J_d$  and the quantity  $(\Delta T)_{\max} = (J_a - J_d)/(R_0 + R_1)$  represents the *relative depth of self-switching* of radiation.

At the middle point M we have  $J_{1l} = (J_a Q + J_d P)/(P + Q) = J_b = J_c$ . The quantity  $P$  at the point M is  $J_a - J_b = J_a - J_c$  and it represents the factor by which the maximum  $J_{1l}$  is greater than the value of  $J_{1l}$  at the point M. The quantity  $Q$  at M is  $J_b - J_d = J_c - J_d$  and it represents the factor by which  $J_{1l}$  at the point M is greater than the minimum  $J_{1l}$ .

In the direct vicinity of the point M when  $r_1^4 \exp(2S)/256 \ll 1$  and  $|P/Q - 1|/(P/Q + 1) \ll 1$  (the latter inequality is obeyed in almost all the cases of practical interest, as discussed above), the slope or steepness of self-switching can be estimated from [62]

$$\begin{aligned} \frac{\partial J_{1l}}{\partial R_j} &\approx -\frac{\partial J_{0l}}{\partial R_j} \approx \frac{J_a - (P/Q)J_d}{8(1+P/Q)} \frac{\partial r_1^2}{\partial R_j} \exp S \\ &\approx \frac{J_a - J_d}{16} \frac{\partial r_1^2}{\partial R_j} \exp S \gg 1. \end{aligned} \quad (4.3.9)$$

It should be pointed out that if  $|P/Q - 1|/(P/Q + 1) \ll 1$ , the approximation represented by expression (4.3.6) simplifies somewhat and becomes [62]

$$J_{1l} \approx \frac{J_a + J_d}{2} + \frac{J_a - J_d}{2} \frac{(r_1^2/8) \exp S}{1 + (r_1^4/256) \exp(2S)}. \quad (4.3.10)$$

In the case of identical UDCWs the self-switching conditions (4.3.1)–(4.3.3) become [36]

$$\exp(2\sqrt{D_+}L) \approx \exp(\sqrt{D}L) \gg 1, \quad (4.3.11)$$

$$|D_-| \ll D_+, \text{ i.e. } \frac{1 + \sqrt{D}}{2} \approx 2(R_0 + R_1), \quad (4.3.12)$$

and the limits of the self-switching region can be estimated from

$$\frac{|D_-|}{D_+} \exp(2\sqrt{D_+}L) \leq 16, \quad (4.3.13)$$

where  $\sqrt{D_+}$  and  $D$  are described by the set of formulas (4.1.2) from which it follows, subject to condition (4.3.12), that in the self-switching region we have  $D_+ \approx (R_0 + R_1)/2 - 1/4$ . In the case of the self-switching region of identical UDCWs, we can obtain the following approximation from expression (4.3.6) or (4.3.10) [36, 54]

$$J_{jl} \approx \frac{R_0 + R_1}{2} + (-1)^j \sqrt{D_+} \frac{-(r_1^2/8) \exp S + \operatorname{sech} S}{1 + (r_1^4/256) \exp(2S)}, \quad (4.3.14)$$

where  $r_1^2 \approx -D_-/D_+$ ,  $S = s + F(\mu, r)m$ ,  $m = \pm 1$ ,

$$\mu = \arccos\left(\frac{R_0 - R_1}{2\sqrt{D_+}}\right),$$

$$\begin{aligned} s &= 2\sqrt{D_+ - D_-}L \approx 2\sqrt{D_+}L \approx \sqrt{D}L \\ &\approx L\sqrt{2(R_0 + R_1) - 1}, \end{aligned}$$

i.e.

$$T_0 \approx 0.5 - (R_0 + R_1)^{-1} \sqrt{\frac{R_1 + R_0}{2} - \frac{1}{4}} \frac{2U}{1 + U^2}, \quad (4.3.14a)$$

where  $U \equiv (r_1^2/16) \exp S$ .

The extrema of  $J_{jl}$  occur under the conditions described by expressions (4.3.7) and (4.3.8), which correspond to the points  $M_1$  ( $J_{1l} = \max$ ) and  $M_0$  ( $J_{0l} = \max$ ). The self-switching depth is

$$(\Delta T)_{\max} = \frac{2\sqrt{D_+}}{R_0 + R_1} = \frac{\sqrt{2(R_0 + R_1) - 1}}{R_0 + R_1}. \quad (4.3.15)$$

Therefore, complete self-switching occurs when  $R_0 + R_1 = 1$ , and if  $R_0 + R_1$  deviates from 1, the self-switching depth decreases even in the case of identical UDCWs ( $\Delta = 0$ )! This is the interesting feature of the situation when both waves are applied to the input.

Near the middle self-switching point M (which corresponds to the condition  $D_- = 0$ ), namely when  $r_1^4 \exp(2S) \ll 256$ , the self-switching slope can be estimated (for  $R_0 \neq R_1$ ) from

$$\frac{\partial J_{0l}}{\partial R_j} \approx -\frac{\partial J_{1l}}{\partial R_j} \approx \frac{(\partial D_- / \partial R_j)}{8\sqrt{D_+}} \exp S \gg 1. \quad (4.3.16)$$

It follows from expressions (4.3.16) and (4.3.14) that an increase in the slope (steepness) of self-switching corresponding to a given value of  $L$  occurs if the self-switching condition is satisfied at higher values of  $R_0 + R_1$ , and that with increase in  $R_0 + R_1$  the self-switching slope increases strongly.

We shall estimate the self-switching slope for the case when  $L = 1.2\pi$ ,  $R_0 = 3$ ,  $R_1 = 1$ ,  $\cos \psi_0 = 0$ ,  $\Delta = 0$ . It then follows from expression (4.3.16) that

$$\frac{\partial I_{0l}}{\partial I_{00}} \approx 3800, \quad \frac{\partial I_{0l}}{\partial I_{10}} \approx -6330, \quad \text{if } \psi_0 = \frac{\pi}{2};$$

$$\frac{\partial I_{0l}}{\partial I_{00}} \approx 798, \quad \frac{\partial I_{0l}}{\partial I_{10}} \approx -1330, \quad \text{if } \psi_0 = -\frac{\pi}{2}.$$

These results are in good agreement with a computer solution of the initial system of equations (2.5.3).

#### 4.4 Switching of a pump by a weak signal. Giant and linear signal amplification

We shall now consider a situation which is of interest in practice when one of the waves (for example, zeroth) reaching the input of the system represents a relatively powerful radiation (pump) and the other (first) wave is a weak control signal. (Figs 5d and 5g, and Fig. 5f with the circular polarisations):  $R_0 \gg R_1 \ll 1$ . If we assume that the nonidentity of UDCWs is small,  $|\Delta| \ll 1$ , the self-switching condition (4.3.2) means that  $R_0 \approx 1$ , i.e. the parameter  $\delta \equiv 1 - R_0$  is also small:  $|\delta| \ll 1$ . Under these assumptions, we have

$$r_1^2 \approx 2(\delta + \Delta - 2\sqrt{R_1} \operatorname{sign} \theta_s \cos \psi_0 + 3R_1 - 2R_1 \cos^2 \psi_0), \quad (4.4.1)$$

$$\begin{aligned} S &\approx L\sqrt{2(R_1 + R_0) - 1} + 2\sin \psi_0 \sqrt{\frac{R_1}{R_0}} \\ &\approx L(R_0 + R_1) + 2\sqrt{\frac{R_1}{R_0}} \sin \psi_0, \end{aligned} \quad (4.4.2)$$

$$\begin{aligned} T_0 &\approx 0.5 - (R_0 + R_1)^{-1} \sqrt{\frac{R_1 + R_0}{2} - \frac{1}{4}} \frac{2U}{1 + U^2} \\ &\approx 0.5 - \frac{U}{1 + U^2}, \end{aligned} \quad (4.4.3)$$

where

$$\begin{aligned} U &\approx \frac{\delta + \Delta - 2\sqrt{R_1} \operatorname{sign} \theta_s \cos \psi_0}{8} \exp S \\ &\approx \frac{1 - R_0 + \Delta - 2\sqrt{R_1} \operatorname{sign} \theta_s \cos \psi_0}{8} \exp L. \end{aligned} \quad (4.4.4)$$

The radiation self-switching is almost complete since

$$(\Delta T)_{\max} \approx \frac{R_0 - R_1 \cos(2\psi_0)}{R_0 + R_1} \approx 1. \quad (4.4.5)$$

The middle self-switching point M is defined by the condition

$$R_1(3 - 2 \cos^2 \psi_0) - 2 \operatorname{sign} \theta_s \cos \psi_0 \sqrt{R_1} + \delta + \Delta = 0. \quad (4.4.6)$$

In the immediate vicinity of the point M, i.e. when condition (4.3.3) is obeyed, the gain representing the change in the signal intensity can be estimated from [70]

$$k_s = \frac{\partial I_{0l}}{\partial I_{10}} = -\frac{\partial I_{1l}}{\partial I_{10}} \approx \frac{\partial J_{0l}}{\partial R_1} \approx \left[ \operatorname{sign} \theta_s \cos \psi_0 \sqrt{\frac{R_0}{R_1}} - 3R_0 + (16R_0^2 + 1)R_1 + 2R_0 \cos^2 \psi_0 \right] \frac{\exp S}{8(R_0 + R_1)}, \quad (4.4.7)$$

and the gain representing the change in the pump intensity is

$$k_p = \frac{\partial I_{0l}}{\partial I_{00}} = -\frac{\partial I_{1l}}{\partial I_{00}} \approx \frac{\partial J_{0l}}{\partial R_0} \approx \frac{\exp S}{8}. \quad (4.4.8)$$

If  $|\delta|$ ,  $R_1$ , and  $|\Delta|$  are sufficiently small, rough estimates of  $k_s$  and  $k_p$  can be obtained by assuming that  $S \approx L$  and ignoring the third term in the square brackets in expression (4.4.7). We then obtain [36]

$$k_s = \frac{\partial I_{0l}}{\partial I_{10}} \approx \left( \frac{\operatorname{sign} \theta_s \cos \psi_0}{\sqrt{R_1}} - 3 + 2R_0 \cos^2 \psi_0 \right) \frac{\exp L}{8}, \quad (4.4.9)$$

$$k_p \approx \frac{\exp L}{8}, \quad (4.4.10)$$

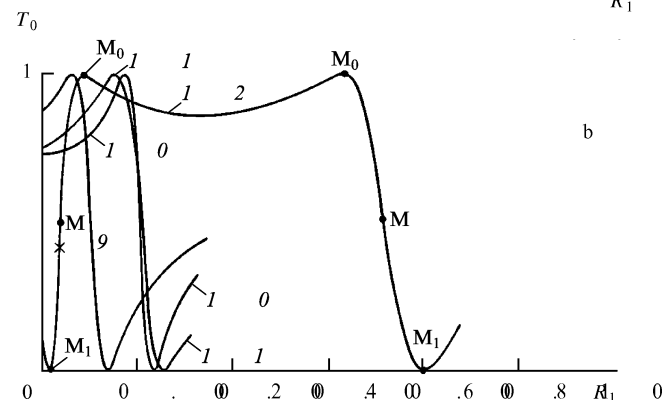
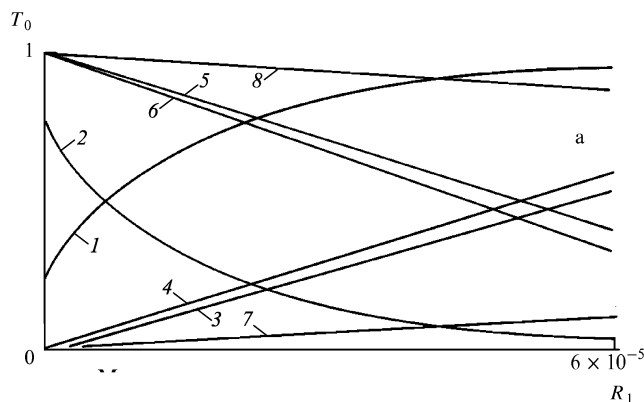
where in practice the last term in parentheses in expression (4.4.9) can also be ignored both for  $|\cos \psi_0| \ll 1$  and for  $|\cos \psi_0| \approx 1$ .

It follows from expression (4.4.9) that if  $|\cos \psi_0| \approx 1$  and the value of  $L$  is given, the gain of a coherent signal is approximately  $(I_{0M}/I_{10})^{1/2} \gg 1$  times higher than the gain of an incoherent signal in the case (Section 3.1) when the pump and signal reach the input of the investigated system in the form of the same wave [this should be compared with expression (3.1.21)]. If  $\cos \psi_0 \neq 0$  and  $R_1 \rightarrow 0$  [and at the same time  $R_0 \rightarrow 1 + \Delta$  in accordance with expression (4.4.6)], then  $|k_s| \rightarrow \infty$ . This situation (represented by curves 1 and 2 in Fig. 10a) is called 'giant amplification' of the change of a small signal [36]. Therefore, if  $|\cos \psi_0| \approx 1$ , the gain representing the change in the signal intensity is  $(I_{0M}/I_{10})^{1/2} \gg 1$  times greater than the gain representing the change in the pump intensity, i.e. the system is much more sensitive to the changes in the signal than those in the pump. This property of the system, in combination with the extremely high gain experienced by a weak alternating signal, is an important practical advantage of the giant amplification regime.

A shortcoming of this regime is nonlinearity of gain, i.e. the signal gain depends on the signal itself. Consequently, the process of signal amplification may distort the signal profile. Therefore, in this regime the system operates as an amplifier with a very high gain and not as an optical transistor. It should be pointed out that the change of the intensity at the output is finite. Let us assume that  $|\cos \psi_0| \approx 1$  and that the signal intensity increases from  $I_{10} = 0$  by a very small amount  $\Delta I_{10}$ , and that  $R_1$  increases correspondingly from  $R_1 = 0$  to  $R_1 = \Delta R_1$ . Then the change in the radiation intensity at the output is, according to expression (4.4.9):

$$|\Delta I_{0l}| \approx \frac{I_{0M} \exp L}{8} \int_0^{\Delta R_1} \frac{dR_1}{\sqrt{R_1}} \approx \frac{I_{0M} \exp L \sqrt{\Delta R_1}}{4}, \quad (4.4.11)$$

so that for  $\Delta R_1 \rightarrow 0$ , we have  $|\Delta I_{0l}| \rightarrow 0$ .



**F i g u r e 10** Efficiency of the system as a function of the signal intensity  $I_{10}$  and the pump intensity  $I_{00}$ . The curves are labeled 1 through 12. The points  $M_0$  and  $M_1$  are marked on the curves. The graph shows the relationship between  $T_0$  and  $R_1$ .

If the phases of the waves are shifted by  $\pi/2$  at the input, the small-signal gain is independent of the signal intensity when the system 'operates' as an optical transistor, but with the gain about three times as high [ $|k_s| \approx (3 \exp L)/8$ ] as in the case when a small signal and a pump are applied to the input in the form of one wave.

Although for  $\cos \psi_0 = 0$  and  $R_1 \ll R_0 \approx 1$  the system operates as an optical transistor [36], we shall show in Section 4.5 that an optical transistor operating in another regime (when  $\cos \psi_0 \neq 0$ ) can also be constructed and it has a much larger gain than in the  $\cos \psi_0 = 0$  case.

According to expressions (4.3.7), (4.3.8), and (4.4.1), if [36, 54, 62]

$$\Delta + \delta - 2\sqrt{R_0 R_1} \operatorname{sign} \theta_s \cos \psi_0 + R_1(3 - 2 \cos^2 \psi_0) = (-1)^{j+1} 8 \exp(-S), \quad (4.4.12)$$

almost all the output radiation is concentrated in the zeroth ( $j=0$  point,  $M_0$ ) or first ( $j=1$ , point  $M_1$ ) wave. The self-switching points  $M_j$  (corresponding to a given

value of  $R_0$ ) correspond to the signal  $R_1 = R_{\text{IM}}^{(j)}$ . If we assume that  $|\cos \psi_0| \gg (3/2)\sqrt{R_1}$ , we obtain [51, 54–56]

$$\sqrt{R_{\text{IM}}^{(j)}} = \left[ (-1)^j 4 \exp(-S) + \frac{\delta + \Delta}{2} \right] \cos^{-1} \psi_0 \text{ sign } \theta_s. \quad (4.4.13)$$

If the right-hand side of the above expression is greater than zero only for one of the values  $j = 0$  or  $1$ , there is only one point  $M_j$  ( $M_0$  or  $M_1$ ), but if it exceeds zero for both values of  $j$ , then both points  $M_j$  exist. In the last case the corresponding value of  $R_{\text{IM}}^{(j)}$  can be estimated from

$$R_{\text{IM}}^{(j)} = \left[ (-1)^j 4 \exp(-S) + \frac{\delta + \Delta}{2} \right]^2 \cos^{-2} \psi_0, \quad (4.4.14)$$

and in the above case the difference between the input intensities of the signal ensuring complete switching of the radiation at the output from one wave to the other can be estimated from

$$R_{\text{IM}}^{(0)} - R_{\text{IM}}^{(1)} \approx 8 \exp(-S) (\delta + \Delta) \cos^{-2} \psi_0. \quad (4.4.15)$$

In the case of very small values of  $|\cos \psi_0| \ll (3/2)\sqrt{R_1}$ , particularly when  $\psi_0 = \pm\pi/2$ , it follows from expression (4.4.12) that

$$\begin{aligned} R_{\text{IM}}^{(0)} &\approx -\frac{8}{3} \exp(-S) - \frac{\delta + \Delta}{3}, \\ R_{\text{IM}}^{(1)} &\approx \frac{8}{3} \exp(-S) - \frac{\delta + \Delta}{3}, \end{aligned} \quad (4.4.16)$$

and the difference between the input signal intensities causing complete switching of the output radiation from one wave to the other is

$$R_{\text{IM}}^{(0)} - R_{\text{IM}}^{(1)} \approx \frac{16}{3} \exp(-S), \quad (4.4.17)$$

i.e. it is approximately one third of that for one wave input [compare with expression (3.1.13)].

A rough estimate of  $R_{\text{IM}}^{(j)}$  in formulas used in this section can be obtained by substituting  $S \approx L$ .

Eqn (4.4.6) has, for a specific ratio of the parameters, two roots  $R_1$  satisfying the condition  $|R_1| \ll 1$ ; this implies double self-switching [70], i.e. switching near two values of  $R_1$  (Fig. 10b), similar to that described in Section 3.3.

#### 4.5 Optical transistor with an enhanced gain, stable against pump intensity instabilities

Analysis of expression (4.3.10) subject to definition (4.4.1) shows that under somewhat different conditions the systems shown in Figs 5d, 5g, and 5f ‘operate’ as optical transistors with an even greater gain than that predicted by formula (4.4.9) for the case when  $\cos \psi_0 = 0$ . In this case the following relationship should be satisfied [51, 54]:

$$\Delta + \delta = (-1)^{j+1} 8 \exp(-L), \quad (4.5.1)$$

which is equivalent to  $R_{\text{IM}}^{(j)} = 0$ , i.e. if  $R_1 = 0$ , we have  $I_{00} = I_{\text{M}}^{(j)}$  [compare with expression 3.3.6]. The meaning of this condition is that, in the absence of a signal, the system is at one of the points  $M_0$  or  $M_1$  (Fig. 2a and Fig. 11). Then, if  $\cos \psi_0 = (-1)^{j+1}$ , a weak signal characterised by [51, 54–56]

$$R_1 \approx R_l \approx 0.15(\Delta + \delta)^2 \approx [3 \exp(-L)]^2 \ll 1 \quad (4.5.2)$$

(where  $R_1$  is found from the condition  $\partial^2 J_{0l} / \partial R_1^2 = 0$ ) should be amplified almost linearly without distortions

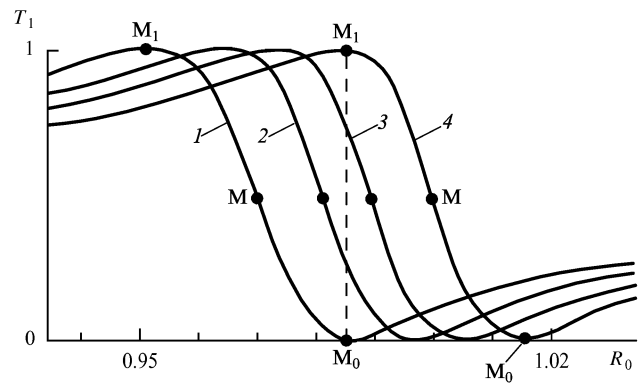


**Figure 11.** Dependence of  $T_1$  on the pump intensity  $R_0$ , plotted for different levels of the signal  $R_1$ . Curves 1 and 2 correspond to  $\Delta = \xi = -16 \exp(-L)$ ;  $R_1 = 0$  for curve 1, and  $R_1 = R_l = 3.25 \times 10^{-5}$  for curve 2;  $\psi_0 = \pi$ . Curves 3 and 4 correspond to  $\Delta = 0$ :  $R_1 = R_l = 2.9 \times 10^{-5}$ ,  $\psi_0 = 0$  for curve 3, and  $R_1 = 0$ ,  $\Delta = 0$  for curve 4 [at the point  $M_1$ ,  $\delta \equiv 1 - R_0 = 0.015 = 8 \exp(-L)$ ].  $L = 2\pi$ ,  $\varepsilon = 0$ ,  $\theta_d = 0$ ,  $\theta_s > 0$ .

(curves 3 and 5 in Fig. 10) and by the very large gain† [51, 54–56, 62]:

$$k_s = \frac{\partial I_{0l}}{\partial I_{10}} \approx (-1)^{j+1} \cos^2 \psi_0 \frac{\exp(2L)}{25}. \quad (4.5.3)$$

Thus, if  $L = 2\pi$ ,  $\cos^2 \psi_0 = 1$ , it follows from expression (4.5.3) that  $|k_s| \sim 10^4$ , whereas according to expression (3.1.21) we have only  $|k_s| \approx 67$  and according to expression (4.4.4) when  $\cos \psi_0 = 0$ , we obtain  $|k_s| \approx 200$ . It is also important to note that in this regime the gain representing the change in the pump [51, 54]

$$k_p = \frac{\partial I_{0l}}{\partial I_{00}} \approx \frac{\exp L}{8} \sqrt{\frac{R_1}{R_l}} \quad (4.5.4)$$

is approximately

$$\frac{|k_s|}{k_p} \approx \cos^2 \psi_0 \frac{\exp L}{3} \sqrt{\frac{R_1}{R_l}} \gg 1 \quad (4.5.5)$$

times less than the signal gain  $k_s$  [51, 54] (this can be seen by comparing Figs 10a and 11). Consequently, the requirement of stability of the pump intensity is relaxed by the same factor as in the case of an optical transistor with  $k_s = k_p$  (see Section 3.1). For example, if  $L = 2\pi$ ,  $\cos^2 \psi_0 \sim 1$ ,  $R_1 \approx R_l$ , we find that  $|k_s|/k_p \approx \exp L/3 \geq 180$ .

In the limit  $R_1 \rightarrow 0$ , the system approaches the point  $M_j$ , where  $k_p = 0$  (curve 2 in Fig. 11) and becomes insensitive to a small change in the pump, but the linearity of the signal amplification for  $R_1 \ll R_l$  is less than for  $R_1 \approx R_l$ .

It therefore follows that it should be possible not only to construct an optical transistor with an extremely high gain, but—which is equally important—such an optical transistor should be much more stable in the presence of pump intensity instabilities than optical transistors discussed in Sections 3.1 and 4.4.

†This optical transistor regime with an enhanced gain can also appear when a pump and a weak coherent signal are applied in the form of one wave to a mixer before this wave enters the system (see Figs 5a–5c, Section 2.5, and Ref. [66]).

An analysis of numerical data [51, 54–56] shows that the set of parameters ensuring that [51, 54–56]

$$A + \delta = (-1)^{j+1} [8 \exp(-L) - \varepsilon] \quad (4.5.6)$$

[where  $|\varepsilon| \ll 8 \exp(-L)$ ] corresponds, for  $\varepsilon > 0$  and small values of  $R_1$  ( $R_1 < R_I$ ), to a larger gain (curves 4 and 6 in Fig. 10a) than in the  $\varepsilon = 0$  case (curves 3 and 5), and the gain can be estimated roughly from [51, 62]

$$k_s \sim (-1)^{j+1} \cos^2 \psi_0 R_0^2 \frac{\exp(2L\sqrt{R_0})}{25}. \quad (4.5.7)$$

The maximum of  $|k_s|$  then shifts to lower and the minimum of the same quantity shifts towards higher values of  $R_1$  compared with the case when  $\varepsilon = 0$ , i.e. the values of  $R_1$  and  $T_j$  at the extrema of  $|k_s|$  come closer together and the signal amplification linearity improves. If  $\varepsilon < 0$ , we have the opposite case when  $|k_s|$  is less than for  $\varepsilon = 0$ . Condition (4.5.6) is also equivalent to  $R_{1M}^{(j)} = 0$ , but at a value of  $\delta$  greater than that given by expression (4.5.1). Selection of  $\delta$ ,  $\varepsilon$ ,  $L$ , and  $A$  can ensure that the linear part of the investigated characteristic becomes very wide. For example, if  $\delta = 0.025$ ,  $\varepsilon = 0.001$ ,  $L = 2\pi$ , and  $A = 0$ , it is found that in the range from  $R_1 = 0.5 \times 10^{-6}$  to  $R_1 = 2.1 \times 10^{-5}$  and, correspondingly, from  $T_0 = 0.067$  to  $T_0 = 0.236$ , the value of  $k_s$  changed from 10170 to 10237, i.e. the deviation from the average value  $k_s = 10204$  does not exceed 0.3%.

If condition (4.5.1) is obeyed, but  $\cos \psi_0 = (-1)^j$ , then for  $R_1 \sim R_I$ , we find from expression (4.3.10) that  $k_s \approx (-1)^{j+1} \exp(2L)/200$  (curves 7 and 10 in Fig. 10a) [54, 56].

It is obvious that the list of examples of optical transistors (see Fig. 5) can be continued. Similar optical transistors can be based on coupled modes in an inhomogeneous waveguide and on other UDCWs [3–6].

Optical transistors can readily be used to construct optical logic elements. The selection of the relationship between the magnitude of the signals and the width of the amplification region of an optical transistor determines the type of logic element, which may be AND or OR. Since the output intensities of the waves 0 or 1 are inversion of one another, a suitable selection of the output wave can readily be used to construct a logic element NOT.

#### 4.6 Self-switching of waves with similar input intensities

If  $R_0 \approx R_1 \approx R \equiv \sqrt{R_0 R_1}$ , self-switching occurs if  $4R > 1$  [36] and  $\psi_0$  is close to zero. The effect is then as follows. If we select  $R_1$  and alter (for example, increase) the value of  $R_0$  near  $R_1$  (Fig. 5e), the output radiation may be switched from the first to the zeroth wave (Fig. 12).

The depth of such self-switching is [54]

$$(\Delta T)_{\max} = \frac{\sqrt{4R-1}}{R_0 + R_1}. \quad (4.6.1)$$

Therefore, complete self-switching  $[(\Delta T)_{\max} = 1]$  occurs for  $R_0 \approx R_1 \approx 0.5$  and, as  $R$  deviates from 0.5, the self-switching depth decreases even in the case of identical waves (Fig. 12b)!

At the middle point M, corresponding to [36, 54]

$$R_0 = R_1 + \frac{2R \sin \psi_0}{\sqrt{4R-1}} + \frac{2R}{4R-1} \Delta, \quad (4.6.2)$$

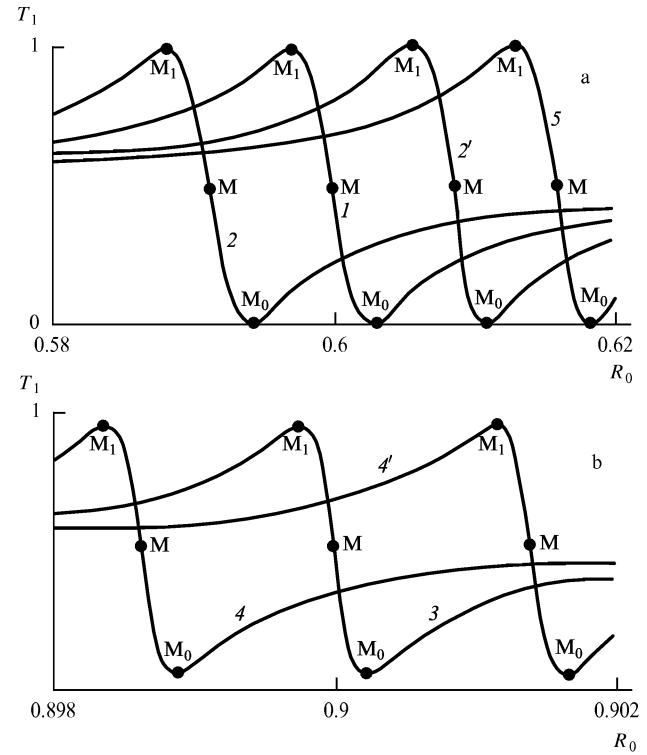


**Figure 12.** Dependence of  $T_1 = 1 - T_0 > 0$  on  $R_0$ , plotted for  $R_0 \approx R_1 = 0.6$  (a),  $0.9$  (b);  $L = 2\pi$ ;  $\xi = 0$  (1, 3, 5),  $-0.01$  (2),  $0.01$  (2'),  $-0.002$  (4),  $0.002$  (4');  $\psi_0 = 0$  (1–4, 2', 4'),  $\pi/200$  (5);  $\theta_d = 0$ ,  $\theta_s > 0$ .

the self-switching slope is [36, 54]

$$\frac{\partial I_{j1}}{\partial I_{00}} = \frac{\partial J_{j1}}{\partial R_0} \approx (-1)^j \left[ 1 - \frac{\Delta}{(4R-1)} \right] \frac{\exp(L\sqrt{4R-1})}{4}, \quad (4.6.3)$$

where  $\Delta = 0$  for identical UDCWs.

If

$$R_0 = R_{0M}^{(j)} \approx R_1 + \frac{2R \sin \psi_0}{\sqrt{4R-1}} + \frac{2R}{4R-1} \Delta \pm 4\sqrt{4R-1} \exp(-L\sqrt{4R-1}), \quad (4.6.4)$$

the wave intensities at the output of the system reach extrema (points belonging to the system  $M_j$ ) [36, 54]. With increase in the input intensity  $R$ , the self-switching slope increases rapidly and the self-switching region rapidly becomes narrower [36]. A shift of the points M and  $M_j$  along the  $R_0$  axis, due to nonidentity of UDCWs ( $\Delta \neq 0$ ), may be compensated by a suitable deviation of  $\psi_0$  from zero when  $\Delta = (4R-1)^{1/2} \sin \psi_0 \approx -\psi_0(4R-1)^{1/2}$ .

#### 4.7 Nonidentical unidirectional distributively coupled waves with $\Delta = 0$

Under certain conditions, namely when [54]

$$\xi = -2 \frac{\theta_d}{\theta_s} (R_0 + R_1), \quad (4.7.1)$$

i.e. when

$$\alpha = \frac{(\theta_1 - \theta_0)(I_{00} + I_{10})}{4\beta} \quad (4.7.2)$$

the 'linear' and 'nonlinear' components  $\Delta$  compensate each other exactly and we have  $\Delta = 0$ . Such compensation is

accompanied by radiation self-switching without the use of the electro-optical effect if  $R_0$  and  $R_1$  in expression (4.7.1) correspond to the point M when  $\alpha = \theta_d = 0$ .

For example, if  $R_0 \approx R_1 = \text{const}$ ,  $\psi_0 = 0$  and we select  $R_0 = R_1$ ,  $\xi = -4(\theta_d/\theta_s)R_1$ , the result is [54]

$$\frac{\partial J_{jl}}{\partial J_{00}} \sim (-1)^{j+1} \frac{[\theta_0(1-8R) + \theta_1] \exp(L\sqrt{4R-1})}{4(\theta_0 + \theta_1)(4R-1)}. \quad (4.7.3)$$

If  $\theta_1 = (8R-1)\theta_0$  no self-switching occurs; for  $\theta_1 = \theta_0$ , formula (4.7.3) reduces to formula (4.6.3). It is evident from formula (4.7.3) that the self-switching direction and slope depend on the ratio of the nonlinear coefficients  $\theta_0$  and  $\theta_1$ . Such wave self-switching is illustrated in Refs [54, 62].

If  $R_1 = 0$  and condition (4.7.2) is fulfilled, complete self-switching occurs, as discussed in Section 3.3 and described by expression (3.3.11).

#### 4.8 Self-phase-matching of waves and limits of changes in the intensities

Wave self-phase-matching occurs at the moment of radiation self-switching (more exactly at the middle point M) also in the general case when both waves are injected into the system. This can be demonstrated quite readily. If we use the second equation from the system of equations (2.5.4), we find that

$$\sin \psi_l = \frac{1}{\sqrt{J_{0l}J_{1l}}} \frac{dJ_{1l}}{dL}, \quad (4.8.1)$$

and it follows from expression (4.3.6) for  $J_{1l}$  that in the direct vicinity of the middle self-switching point M [i.e. when  $r_1^4 \exp(2S) \ll 16$ ], the result is

$$\sin \psi_l \approx \frac{(J_a - J_d)(r_1^2/8) \exp(S) 2\sqrt{PQ}}{2[1 + r_1^2 \exp(2S)/256]}. \quad (4.8.2)$$

Since  $r_1 = 0$  at the middle point M and since  $r_1^2$  changes sign, it follows that at this point we have  $\sin \psi_l = 0$  (Fig. 13).

Let us consider the change in the difference between the wave phases in the self-switching region and not only in the direct vicinity of the point M. For simplicity, let us consider the case of identical waves. If we use the approximations for the elliptic functions in the switching region (Appendix II), we obtain

$$\begin{aligned} \sin \psi_l \approx & \frac{1 - (r_1^4/256) \exp S}{1 + (r_1^4/256) \exp S} \times \frac{2 \exp(-S) + (r_1^2/8) \exp S}{1 + (r_1^4/256) \exp(2S)} \\ & \times \frac{2D_+}{[(R_0 + R_1)/2 - D_+ \text{cn}^2(S, r)]^{1/2}}. \end{aligned} \quad (4.8.3)$$

We can see that  $\sin \psi_l$  vanishes not only for  $r_1 = 0$ , but also for  $r_1^2 \exp S = \pm 16$ , i.e. it vanishes at the points  $M_j$  and at these points we have  $\cos \psi_l = -1$ , i.e. the phases are opposite (Fig. 13).

Some relationships governing the interaction of UDCWs are revealed by an analysis of integrals described by expressions (2.5.5) and (2.5.6) without complete analytic solution of the system of equations (2.5.3). The same integrals yield an expression (2.5.9) and values of  $\cos \psi$  along the system. It follows from formula (2.5.9) and the condition  $|\cos \psi| \leq 1$  that for certain relationships between  $R_0$ ,  $R_1$ ,  $\psi_0$ , and  $\Delta$ , the UDCW intensities may vary not over

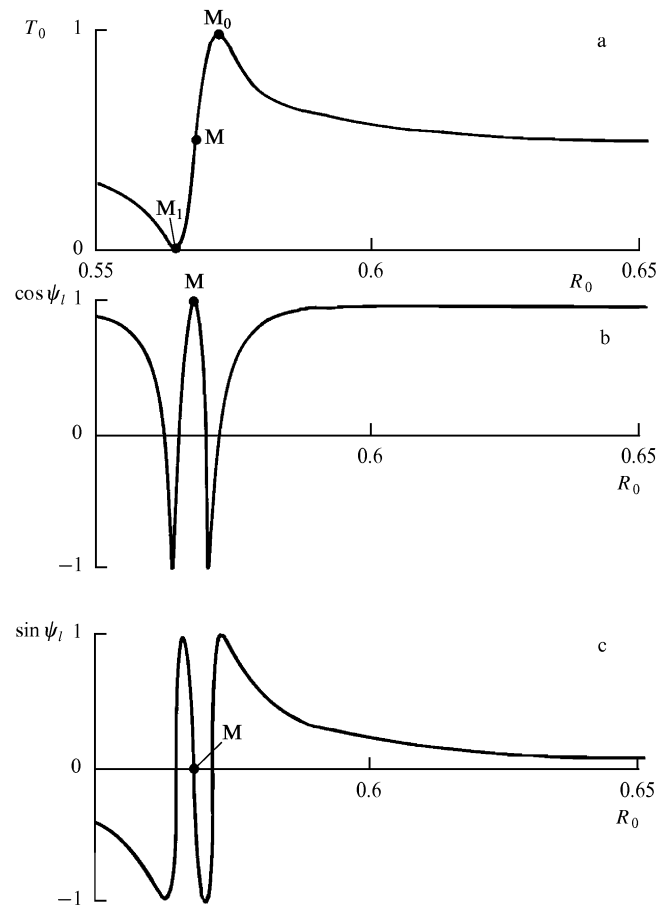


**Figure 13.** Dependences of  $T_0$  (a),  $\cos \psi_l$  (b), and  $\sin \psi_l$  (c) on  $R_0$  for  $R_0 \approx R_1 = 0.6$ ,  $L = 2\pi$ ,  $\psi_0 = -\pi/100$ .

the whole range  $0 \leq J_{0,1} \leq R_0 + R_1$ , but only in certain 'allowed' intervals. In the case of identical UDCWs, formula (2.5.9) becomes

$$\begin{aligned} \cos \psi = & 2 \text{sign } \theta \sqrt{J_0 J_1} \\ & + \sqrt{\frac{R_0 R_1}{J_0 J_1}} (\cos \psi_0 - 2 \text{sign } \theta \sqrt{R_0 R_1}). \end{aligned} \quad (4.8.4)$$

It follows directly from formula (4.8.4) that if radiation is coupled into the system in the form of both waves, i.e. if  $R_0 R_1 \neq 0$  and  $2\sqrt{R_0 R_1} \neq \text{sign } \theta \cos \psi_0$ , then  $J_0 J_1 \neq 0$  [in the opposite case the second term in formula (4.8.4) would have become infinite]. We then have  $J_d \leq J_{0,1} \leq J_a$  and if  $D < 1$  [i.e. if  $2(R_0 R_1)^{1/2} < \text{sign } \theta \cos \psi_0$ ], then for extremal values of the intensity which are  $J_{a,d} = (R_0 + R_1)/2 \pm \sqrt{D_+}$ , the waves 0 and 1 are in phase, but if  $D > 1$  [i.e. if  $2(R_0 R_1)^{1/2} < \text{sign } \theta \cos \psi_0$ ], then for  $J_{0,1} = J_{a,d}$  the waves are in antiphase. If the input radiation is in the form of one wave ( $R_0 R_1 = 0$ ), then  $\cos \psi = \text{sign } \theta 2(J_0 J_1)^{1/2}$  (Section 3.2) and for  $J_0 J_1 = 0$  the wave phases are shifted by  $\pi/2$ .

If  $D_- \geq 0$ , i.e. if  $2(R_0 + R_1) \geq 1 + \sqrt{D}$ , then  $J_b \leq J_0 \leq R_0 + R_1$  and  $0 < J_1 < J_c$  (it is assumed that  $R_0 > R_1$ ), and for  $J_{0,1} = J_{b,c} = (R_0 + R_1)/2 \pm \sqrt{D_-}$  the waves 0 and 1 are in phase.

When the inequalities  $R_0 R_1 \neq 0$  ( $D \neq 0$ ) and  $D_- \geq 0$  are satisfied simultaneously, we find that  $J_c \leq J_0 \leq J_a$  and  $J_d \leq J_1 \leq J_c$ , and the range of variation of  $I_j$  is

$\sqrt{D_+} - \sqrt{D_-}$ . If  $\text{sign } \theta \cos \psi_0 = 1$  and  $4\sqrt{R_0 R_1} = 1$ , then  $D = 0$ ,  $D_+ = D_-$ ,  $J_0 = J_c = J_a = R_0$ ,  $J_1 = J_d = J_b = R_1$ , i.e. the wave powers do not vary along the waveguides and are equal to their initial values.

These ideas are illustrated in Ref. [36] by computer calculations.

#### 4.9 Dependence of the intensities on the input phase difference

It is evident from formula (4.4.3) that near the middle switching point M the output characteristics depend strongly not only on  $R_0$  and  $R_1$ , but also on the input phase difference  $\psi_0$  (Fig. 14).

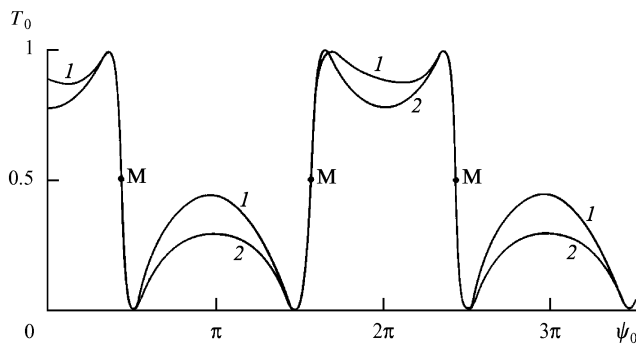


**Figure 14.** Dependences of  $T_0$  on the initial phase difference  $\psi_0$ : (1) solution of the system of equations (2.5.3); (2) approximation by formula (4.4.3);  $R_0 = 0.99$ ,  $R_1 = 0.005$ ;  $\Delta = 0$ ,  $\theta_d = 0$ ,  $\theta_s > 0$ ;  $L = 1.6\pi$ .

From the point of view of mathematics the essential fact is that at  $r \approx 1$  the output characteristics depend strongly on  $r$  and that  $r$  in turn depends on both  $R_0$  and  $R_1$  as well as on  $\cos \psi_0$ , i.e. the dependence on  $\psi_0$  is periodic and near a certain value of  $\cos \psi_0$ , found from the condition  $r = 1$  and for  $\Delta = 0$  equal to

$$\cos \psi_0 \approx \frac{4R_0 R_1 - (R_0 + R_1)(R_0 + R_1 - 1)}{2\sqrt{R_0 R_1} \text{sign } \theta}, \quad (4.9.1)$$

this dependence on  $\psi_0$  is strong: optical switching of waves takes place. If  $\Delta = 0$ , then near the switching point M, we have

$$\frac{\partial J_{1l}}{\partial \psi_0} \approx -\frac{(R_0 + R_1)\sqrt{R_0 R_1} \sin \psi_0 \text{sign } \theta \exp S}{[2(R_0 + R_1) - 1]^{3/2} 8}. \quad (4.9.2)$$

This formula can be used to estimate the sensitivity of the system to changes in  $\psi_0$ , which for points  $|\sin \psi_0| \sim 1$  is very high (Fig. 14).

It is evident that the strong dependence of  $J_{1l}$  on  $\psi_0$  creates favourable conditions for the control of the output power because of a change in  $\psi_0$ . The possibility of such control was pointed out in Ref. [82]. However, in some cases it is desirable to eliminate this dependence (Sections 3.5 and 5.4).

#### 4.10 Comparison with Winful's results

It is shown in Section 4.6 and in Refs [36, 54] that self-switching takes place when  $R_0 \approx R_1$  provided  $\psi_0 \approx 0$ . However, if  $\psi_0 = \pi/2$ , as in Winful's work [78], there is no self-switching in the sense understood here. We recall

that Winful [78] considered the situation when two identical ( $\alpha = 0$ ) circularly polarised waves of equal intensity,  $R_0 = R_1 = R$ , are injected into a birefringent waveguide or crystal. The situation corresponds to the arrival at the input of a linearly polarised wave with the vector  $\mathbf{E}$  which makes an angle  $\vartheta_0 = \pi/4$  with the optic axis. However, in this case it is found that  $\psi_0 = 2\vartheta_0 = \pi/2$  [78] and in the solution described by expression (4.1.3) we have  $r^2 = \frac{1}{2}(1 - \sqrt{16R^2 + 1})$ , i.e.  $r^2$  varies from zero to  $\frac{1}{2}$  and nowhere does it even approach unity. Therefore, in the sense understood here, there was no self-switching in the case discussed by Winful [78]. This evidently accounts for the relatively smooth changes in the output intensity caused by changes in the input intensity, which are predicted in Ref. [78] even in the case when  $L/\pi \gg 1$ , when—according to expression (4.6.3)—the changes in the output intensity and the self-switching slope should be fantastically high. Therefore, from the standpoint adopted here, the case discussed by Winful [78] represents 'nonlinear radiation transfer' or 'nonlinear pumping over', but not 'self-switching' of light.

It is worth pointing out also a fundamental difference between our approach [33, 36, 54] and that of Winful [78]. In our case the input intensity of one (for example,  $R_0$ ) of the UDCWs is varied and the input intensity of the other wave ( $R_1$ ) is fixed. In Winful's work [78] the total intensity of waves at the input (i.e. the quantity  $2R$ ) is varied; naturally, there are simultaneous and identical changes in the input intensities of both waves, i.e.  $R_0 = R_1 = R$ . The normalised total intensity, which in our notation is  $2R$ , is increased in Ref. [78] passing through the values 1, 2, 3, 4, 5, etc. ( $\psi_0 = \pi/2$ ). The ratio of the output intensities ('output ellipticity') changes smoothly, i.e. there is no self-switching.

#### 4.11 Special features of self-switching of unidirectional distributively coupled waves with orthogonal polarisations

As pointed out in Sections 2.3 and 2.6, self-switching of UDCWs with orthogonal polarisations has certain specific features associated with the presence of an additional term in the system of equations (2.6.4). It is appropriate to consider the special features of such switching in this section, because effective self-switching of these waves requires the presence of both waves at the input (Fig. 5f with the TE and TM polarisations at the input).

Let us consider the system of equations (2.6.4) in a coordinate system with its axes rotated relative to the  $x$  and  $y$  axes by an angle  $\varphi$ :

$$\kappa = \kappa_n \cos \varphi - \eta_n \sin \varphi, \quad \eta = \kappa_n \sin \varphi + \eta_n \cos \varphi, \quad (4.11.1)$$

and let us select such an angle  $\varphi$  that  $\sin \varphi = K/\gamma$ ,  $\cos \varphi = \alpha/\gamma$  [71], where  $\gamma \equiv (\alpha^2 + K^2)^{1/2}$ . Let us also use the set of expressions (2.3.10) which give the relationships between the nonlinear coefficients  $\theta_x = \theta_y = \theta$ ,  $\theta_{xy} = \theta_{yx} = 2\theta/3$ ,  $\theta = \theta/3$ ; these relationships are conserved after rotation. The system of equations (2.6.4) expressed in terms of the variables  $\kappa_n$  and  $\eta_n$  then simplify to [71]

$$\begin{cases} \kappa'_n = (I_n \eta_n) \sqrt{1 - \kappa_n^2 - \eta_n^2}, \\ \eta'_n = -(I_n \kappa_n + \gamma) \sqrt{1 - \kappa_n^2 - \eta_n^2}, \end{cases} \quad (4.11.2)$$

where  $I_n = \theta I/3$ . The analytic solution of the above system of equations can be found easily.

If we go back to the ‘old’ variables, we find that the solution is [71]

$$\begin{aligned} \varkappa_l &= \varkappa_0 - \frac{\alpha}{\gamma} \frac{2\rho}{I_n} r^2 [\operatorname{sn}^2(S, r) - \operatorname{sn}^2(s_0, r)] \\ &\quad + \frac{K}{\gamma} \frac{2\rho}{I_n} r [\operatorname{sn}(S, r) \operatorname{dn}(S, r) - \operatorname{sn}(s_0, r) \operatorname{dn}(s_0, r)], \\ \eta_l &= \eta_0 - \frac{K}{\gamma} \frac{2\rho}{I_n} r^2 [\operatorname{sn}^2(S, r) - \operatorname{sn}^2(s_0, r)] \\ &\quad - \frac{\alpha}{\gamma} \frac{2\rho}{I_n} r [\operatorname{sn}(S, r) \operatorname{dn}(S, r) - \operatorname{sn}(s_0, r) \operatorname{dn}(s_0, r)], \end{aligned} \quad (4.11.3)$$

where  $S = s + F(\mu_0, r) \equiv s + s_0$ ,  $s = \sqrt{\rho/\gamma} L$ ,  $L = 2\pi l/\lambda\beta$ ,

$$\mu_0 = \arcsin \left[ \frac{2(K\varkappa_0 - \alpha\eta_0)}{I_n \sqrt{(1-u_b)(u_a-u_0)}} \right],$$

$$u_a = I_n^{-2}(\gamma + \rho)^2, \quad u_b = I_n^{-2}(\gamma - \rho)^2,$$

$$u_0 = \varkappa_0^2 + \eta_0^2, \quad \varkappa_0 = \varkappa(z=0), \quad \eta_0 = \eta(z=0),$$

$$\rho^2 = (I_n \varkappa_0 + \alpha)^2 + (I_n \eta_0 + K)^2 = \gamma^2 + I_n \Gamma$$

$$= \gamma^2 + 2I_n(K \cos \psi_0 \sqrt{1 - \varkappa_0^2} + \alpha \varkappa_0)$$

$$+ I_n^2(\cos^2 \psi_0 + \varkappa_0^2 \sin^2 \psi_0),$$

$\Gamma = 2K\eta_0 + 2\alpha\varkappa_0 + I_n u_0$  is the integral in the system of equations (2.6.4), and

$$r^2 = \frac{I_n^2 - (\gamma - \rho)^2}{4\rho\gamma} = 1 - r_1^2, \quad r_1^2 = \frac{(\gamma + \rho)^2 - I_n^2}{4\rho\gamma}. \quad (4.11.4)$$

Self-switching of UDCWs occurs near the middle self-switching point M, which is defined by condition (4.3.4):  $r = 1$  or  $r_1 = 0$ , i.e. in this case we have the relationship [71]

$$\gamma + \rho = |I_n|, \quad (4.11.5)$$

which leads to the equation for the determination of  $\varkappa_0$  at the point M

$$\begin{aligned} R \sin^2 \psi_0 (1 + \varkappa_0) &= \frac{K}{\gamma} \sqrt{(1 - \varkappa_0)} \operatorname{sign} \theta \cos \psi_0 \\ &\quad + \frac{\alpha}{\gamma} \varkappa_0 \operatorname{sign} \theta + 1, \end{aligned} \quad (4.11.6)$$

where  $R \equiv |\theta| I_{y0}/3\gamma \equiv 4R_y/3$ .

The behaviour of the solution described by the set of expressions (4.11.3) is governed by two key terms which can be approximated as follows in the self-switching region (Appendix II):

$$\operatorname{sn}(S, r) \operatorname{dn}(S, r) \approx \frac{2U(1 - U^2)}{(1 + U^2)^2}, \quad (4.11.7a)$$

$$\operatorname{sn}^2(S, r) \approx \left( \frac{1 - U^2}{1 + U^2} \right)^2, \quad (4.11.7b)$$

where  $U = r_1^2 \exp S/16$ .

Let us now consider two important limiting cases of self-switching.

(1)  $K \gg |\alpha|$ . The solution described by expression (4.11.3) is dominated by the term given by

formula (4.11.7a), which reaches its extremal values  $\pm 0.5$  for  $U = \pm(1 \pm \sqrt{2})$ . If  $U = U_y = \sqrt{2} - 1$ , then  $\operatorname{sn}(S, r) \operatorname{dn}(S, r) = 0.5$  and

$$T_x = T_{x,\min} = \frac{\gamma}{2} |I_n|^{-1} = \frac{3}{8(R_x + R_y)}. \quad (4.11.8a)$$

If  $U = U_x = -(\sqrt{2} - 1)$ , then  $\operatorname{sn}(S, r) \operatorname{dn}(S, r) = -0.5$  and

$$T_x = T_{x,\max} = 1 - \frac{\gamma}{2} |I_n|^{-1} = 1 - \frac{3}{8(R_x + R_y)}. \quad (4.11.8b)$$

The switching depth

$$(\Delta T)_{\max} = T_{x,\max} - T_{x,\min} = 1 - \frac{\gamma}{|I_n|} = 1 - \frac{3}{4(R_x + R_y)} \quad (4.11.8c)$$

increases with increase in  $I_n$ , i.e. with increase in  $R_x + R_y$ . If  $|I_n| \gg \gamma \approx K$ , i.e. if  $R_x + R_y \gg 3/4$ , we find that  $(\Delta T)_{\max} \approx 1$ , i.e. at sufficiently high pump intensities the process of self-switching becomes almost complete.

A characteristic feature of such switching in the case when  $K \gg |\alpha|$  (compared with that described in Section 4.6) is the presence of two additional extrema: if  $U = \tilde{U}_x = (\sqrt{2} + 1)$ , then  $\operatorname{sn}(S, r) \operatorname{dn}(S, r) = -0.5$  and  $T_x = \max = T_{x,\max}$ ; if  $U = \tilde{U}_y = -(\sqrt{2} + 1)$ , then  $\operatorname{sn}(S, r) \operatorname{dn}(S, r) = 0.5$  and  $T_x = \min = T_{x,\min}$ . The same values given by the set of expressions (4.11.8) apply for  $T_{x,\min}$ ,  $T_{x,\max}$ , and  $(\Delta T)_{\max}$  as for  $U = U_{x,y}$ , but in the former case these values are reached for larger deviations from the middle switching point M. Thus, near one point M there are two points  $M_x$  ( $U = U_x$ ) and  $\tilde{M}_x$  ( $U = \tilde{U}_x$ ), where  $T_x = T_{x,\max}$ ; there are also two points  $M_y$  ( $U = U_y$ ) and  $\tilde{M}_y$  ( $U = \tilde{U}_y$ ), where  $T_x = T_{x,\min}$  (Fig. 15a).

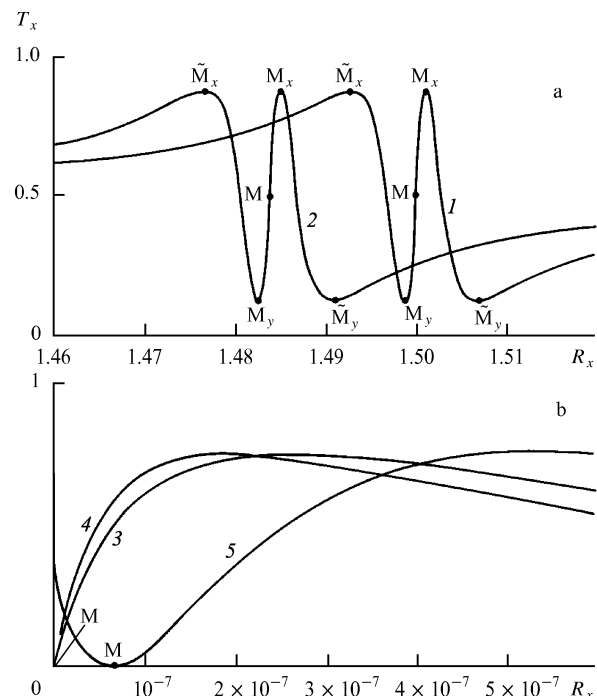


**Figure 15.** Dependences of  $T_x \equiv I_{xl}/(I_{x0} + I_{y0})$  on  $R_x \equiv I_{x0}|\theta|/4\gamma$ : (a)  $R_x \approx R_y \equiv I_{y0}|\theta|/4\gamma = 1.5$ ,  $\alpha = 0$ ,  $\psi_0 = \pi$  (1),  $\psi_0 = \pi - 0.001$  (2); (b)  $R_x \ll R_y = 3$ ;  $K/\alpha = 0$  (3, 4), 0.0005 (5);  $\cot \psi_0 = 0$  (3, 5),  $-1/(R - 1)^{1/2}$  (4).  $L = 2\pi\gamma l/\lambda\beta = 1.6\pi$ ,  $\gamma \equiv (\alpha^2 + K^2)^{1/2}$ ,  $R = 4R_y/3$ .

Self-switching occurs for  $|\varkappa_0| \ll 1$  (i.e. for  $R_x \approx R_y$ ) and  $|\sin \psi_0| \ll 1$ . If we assume that  $|2R - 1| \gg |\varkappa_0|$  and  $|\alpha|/K, |\psi_0|$ , we find that

$$r_1^2 = \frac{R^2}{(2R - 1)^2} \left[ \left( \varkappa_0 - \frac{\alpha}{K} \operatorname{sign} \theta \right)^2 - \sin^2 \psi_0 (2R - 1) \right], \quad (4.11.9a)$$

$$U = \frac{\exp s}{4} \frac{R}{2R - 1} \left( \varkappa_0 - \frac{\alpha}{K} \operatorname{sign} \theta - \sin \psi_0 \sqrt{2R - 1} \right). \quad (4.11.9b)$$

Expression (4.11.9b) and the values of  $U_x, \tilde{U}_x, U_y,$  and  $\tilde{U}_y$  given above readily yield the values of  $R_x$  at which  $T_x$  reaches extremal values.

The point M is then described by the formula

$$\varkappa_{0M} = \frac{\alpha}{K} \operatorname{sign} \theta - \sin \psi_0 (2R - 1)^{1/2}. \quad (4.11.10)$$

If  $\alpha = \sin \psi_0 = 0$ , the point M is reached at  $\varkappa_{0M} = 0$ , i.e. at  $R_x = R_y$ , and the pump  $R_y$  can have any value not exceeding  $3/4$  (i.e.  $R > 0.5$  and  $I_{y0} > 1.5K/|\theta|$ ). If  $\alpha \neq 0$  and  $\sin \psi_0 \neq 0$ , the point M shifts along the scale  $R_x$  in accordance with expression (4.11.10) (Fig. 15a). If  $\alpha/K = \sqrt{2R - 1} \operatorname{sign} \theta \sin \psi_0$ , the shift caused by  $\alpha$  compensates the shift caused by  $\sin \psi_0 \neq 0$  and the point M is reached at  $R_x = R_y$ .

The gain corresponding to a small change in the intensity at the point M can be calculated from [71]

$$\frac{\partial I_{xl}}{\partial I_{x0}} \approx \frac{\exp s}{4}, \quad (4.11.11)$$

where

$$s \approx L \sqrt{2R(1 + \xi_{0M}) - 1} \approx L \sqrt{\frac{|I_n|}{K} - 1} \\ = L \sqrt{\frac{4(R_x + R_y)}{3} - 1}$$

and  $L = 2\pi Kl/\lambda\beta$ ; this is almost identical with expression (4.6.3).

(2)  $|\alpha| \gg K$ . In expression (4.11.3) the dominant term is (4.11.7b), which has the extremal values 0 and 1 for  $U^2 = 1$  and  $U = 0$ , respectively. Self-switching occurs for  $R_x \ll R_y$ . The assumption that  $(R - 1)^2 \gg K^2/\alpha^2$ ,  $R_x/R_y$ , and  $(K/|\alpha|) \cos \psi_0 \sqrt{R_x/R_y}$  leads to

$$r_1^2 \approx -\frac{R_x}{R_y} \frac{R^2}{(R - 1)^2} \left[ \sin \psi_0 \sqrt{R - 1} - (\cos \psi_0 + \Omega) \right] \\ \times \left[ \sin \psi_0 \sqrt{R - 1} + (\cos \psi_0 + \Omega) \right], \quad (4.11.12a)$$

$$U^2 \approx \frac{R^2}{(R - 1)^2} \frac{\exp(2s)}{16} \frac{R_x}{R_y} \\ \times \left[ \sin \psi_0 \sqrt{R - 1} - (\cos \psi_0 + \Omega) \right]^2, \quad (4.11.12b)$$

where  $\Omega = [K/(2\alpha)](R_y/R_x)^{1/2}$ ,  $s \approx L(R - 1)^{1/2} = L(4R_y/3 - 1)^{1/2}$ ,  $L = 2\pi|\alpha|l/\lambda\beta$ ,  $R_y = I_{y0}|\theta|/(4|\alpha|) = 3R/4$ ,  $R_x = I_{x0}|\theta|/(4|\alpha|)$ ,  $R = I_{y0}|\theta|/(3|\alpha|) = 4R_y/3$ . The gain resulting from a small change in the intensity near the point M is

$$\frac{\partial T_x}{\partial R_x} \approx \frac{\partial I_{xl}}{R_y \partial I_{x0}} \approx \frac{\exp(2s)}{3(R - 1)} \left( \sin \psi_0 \sqrt{R - 1} - \cos \psi_0 - \Omega \right) \\ \times \left( \sin \psi_0 \sqrt{R - 1} - \cos \psi_0 \right). \quad (4.11.13)$$

The point M is reached at

$$R_x = R_{xM} \approx \frac{K^2}{4\alpha^2} \frac{R_y}{(\pm\sqrt{R - 1} \sin \psi_0 - \cos \psi_0)^2} \quad (4.11.14)$$

and at this point we have  $T_x = \min = 0$ ,  $U = 0$ ,  $\partial T_x/\partial R_x = 0$ . Therefore, the point M coincides with the point  $M_y$  (which is an analogue of the point  $M_1$  discussed in Section 4.3)! This is one of the special features of the self-switching process considered here. If  $|\sin \psi_0 \sqrt{R - 1} - \cos \psi_0| \ll |\Omega|$ , then

$$\frac{\partial T_x}{\partial R_x} \approx \frac{\partial I_{xl}}{R_y \partial I_{x0}} \approx -\frac{K}{2\alpha(R - 1)} \frac{\exp(2s)}{3} \sqrt{\frac{R_y}{R_x}}, \quad (4.11.15)$$

and we are dealing with giant amplification (Section 4.4): in the limit  $R_x \rightarrow 0$ , we obtain  $\partial T_x/\partial R_x \rightarrow \infty$  (curve 5 in Fig. 15b).

If  $|\sin \psi_0 \sqrt{R - 1} - \cos \psi_0| \gg |\Omega|$ , then

$$\frac{\partial T_x}{\partial R_x} \approx \frac{\exp(2s)}{3(R - 1)} \left( \sin \psi_0 \sqrt{R - 1} - \cos \psi_0 \right)^2 \\ = \frac{(\sqrt{R - 1} - \cot \psi_0)^2 \exp(2s)}{(R - 1)(1 + \cot^2 \psi_0) 3}, \quad (4.11.16)$$

and the amplification is linear. If the optimal initial phase, defined by  $\cot \psi_0 = -1/\sqrt{R - 1}$ , is selected the gain is maximal and its value is

$$\frac{\partial I_{xl}}{\partial I_{x0}} \approx R_y \frac{R}{R - 1} \frac{\exp(2s)}{3} \quad (4.11.17)$$

(curve 4 in Fig. 15b). The closest approach to linearity occurs in the same phase because then the influence of the term proportional to  $\Omega$  is smallest.

If  $\cos \psi_0 = 0$ , expression (4.11.16) reduces to [17]

$$\frac{\partial I_{xl}}{\partial I_{x0}} \approx R_y \frac{\exp(2s)}{3} \quad (4.11.18)$$

(curve 3 in Fig. 15b). If  $K = 0$ , then expressions (4.11.16)–(4.11.18) give the best approximation and, according to formula (4.11.14), the point M is reached at  $I_{x0} = R_x = 0$  (for an infinitesimally small signal) even if  $\cos \psi_0 \neq 0$ . At the point M we have  $\varkappa_{0M} = -\operatorname{sign} \theta \operatorname{sign} \alpha$ ,  $\eta_{0M} = 0$ .

Self-switching occurs for any (sufficiently strong) pump such that  $R > 1$ , i.e.  $R_y > 3/4$  or  $I_{y0} > 3|\alpha/\theta|$ ; if  $K = 0$ , the point M is still reached at  $I_{x0} = R_x = 0$  as the pump is increased.

The extremal values of  $T_x$  and the switching depth  $(\Delta T)_{\max}$  are described by the formulas

$$T_{x,\min} = 0, \quad (\Delta T)_{\max} = T_{x,\max} = 1 - \frac{\gamma}{|I_n|} = 1 - \frac{3}{4R_y}. \quad (4.11.19)$$

The switching depth increases with increase in  $R_y$ . If  $R_y \gg 3/4$ , i.e. if  $|I_n| \gg \gamma \approx |\alpha|$ , we have  $(\Delta T)_{\max} \approx 1$ ; self-switching becomes almost complete at sufficiently high pump intensities.

Formula (4.11.16) predicts a much higher gain than does formula (4.11.11). The gain becomes extremely high even at relatively low values of  $L$ . For example, if  $L = \pi$ ,  $R_y = 5$ , and  $\psi_0 = \pi/2$ , we have  $\partial I_{xl}/\partial I_{x0} \approx 10^6 R_y$  and  $(\Delta T)_{\max} \approx 0.85$ ; if  $L = 1.6\pi$ ,  $R_y = 3$ , we obtain  $\partial I_{xl}/\partial I_{x0} \approx 12 \times 10^6 R_y \approx 36 \times 10^6$  and  $(\Delta T)_{\max} \approx 0.75$ . These results are in good agreement with the numerical solutions of the initial system of equations (2.3.7) (curve 3 in Fig. 15b).

One of the most interesting features of such self-switching is that it occurs even for  $K = 0$  and that in this case the amplification is closest to linearity! The results reported in Ref. [71] and those given above contradict the hypothesis [83] that if  $|\alpha| \gg K$ , we can ignore the term with  $\tilde{\theta}$  in the system of equations (2.3.7). The situation is just the opposite: this term plays a key and positive role.

This paradoxical situation occurs because in the linear regime for the selected parameters there is no coupling between the waves and no transfer of energy between them (see Fig. 1). The coupling, which is purely nonlinear, appears only in the nonlinear regime. Therefore, switching in the regime under discussion is very similar to switching from one frequency to another described in Refs [50, 52, 53].

The regime in question is most interesting in practical applications—such as optical transistors, logic elements, and switching—for the following reasons. First, if  $K = 0$ , the middle self-switching point M is stable against changes in  $\psi_0$  and changes in the pump intensity. In other words, when the initial phase difference between the pump and signal or the pump intensity is changed, the signal gain maximum is still achieved for an infinitesimally small signal simply by variation of the signal gain. Moreover, the signal gain is extremely high. This case is of interest also for the development of optical switches for lasers and for pulse limiters.

We shall now give two specific examples of possible realisations of such self-switching.

*Example 1.* A pump wave with the wavelength  $\lambda = 0.51 \mu\text{m}$ , generated in an argon laser polarised along the vertical  $y$  axis, is coupled into a fibre waveguide made of fused quartz and characterised by a birefringence  $\Delta n \sim 5 \times 10^{-8}$ , a nonlinear coefficient  $\theta \sim 10^{-12}$  esu, and a cross-sectional area of about  $5 \times 10^{-8} \text{ cm}^2$ . Let us assume that the fibre orientation is such that  $K = 0$  and  $\alpha = \Delta n$  (so that the optic axis in the fibre cross section coincides with the  $y$  axis or is perpendicular to the latter). Then, the threshold pump intensity (deduced from the condition  $R > 1$ ) is  $3(\text{cn}/2\pi)(\Delta n/|\theta|) \sim 10^8 \text{ W cm}^{-2}$  and the corresponding threshold power is  $\sim 5 \text{ W}$ . Let us assume that the fibre length is 12 m ( $L \approx 1.6\pi$ ) and the input pump power is 10 W ( $R = 2$ ). A weak signal (of the same wavelength), polarised along the horizontal  $x$  axis, is coupled into the same fibre and the power of the signal is varied by about 0.1 mW. The power at the output in each polarisation should then change to about 1.2 W, i.e. the differential gain is  $\approx 12000$ .

*Example 2.* A pump wave with the wavelength  $\lambda \approx 0.9 \mu\text{m}$  is generated in a semiconductor laser. It is polarised along the vertical  $y$  axis and coupled into a fibre waveguide in which the core is a layer structure of the GaAs–Ga<sub>0.3</sub>Al<sub>0.7</sub>As type (here,  $n \approx 3.5$ ), which represents a multiquantum-well structure with a nonlinear coefficient  $\theta \sim 10^{-4}$  esu and the difference between the refractive indices for two orthogonally polarised waves  $\Delta n = 3 \times 10^{-4} = \alpha$ . The cross-sectional area of the core is  $\sim 10^{-7} \text{ cm}^2$ . Then, the threshold pump intensity is  $2 \times 10^4 \text{ W cm}^{-2}$  and the corresponding threshold power is  $\approx 2 \text{ mW}$ . Let us assume that the fibre length is  $\approx 1.5 \text{ mm}$  ( $L \approx \pi$ ) and that the pump intensity is  $8 \times 10^4 \text{ W cm}^{-2}$  ( $R = 4$ ), i.e. the input pump power is  $\approx 8 \text{ mW}$ . Then, the coupling into the same waveguide of a small signal (of the same wavelength), polarised along the  $x$  horizontal axis,

and a change in the power of the signal by 0.01  $\mu\text{W}$  alters the output power in each polarisation by about 0.53 mW, i.e. the differential gain is  $\approx 53000$ .

The small coupling coefficient ( $K \ll |\alpha|$ ) results, on the one hand, in a deviation from the amplification linearity and, on the other, it increases even further the small-signal gain which even for low values  $L \approx \pi$  can reach—according to expression (4.11.15)—fantastically high values ( $\sim 10^9$ ).

Another interesting feature is that in the range of high intensities where  $I_n^{-2}(\gamma + \rho)^2 \ll 1$ , an increase in  $I_{x0}$  may generate output intensity beats with increasing amplitude. This is physically due to the nonlinear coupling represented by the term with  $\tilde{\theta}$ , which (in contrast to the case of tunnel-coupled optical waveguides), seems to increase with increase in the input intensity.

Characteristic features of the self-switching of TE and TM waves are due to the fact that, in accordance with the classification given in the Introduction, if  $K \neq 0$ , they belong to both the first and second groups of UDCWs; if  $K = 0$ , they belong only to the second group.

## 5. Optical switching in a cubically nonlinear system with unidirectional distributively coupled waves by a signal of different frequency or with different polarisation

In Sections 2 and 3 it is shown that radiation self-switching can occur in a cubically nonlinear system with single-frequency UDCWs. The question arises whether a major transfer of high-power radiation (of a given frequency) can take place, at the output of a nonlinear system with UDCWs, from one wave to another as a result of a small change in the power of weak radiation of different frequency reaching the same system in one of two waves. The results of a theoretical investigation [40], presented in this section, give a positive answer to this question. This makes it possible to transform and amplify greatly the modulation of radiation from a low-power laser into the modulation of strong radiation from a high-power laser operating at a different frequency.

### 5.1 Equations for the wave amplitudes

We shall begin with Eqn (2.1). We shall consider a field which is a sum of fields with two different frequencies  $\omega$  and  $\nu$ . Under steady-state conditions the two fields can be represented in the form

$$E(x, y, z, t) = E_\omega(x, y, z) \exp(i\omega t) + E_\omega^*(x, y, z) \exp(-i\omega t) + E_\nu(x, y, z) \exp(i\nu t) + E_\nu^*(x, y, z) \exp(-i\nu t). \quad (5.1.1)$$

Under such conditions the fields with the frequencies  $\omega$  and  $\nu$  obey the equations [13–14]

$$\nabla^2 E_\omega + \frac{\omega^2}{c^2} \hat{\epsilon} E_\omega = -\frac{\omega^2}{c^2} P_{\text{nl},\omega}, \quad \nabla^2 E_\nu + \frac{\nu^2}{c^2} \hat{\epsilon} E_\nu = -\frac{\nu^2}{c^2} P_{\text{nl},\nu} \quad (5.1.2)$$

and their nonlinear polarisations are

$$P_{\text{nl},\omega} = \hat{\theta} : (E_\omega^* E_\omega E_\omega + E_\omega E_\omega^* E_\omega + E_\omega E_\omega E_\omega^* + E_\nu^* E_\nu E_\omega + E_\nu E_\nu^* E_\omega + E_\omega E_\nu^* E_\nu + E_\omega E_\nu E_\nu^* + E_\nu^* E_\omega E_\nu) \quad (5.1.3)$$

( $P_{\text{nl},\nu}$  is obtained from  $P_{\text{nl},\omega}$  by the transposition of the subscripts  $\omega \Rightarrow \nu$ ,  $\nu \Rightarrow \omega$ ).

At each of these frequencies the field is in turn a superposition of two coupled waves (zeroth with  $j = 0$  and first with  $j = 1$ )

$$\begin{aligned} E_\omega(x, y, z) &= \sum_j e_{\omega j} A_{\omega j}(z) E_{\omega j}(x, y) \exp\left(\frac{\omega}{c} z i \beta_{\omega j}\right), \\ E_\nu(x, y, z) &= \sum_j e_{\nu j} A_{\nu j}(z) E_{\nu j}(x, y) \exp\left(\frac{\nu}{c} z i \beta_{\nu j}\right), \end{aligned} \quad (5.1.4)$$

where  $A_{\omega j}(z)$ ,  $A_{\nu j}(z)$  are the slowly varying amplitudes of the waves;  $e_{\omega, \nu, j}$  are the polarisation unit vectors of these waves;  $E_{\omega, \nu, j}(x, y)$  are the field profiles;  $\beta_{\omega, \nu, j}$  are the effective refractive indices for the waves with  $j = 0$  or 1.

The equations for the amplitudes of the waves with the frequencies  $\omega$  and  $\nu$  propagating in cubically nonlinear tunnel-coupled optical waveguides can be derived by analogy with the system of equations (2.1.7) and are [40]

$$\begin{aligned} 2i\beta_\omega \frac{c}{\omega} \frac{dA_{\omega 0}}{dz} + K_{01}^\omega A_{\omega 1} \exp\left(i\alpha_\omega \frac{\omega}{c} z\right) &= -\theta_{\omega 0} |A_{\omega 0}|^2 A_{\omega 0} - 2\theta_{\omega \nu 0} |A_{\nu 0}|^2 A_{\omega 0}, \\ 2i\beta_\omega \frac{c}{\omega} \frac{dA_{\omega 1}}{dz} + K_{10}^\omega A_{\omega 0} \exp\left(-i\alpha_\omega \frac{\omega}{c} z\right) &= -\theta_{\omega 1} |A_{\omega 1}|^2 A_{\omega 1} - 2\theta_{\omega \nu 1} |A_{\nu 1}|^2 A_{\omega 1}, \\ 2i\beta_\nu \frac{c}{\nu} \frac{dA_{\nu 0}}{dz} + K_{01}^\nu A_{\nu 1} \exp\left(i\alpha_\nu \frac{\nu}{c} z\right) &= -\theta_{\nu 0} |A_{\nu 0}|^2 A_{\nu 0} - 2\theta_{\nu \omega 0} |A_{\omega 0}|^2 A_{\nu 0}, \\ 2i\beta_\nu \frac{c}{\nu} \frac{dA_{\nu 1}}{dz} + K_{10}^\nu A_{\nu 0} \exp\left(-i\alpha_\nu \frac{\nu}{c} z\right) &= -\theta_{\nu 1} |A_{\nu 1}|^2 A_{\nu 1} - 2\theta_{\nu \omega 1} |A_{\omega 1}|^2 A_{\nu 1}, \end{aligned} \quad (5.1.5)$$

where  $\alpha_\omega = \beta_{\omega 1} - \beta_{\omega 0}$ ,  $\alpha_\nu = \beta_{\nu 1} - \beta_{\nu 0}$ ,  $\beta = (\beta_{\omega 1} + \beta_{\omega 0} + \beta_{\nu 1} + \beta_{\nu 0})/4$ . The coupling coefficient at the frequency  $\omega$  is [3–8]

$$K_{01}^\omega = \frac{(\mathbf{e}_{\omega 0} \mathbf{e}_{\omega 1}) \iint (n_{\omega 0}^2 - n_{\omega 1}^2) E_{\omega 1}(x, y) E_{\omega 0}^*(x, y) dx dy}{\iint |E_{\omega 0}(x, y)|^2 dx dy}$$

and  $K_{10}^\omega$  can be obtained from the above expression by the subscript transpositions  $0 \Rightarrow 1$  and  $1 \Rightarrow 0$ . The corresponding coupling coefficients  $K_{01}^\nu$  and  $K_{10}^\nu$  are obtained from  $K_{01}^\omega$  and  $K_{10}^\omega$  by the subscript transition  $\omega \Rightarrow \nu$ ,  $\nu \Rightarrow \omega$ . The nonlinear coefficients of the waveguides are

$$\begin{aligned} \theta_{\omega j} &= \frac{3 \iint \bar{\theta}_{\omega j} |E_{\omega j}(x, y)|^4 dx dy}{\iint |E_{\omega j}|^2 dx dy}, \\ \theta_{\omega \nu j} &= \frac{\iint \bar{\theta}_{\omega \nu j} |E_{\omega j}|^2 |E_{\nu j}|^2 dx dy}{\iint |E_{\omega j}|^2 dx dy}, \end{aligned} \quad (5.1.6)$$

where convolutions of the tensor  $\hat{\theta}$  are  $\bar{\theta}_{\omega j} = \mathbf{e}_{\omega j} \hat{\theta} : \mathbf{e}_{\omega j} \mathbf{e}_{\omega j} \mathbf{e}_{\omega j}$ ,  $\bar{\theta}_{\omega \nu j} = \mathbf{e}_{\omega j} \hat{\theta} : (\mathbf{e}_{\nu j} \mathbf{e}_{\omega j} \mathbf{e}_{\nu j} + \mathbf{e}_{\nu j} \mathbf{e}_{\nu j} \mathbf{e}_{\omega j} + \mathbf{e}_{\omega j} \mathbf{e}_{\nu j} \mathbf{e}_{\nu j})$ ;  $\theta_{\nu j}$ ,  $\theta_{\nu \omega j}$ ,  $\theta_{\nu j}$  and  $\bar{\theta}_{\nu \omega j}$  are derived from the above expressions by the subscript transposition  $\omega \Rightarrow \nu$ ,  $\nu \Rightarrow \omega$ .

If the polarisations of all the waves are identical at the input, then  $\bar{\theta}_{\omega j} = \bar{\theta}_{\nu \omega j} = 3\theta_{\omega j} = 3\bar{\theta}_{\nu j}$ .

Usually, the anisotropy with the tensor  $\hat{\theta}$  of the waveguides can be ignored. It then follows from expression (1.2) in Appendix I that the convolutions are

$$\begin{aligned} \bar{\theta}_{\omega j} &= \theta_{xxxx}^{(j)}(\omega) = \theta_{yyyy}^{(j)}(\omega) = \theta_{zzzz}^{(j)}(\omega), \\ \bar{\theta}_{\nu j} &= \theta_{xxxx}^{(j)}(\nu) = \theta_{yyyy}^{(j)}(\nu) = \theta_{zzzz}^{(j)}(\nu), \\ \bar{\theta}_{\nu \omega j} &= \bar{\theta}_{\omega \nu j} = \theta_{xxxx}^{(j)}(\omega, \nu)(1 + 2 \cos^2 \vartheta_{\omega j, \nu j}), \\ \bar{\theta}_{\omega \nu j} &= \theta_{kkkk}^{(j)}(\omega, \nu) = \theta_{mmmm}^{(j)}(\omega, \nu), \end{aligned} \quad (5.1.7)$$

where  $\vartheta_{\omega j, \nu j}$  are the angles between the unit vectors  $\mathbf{e}_{\omega j}$  and  $\mathbf{e}_{\nu j}$  and the subscripts  $k, m$  assume the values  $x, y, z$ .

It is evident from the set of expressions (5.1.7) that the influence of the signal is maximal when the vectors of the signal and pump fields are collinear:  $\cos^2 \vartheta_{\omega j, \nu j} = 1$ ; this influence is minimal when these vectors are orthogonal:  $\cos^2 \vartheta_{\omega j, \nu j} = 0$ .

Since the waveguides support only a single mode at the two frequencies, the field profiles  $E_{\omega j}(x, y)$  and  $E_{\nu j}(x, y)$  are the same dome shape, but they differ in the degree of spreading. At the higher frequency, the profile spreads out less and the energy concentration is greater. However, if the wavelengths do not differ greatly, for example, if  $\lambda_\nu = 1.06 \mu\text{m}$  and  $\lambda_\omega = 1.15 \mu\text{m}$ , these differences in the degree of energy concentration are not large. For example, in the case of a fibre waveguide made of fused quartz with the core  $a = 1.97 \mu\text{m}$  in diameter when the difference between the refractive indices of the core and cladding is  $n_{\omega j} - n_{\omega 0} = 0.01$ , we find that the parameter  $V_{\omega j} = 2\pi a (n_{\omega j}^2 - n_{\omega 0}^2)^{1/2} / \lambda_{\omega 0}$ , which represents the fraction of the energy concentrated in the core, amounts to  $V_{\nu j} = 2$  and  $V_{\omega j} = 1.84$  for  $\lambda_\nu = 1.06 \mu\text{m}$  and  $\lambda_\omega = 1.15 \mu\text{m}$ , respectively. It therefore follows from Ref. [124] that the energy concentration in the core is 74% and 70% in these two cases, i.e. the difference is small and we can ignore the difference between the overlap integrals in the set of expressions (5.1.6) if the wavelengths do not differ too much. For similar wavelengths the cubic susceptibilities of the waveguide materials are also similar. Therefore, in the case of radiations with somewhat different wavelengths propagating in identical tunnel-coupled optical waveguides we can assume that in the set of expressions (5.1.5), we have

$$\theta_{\omega \nu j} \approx \theta_{\omega j} \frac{1 + 2 \cos^2 \vartheta_{\omega j, \nu j}}{3}, \quad \theta_{\nu \omega j} \approx \theta_{\nu j} \frac{1 + 2 \cos^2 \vartheta_{\omega j, \nu j}}{3}, \quad (5.1.8)$$

where  $\theta_{\omega j} \approx \theta_{\nu j}$ .

If the wave polarisations are also identical, then

$$\theta_{\omega 0} \approx \theta_{\omega 1} \approx \theta_{\nu 1} \approx \theta_{\nu 0} \approx \theta_{\nu \omega 0} \approx \theta_{\omega \nu 0} \approx \theta_{\omega \nu 1} \approx \theta_{\nu \omega 1} = \theta. \quad (5.1.9)$$

The difference between the nonlinear coefficients does not alter the nature of the dependences of the output wave

intensities and of the phase differences between them on the input intensity of the signal wave [40].

For an *arbitrary* cubically nonlinear system with UDCWs the equations for the amplitudes of the waves with the frequencies  $\omega$  and  $\nu$  may be written in the form

$$\begin{aligned}
2i\beta \frac{c}{\omega} \frac{d\tilde{A}_{\omega 0}}{dz} + K_{01}^{\omega} \tilde{A}_{\omega 1} \exp\left(i\tilde{\alpha}_{\omega} \frac{\omega}{c} z\right) \\
&= -\theta_{\omega 00} |\tilde{A}_{\omega 0}|^2 \tilde{A}_{\omega 0} - 2\theta_{\omega \nu 00} |\tilde{A}_{\nu 0}|^2 \tilde{A}_{\omega 0} \\
&\quad -\theta_{\omega 01} |\tilde{A}_{\omega 1}|^2 \tilde{A}_{\omega 0} - 2\theta_{\omega \nu 01} |\tilde{A}_{\nu 1}|^2 \tilde{A}_{\omega 0}, \\
2i\beta \frac{c}{\omega} \frac{d\tilde{A}_{\omega 1}}{dz} + K_{10}^{\omega} \tilde{A}_{\omega 0} \exp\left(-i\tilde{\alpha}_{\omega} \frac{\omega}{c} z\right) \\
&= -\theta_{\omega 11} |\tilde{A}_{\omega 1}|^2 \tilde{A}_{\omega 1} - 2\theta_{\omega \nu 11} |\tilde{A}_{\nu 1}|^2 \tilde{A}_{\omega 1} \\
&\quad -\theta_{\omega 10} |\tilde{A}_{\omega 0}|^2 \tilde{A}_{\omega 1} - 2\theta_{\omega \nu 10} |\tilde{A}_{\nu 0}|^2 \tilde{A}_{\omega 1}, \\
2i\beta \frac{c}{\nu} \frac{d\tilde{A}_{\nu 0}}{dz} + K_{01}^{\nu} \tilde{A}_{\nu 1} \exp\left(i\tilde{\alpha}_{\nu} \frac{\nu}{c} z\right) \\
&= -\theta_{\nu 00} |\tilde{A}_{\nu 0}|^2 \tilde{A}_{\nu 0} - 2\theta_{\nu \omega 00} |\tilde{A}_{\omega 0}|^2 \tilde{A}_{\nu 0} \\
&\quad -\theta_{\nu 01} |\tilde{A}_{\nu 1}|^2 \tilde{A}_{\nu 0} - 2\theta_{\nu \omega 01} |\tilde{A}_{\omega 1}|^2 \tilde{A}_{\nu 0}, \\
2i\beta \frac{c}{\nu} \frac{d\tilde{A}_{\nu 1}}{dz} + K_{10}^{\nu} \tilde{A}_{\nu 0} \exp\left(-i\tilde{\alpha}_{\nu} \frac{\nu}{c} z\right) \\
&= -\theta_{\nu 11} |\tilde{A}_{\nu 1}|^2 \tilde{A}_{\nu 1} - 2\theta_{\nu \omega 11} |\tilde{A}_{\omega 1}|^2 \tilde{A}_{\nu 1} \\
&\quad -\theta_{\nu 10} |\tilde{A}_{\nu 0}|^2 \tilde{A}_{\nu 1} - 2\theta_{\nu \omega 10} |\tilde{A}_{\omega 0}|^2 \tilde{A}_{\nu 1}.
\end{aligned} \tag{5.1.10}$$

The system of equations (5.1.10) is put forward here for the first time. Simple substitutions

$$\begin{aligned}
\tilde{A}_{\omega 0} &= A_{\omega 0} \exp\left[i\left(\frac{\theta_{\omega 01} I_{\omega}}{2} + \theta_{\omega \nu 01} I_{\nu}\right) \frac{z\omega}{c\beta}\right], \\
\tilde{A}_{\omega 1} &= A_{\omega 1} \exp\left[i\left(\frac{\theta_{\omega 10} I_{\omega}}{2} + \theta_{\omega \nu 10} I_{\nu}\right) \frac{z\omega}{c\beta}\right], \\
\tilde{A}_{\nu 0} &= A_{\nu 0} \exp\left[i\left(\frac{\theta_{\nu 01} I_{\nu}}{2} + \theta_{\nu \omega 01} I_{\omega}\right) \frac{z\nu}{c\beta}\right], \\
\tilde{A}_{\nu 1} &= A_{\nu 1} \exp\left[i\left(\frac{\theta_{\nu 10} I_{\nu}}{2} + \theta_{\nu \omega 10} I_{\omega}\right) \frac{z\nu}{c\beta}\right], \\
\theta_{\omega 0} &= \theta_{\omega 00} - \theta_{\omega 01}, \quad \theta_{\omega \nu 0} = \theta_{\omega \nu 00} - \theta_{\omega \nu 01}, \\
\theta_{\omega 1} &= \theta_{\omega 11} - \theta_{\omega 10}, \quad \theta_{\omega \nu 1} = \theta_{\omega \nu 11} - \theta_{\omega \nu 10}, \\
\tilde{\alpha}_{\omega} &= \alpha_{\omega} + \frac{(\theta_{\omega 10} - \theta_{\omega 01})I_{\omega}/2 + (\theta_{\omega \nu 10} - \theta_{\omega \nu 01})I_{\nu}}{\beta}, \\
\tilde{\alpha}_{\nu} &= \alpha_{\nu} + \frac{(\theta_{\nu 10} - \theta_{\nu 01})I_{\nu}/2 + (\theta_{\nu \omega 10} - \theta_{\nu \omega 01})I_{\omega}}{\beta},
\end{aligned} \tag{5.1.11}$$

where  $I_{\omega} = I_{\omega 0} + I_{\omega 1}$ ,  $I_{\nu} = I_{\nu 0} + I_{\nu 1}$ , make it possible to transform the system of equations (5.1.10) to the system (5.1.5). We shall therefore analyse specifically the system of equations (5.1.5).

## 5.2 Integrals of equations

We shall introduce the moduli  $\rho_{\omega j}$ ,  $\rho_{\nu j}$  and phases  $\varphi_{\omega j}$ ,  $\varphi_{\nu j}$  of the amplitudes  $A_{\omega j} = \rho_{\omega j} \exp(i\varphi_{\omega j})$ ,  $A_{\nu j} = \rho_{\nu j} \exp(i\varphi_{\nu j})$ , as well as quantities  $I_{\omega j} \equiv \rho_{\omega j}^2$ ,  $I_{\nu j} \equiv \rho_{\nu j}^2$ , which are proportional to the wave intensities. The initial conditions are specified at the input ( $z = 0$ ):

$$\begin{aligned}
I_{\omega j}(z = 0) &= I_{\omega j 0}, \quad I_{\nu j}(z = 0) = I_{\nu j 0}, \\
\varphi_{\omega j}(z = 0) &= \varphi_{\omega j 0}, \quad \varphi_{\nu j}(z = 0) = \varphi_{\nu j 0}.
\end{aligned}$$

We are interested in the intensities and phases at the output  $z = l$ :

$$\begin{aligned}
I_{\omega j}(z = l) &= I_{\omega j l}, \quad I_{\nu j}(z = l) = I_{\nu j l}, \\
\varphi_{\omega j}(z = l) &= \varphi_{\omega j l}, \quad \varphi_{\nu j}(z = l) = \varphi_{\nu j l}.
\end{aligned}$$

We can readily show that if  $K_{01}^{\omega} = K_{10}^{\omega} = K_{\omega}$ ,  $K_{01}^{\nu} = K_{10}^{\nu} = K_{\nu}$ , the energies of the waves at each frequency are conserved along the longitudinal coordinate  $z$  and in the linear case ( $\theta \neq 0$ ), we have

$$I_{\omega 0} + I_{\omega 1} = I_{\omega} = \text{const}, \quad I_{\nu 0} + I_{\nu 1} = I_{\nu} = \text{const} \tag{5.2.1}$$

and we can introduce the coefficients representing power transfer by each wave:  $T_{\omega j} = I_{\omega j l}/I_{\omega}$ ,  $T_{\nu j} = I_{\nu j l}/I_{\nu}$ .

If  $\theta_{\nu \omega 0} = \theta_{\omega \nu 0}$  and  $\theta_{\nu \omega 1} = \theta_{\omega \nu 1}$ , then in addition to expressions (5.2.1), it is possible to write down one further integral of the system of equations (5.1.5):

$$\begin{aligned}
\Gamma_{\omega \nu} &= K_{\omega} \sqrt{I_{\omega 0} I_{\omega 1}} \cos \psi_{\omega} + K_{\nu} \sqrt{I_{\nu 0} I_{\nu 1}} \cos \psi_{\nu} \\
&\quad - \alpha_{\omega} \beta_{\omega 0} I_{\omega 0} - \alpha_{\nu} \beta_{\nu 0} I_{\nu 0} + \frac{\theta_{\omega 0} I_{\omega 0}^2}{4} + \frac{\theta_{\nu 0} I_{\nu 0}^2}{4} + \frac{\theta_{\omega 1} I_{\omega 1}^2}{4} \\
&\quad + \frac{\theta_{\nu 1} I_{\nu 1}^2}{4} + \theta_{\nu \omega 0} I_{\omega 0} I_{\nu 0} + \theta_{\nu \omega 1} I_{\omega 1} I_{\nu 1},
\end{aligned} \tag{5.2.2}$$

where  $\psi_{\omega} = \alpha_{\omega} z \omega / c + \varphi_{\omega 1} - \varphi_{\omega 0}$ ,  $\psi_{\nu} = \alpha_{\nu} z \nu / c + \varphi_{\nu 1} - \varphi_{\nu 0}$ .

We can normalise the system of equations (5.1.5) by introducing dimensionless variables [40]. For example, if we assume that expressions (5.1.9) are valid, we can introduce the variables  $R_{\nu j} = |\theta| I_{\nu j 0} / (4K_{\nu})$ ,  $L_{\nu} = K_{\nu} l \nu / c \beta$ .

## 5.3 Numerical analysis of equations

Numerical analysis of the system of equations (5.1.5) shows [40] that if a pump satisfies the self-switching condition, described by expressions (4.3.1)–(4.3.3), then the pump at the output can be switched by a small change in the intensity of a weak signal even if the frequency of this signal is not equal to the pump frequency. Such pump switching is accompanied by self-phase-matching of the zeroth and first pump waves at the point M and also by switching of the signal and self-phase-matching of the signal waves. The relationships between these mutually coupled processes have been investigated [40] and some of the results obtained are presented in Fig. 16. If the signal and pump are fed in the form of one of the waves [in the case of TCOWs this means they are fed into the same waveguide (Fig. 5a)], then the pump intensity needed for switching should be slightly less than the critical value (Fig. 16a). However, if the signal and pump reach the input in the form of different waves, entering different

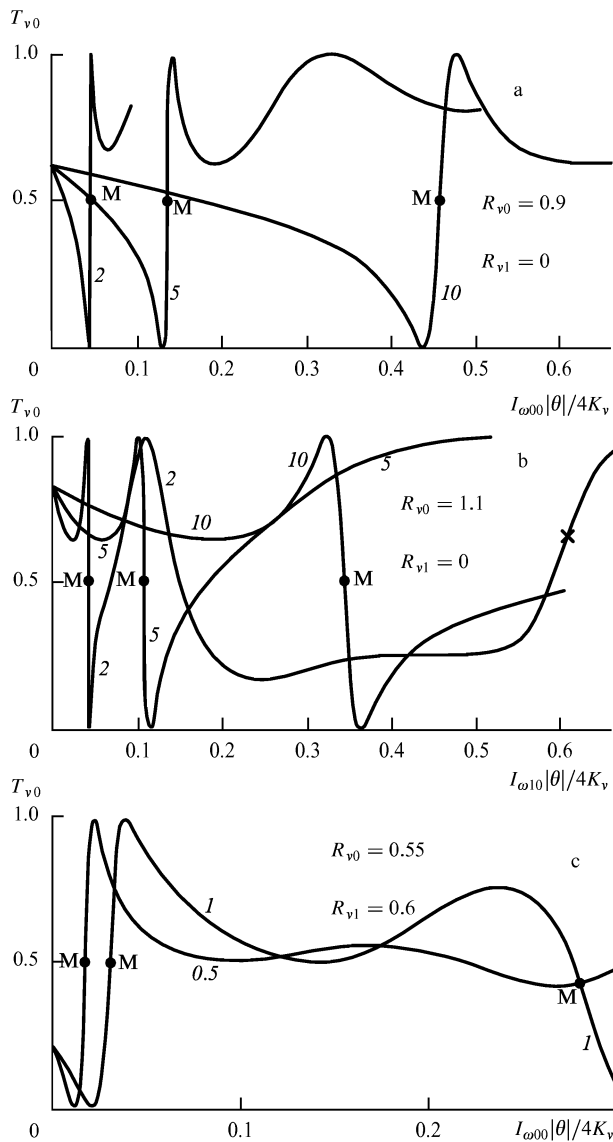


**Figure 16.** Dependences of the coefficient representing the transfer of the pump power by the zeroth wave  $T_{v0} \equiv I_{v0l}/(I_{v0} + I_{v1})$  on the normalised intensity of the control signal  $I_{\omega 00}|\theta|/4K_v$ . The values of the ratio  $K_{\omega}/K_v$  are given.  $L_v = 2.5\pi$  (a, b),  $1.6\pi$  (c). (a)  $R_{v0} = 0.9$ ,  $R_{v1} = 0$ ; (b)  $R_{v0} = 1.1$ ,  $R_{v1} = 0$ ; (c)  $R_{v0} = 0.55$ ,  $R_{v1} = 0.6$ .  $\lambda_{\omega}/\lambda_v = 1.15/1.06$  (a, b),  $0.85/1.06$  (c, curve labelled 0.5); 1 (c, curve labelled 1). The approximations described by expression (5.1.9) are assumed to be satisfied;  $\alpha_{\omega} = \alpha_v = 0$ . At the points M, we have  $\cos(\varphi_{v1l} - \varphi_{v0l}) = 1$  and near the points M, the slope is  $|\partial I_{v0l}/\partial I_{\omega 00}| = \max$ .

waveguides in the case of a tunnel-coupled system of waveguides (Fig. 5d), the switching pump intensity should be slightly higher than the critical value (Fig. 16b).

The amplitude  $\Delta I_{v0l}$  of the change in the power  $I_{v0l}$  of the pump at the output can be tens, hundreds, or thousands of times higher than the amplitude of the power change  $\Delta I_{\omega 00}$  of the control signal at the input. This gives rise to the transistor effect. A rough estimate of the gain of an optical transistor at the middle switching point can be made on the basis of expression (3.1.21) where, however, one must include a coefficient of the order of 0.1–1.5; the value of this coefficient is given for different parameters  $K_{\omega}/K_v$ ,

$R_{v0}$ ,  $R_{v1}$  in Ref. [40]. Examples of possible realisation of different-frequency switching are given in Ref. [40] together with estimates of the signal and pump intensities when a fibre waveguide is pumped by radiation from a single-mode Nd:YAG laser ( $\lambda = 1.06 \mu\text{m}$ ) and the signal represents He–Ne laser radiation ( $\lambda = 1.15 \mu\text{m}$ ).

The switching efficiency (gain) decreases with reduction in the signal coupling coefficient, more precisely, with reduction in the ratio and  $K_{\omega}/K_v$  (see Fig. 16) [40, 65], which means that this increase occurs when  $\lambda_{\omega}/\lambda_v = v/\omega$  becomes smaller.

When the signal and pump are coupled into different waveguides (Fig 16c,  $K_{\omega}/K_v = 1$ ), double switching of the pump may take place. The second switching occurs at higher values of the signal intensity and its slope is considerably less than the slope of the first switching [65]. The signal intensity plotted along the abscissa in various figures in this review is normalised to the critical pump intensity, but in Ref. [40] it is normalised to the critical signal intensity.

In Sections 3 and 4 we defined the middle self-switching point M by the condition (4.3.2):  $r = 1$ . The question may be asked: how to find the middle point M in a given situation when the solution and the expression for  $r$  are not known? This can be done by applying two conditions: (1) this is the point in the close vicinity of which the slope (differential gain) reaches its maximum  $\partial I_{v0l}/\partial I_{\omega 00} = \max$ ; (2) at this point the pump waves become phase-matched:  $\cos \psi_v = 1$ . This definition is more general than that set by the condition  $r = 1$ , although it is equivalent to the former definition.

#### 5.4 Elimination of the influence of the phase of a signal on its amplification in tunnel-coupled optical waveguides

It is shown in Sections 3 and 4, and in Refs [36, 54], that if the signal and pump are coherent, the output characteristics of the waves and the signal gain may all depend strongly on the difference between the input phases of the signal and pump. The positive and negative aspects of this effect are considered in Section 3.5.

It is shown in Section 3.5 and in Ref. [66] that in some cases it is desirable to eliminate the parasitic influence of the input phase of the signal on the characteristics of a switch or an optical transistor based on TCOWs. This can be done in a variety of ways [66].

One trivial way is to make the signal incoherent with the pump. However, this is not always the optimal approach, since it requires a fairly large difference between the signal and pump paths (it requires greater coherence length), which increases the delay time and enhances the influence of various parasitic factors such as deformation of the waveguide, losses, noise, etc. (See also Section 6.2).

Secondly, it can also be done by applying the pump at one carrier frequency and the signal at another frequency [40]. This approach is discussed in the preceding sections (5.1–5.3).

The third way of tackling the same problem is to feed the signal and pump with *different circular polarisations* (it is assumed that TCOWs are isotropic in a transverse direction, and that the signal and pump can have the same frequency). Then, the equations for the signal and pump wave amplitudes are [66]

$$\begin{aligned}
i\beta \frac{\lambda_p}{\pi} \frac{dA_{0p}}{dz} + K_p \exp\left(\frac{i\alpha_p z 2\pi}{\lambda_p}\right) A_{1p} &= -\theta_{0p} (|A_{0p}|^2 + 2|A_{0s}|^2) A_{0p}, \\
i\beta \frac{\lambda_p}{\pi} \frac{dA_{1p}}{dz} + K_p \exp\left(-\frac{i\alpha_p z 2\pi}{\lambda_p}\right) A_{0p} &= -\theta_{1p} (|A_{1p}|^2 + 2|A_{1s}|^2) A_{1p}, \\
i\beta \frac{\lambda_s}{\pi} \frac{dA_{0s}}{dz} + K_s \exp\left(\frac{i\alpha_s z 2\pi}{\lambda_s}\right) A_{1s} &= -\theta_{0s} (|A_{0s}|^2 + 2|A_{0p}|^2) A_{0s}, \\
i\beta \frac{\lambda_s}{\pi} \frac{dA_{1s}}{dz} + K_s \exp\left(-\frac{i\alpha_s z 2\pi}{\lambda_s}\right) A_{0s} &= -\theta_{1s} (|A_{1s}|^2 + 2|A_{1p}|^2) A_{1s},
\end{aligned} \tag{5.4.1}$$

where for the same frequencies (but different circular polarisations) of the signal and pump we have  $\lambda_s = \lambda_p = \lambda$ ,  $K_s = K_p = K$ ,  $\theta_{0p} = \theta_{0s} = \theta_0$ ,  $\theta_{1p} = \theta_{1s} = \theta_1$ ,  $\alpha_s = \alpha_p = \alpha$  and for the identical TCOWs, the parameters are  $\alpha_s = \alpha_p = 0$ ,  $\theta_{0p} = \theta_{1p} = \theta_p$ ,  $\theta_{0s} = \theta_{1s} = \theta_s$ .

It therefore follows that the system of equations (5.4.1) is of the same form as the system of equations (5.1.5) and it has the same integrals (5.2.2), apart from the notation. The solution of the system of equations (5.4.1) for identical signal and pump frequencies and identical TCOWs is discussed in detail in Ref. [66]; the results do not differ qualitatively from those plotted in Fig. 16.

There is another, fourth, way of eliminating the influence of the input phase difference on the output powers of a switch and of an optical transistor based on tunnel-coupled optical waveguides: the *polarisations of the signal and pump should be orthogonal* to one another. The waveguide parameters should satisfy special conditions [66] given below. The equations for the amplitudes of the orthogonally polarised signal and pump amplitudes are [66]

$$\begin{aligned}
i\beta \frac{\lambda}{\pi} \frac{dA_{0p}}{dz} + K_p \exp\left(\frac{i\alpha_p z 2\pi}{\lambda}\right) A_{1p} &= -(\theta_{0p} |A_{0p}|^2 + \theta_{0ps} |A_{0s}|^2) A_{0p} \\
&\quad - \tilde{\theta}_{0ps} A_{0s}^2 A_{0p}^* \exp\left(\frac{i2\alpha_{sp0} z 2\pi}{\lambda}\right), \\
i\beta \frac{\lambda}{\pi} \frac{dA_{1p}}{dz} + K_p \exp\left(-\frac{i\alpha_p z 2\pi}{\lambda}\right) A_{0p} &= -(\theta_{1p} |A_{1p}|^2 + \theta_{1ps} |A_{1s}|^2) A_{1p} \\
&\quad - \tilde{\theta}_{1ps} A_{1s}^2 A_{1p}^* \exp\left(\frac{i2\alpha_{sp1} z 2\pi}{\lambda}\right), \\
i\beta \frac{\lambda}{\pi} \frac{dA_{0s}}{dz} + K_s \exp\left(\frac{i\alpha_s z 2\pi}{\lambda}\right) A_{1s} &= -(\theta_{0s} |A_{0s}|^2 + \theta_{0sp} |A_{0p}|^2) A_{0s} \\
&\quad - \tilde{\theta}_{0sp} A_{0p}^2 A_{0s}^* \exp\left(-\frac{i2\alpha_{sp0} z 2\pi}{\lambda}\right), \\
i\beta \frac{\lambda}{\pi} \frac{dA_{1s}}{dz} + K_s \exp\left(-\frac{i\alpha_s z 2\pi}{\lambda}\right) A_{0s} &= -(\theta_{1s} |A_{1s}|^2 + \theta_{1sp} |A_{1p}|^2) A_{1s} \\
&\quad - \tilde{\theta}_{1sp} A_{1p}^2 A_{1s}^* \exp\left(-\frac{i2\alpha_{sp1} z 2\pi}{\lambda}\right),
\end{aligned} \tag{5.4.2}$$

where  $\alpha_{spj} = \beta_{sj} - \beta_{pj}$ ,  $\alpha_s = \beta_{s1} - \beta_{s0}$ ,  $\alpha_p = \beta_{p1} - \beta_{p0}$ ,  $\beta = (\beta_{s0} + \beta_{s1} + \beta_{p0} + \beta_{p1})/4$ , and the nonlinear coefficients are

related approximately by  $\theta_{jp} \approx \theta$ ,  $\theta_{jps} \approx 2\theta/3$ ,  $\tilde{\theta}_{jsp} \approx \theta/3$  [see the set of expressions (2.3.10)].

In this case the nonlinear parts of the equations generally include one more term, which contains a complex-conjugate amplitude. Its presence describes the dependences of the output intensities of the waves on the input difference between the phases, even in the case of orthogonally polarised signal and pump waves in TCOWs isotropic in the transverse direction, when the linear coefficient of the coupling between the signal and pump waves vanishes. However, we can select conditions under which the influence of this term is negligible. This can be done by employing waveguides which are transversely anisotropic, have an elliptic distribution of the effective refractive indices, and the polarisation unit vectors of the pump and signal waves which are mutually perpendicular and directed along the principal axes  $x$  and  $y$ . The optical anisotropy should be sufficiently strong so that the difference between the effective refractive indices of the waves polarised along the principal axes  $x$  and  $y$  (i.e. the quantity  $\alpha_{spj}$ ) is considerably greater than the coefficient  $K$  representing the linear coupling between the waveguides. It follows from numerical calculations [66] that this term can definitely be ignored if  $|\alpha_{spj}| \geq 5K$ . The output intensities of the waves are then almost completely independent of the input phase difference.

The system of equations (5.4.2) had been derived and investigated also in Ref. [87], but without a discussion of the influence of the signal phase on the switching process. Numerical calculations are used in Ref. [87] to draw the conclusion that chaos appears in the system at large values of  $L$  ( $L \geq 6\pi$ ) and that the term with  $\theta_{0sp}$  has an important influence. A similar conclusion about chaos in TCOWs made of an isotropic nonlinear material, when the polarisation vector is tilted relative to the geometric axis of the tunnel-coupled waveguides, is reached in Ref. [88] where the values of  $L$  are assumed to be even larger than those given in Ref. [87]. Moreover, Ref. [88] deals also with the case when pump waves of similar intensities (one equal to four critical values and the other close to four critical values) are coupled into both waveguides. According to expression (4.6.3) [36], this enhances strongly the gain and makes it fantastically large.

The existence of chaos is deduced in Refs [87, 88] on the basis of computer calculations. However, for the values of  $L$  selected in Refs [87, 88] the values of the gain estimated on the basis of expressions (3.1.21) and (4.6.3) are so high that the computer is unable to ‘track’ the very abrupt changes of the output intensities, and this may be the reason for the appearance of random jump-like graphs representing the output intensities [87, 88]. Therefore, the conclusion on the chaos reached in Refs [87, 88] should, in our opinion, be checked additionally and physically analysed.

## 6. Optical multivibrators based on unidirectional distributively coupled waves

### 6.1 Optical multivibrators unstable against a phase shift in a feedback loop

The results presented in Sections 3–5 can be used to design and forecast the characteristics of feedback devices based on nonlinear systems with UDCWs, i.e. of devices in which part of the radiation from the output of the system is fed to the input [51, 56, 62]. We shall discuss one such device in

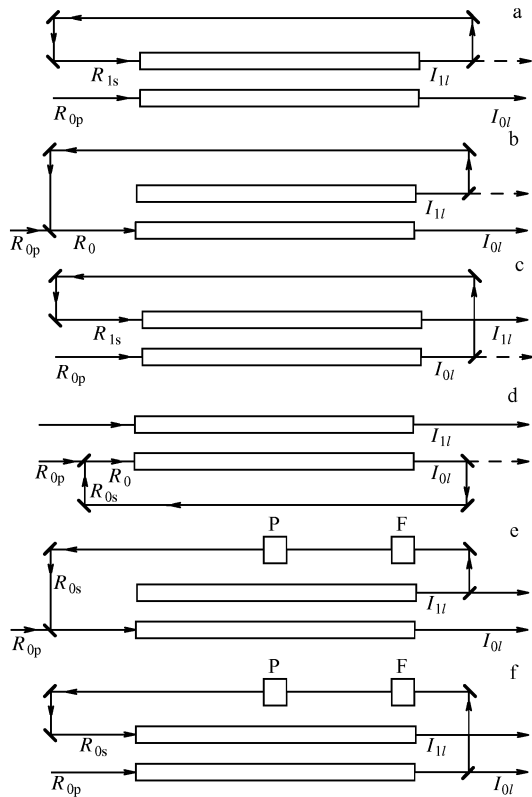


**Figure 17.** Optical multivibrator configurations, which are unstable (a–d) and stable (e, f) against a deviation of the phase in the feedback loop from the calculated value; P is a device which transforms the polarisation or frequency, and F is a polarisation filter which prevents admission to the feedback channel of the radiation with the polarisation other than the required one.

the specific case of TCOWs with feedback (Fig. 17). Similar devices can be based also on other systems with UDCWs.

Let us assume that, for example, a pump wave with a constant normalised intensity  $R_{0p}$  reaches the input of the zeroth waveguide without losses and that the radiation from the output of the first waveguide is returned, by mirrors or a feedback waveguide (completely or partly), to the input of the same waveguide (Fig. 17a). The coefficient representing energy transfer from the output of the first waveguide to its input is  $\sigma$  (usually  $\sigma \ll 1$ ), i.e. the boundary conditions for the amplitudes are

$$\begin{aligned} A_{10}(t) &= \sqrt{\sigma} A_{1l}(t - \tau_f) \exp(i\varphi_f), \\ A_{00}(t) &= \sqrt{R_{0p} I_{0M}} = \text{const}, \end{aligned} \quad (6.1.1)$$

where  $\tau_f$  is the time taken by radiation to travel along the feedback channel,  $t$  is an arbitrary moment in time, and  $\varphi_f$  is the phase shift during the passage along the feedback channel.

Let us select  $R_{0p}$  so that for  $R_1 = 0$  the radiation emerges entirely from the first waveguide. The coefficient  $\sigma$  is selected so that the signal entering the input of the first waveguide is such that, for the selected value of  $R_{0p}$ , all the radiation emerges from the zeroth waveguide. This selection of the parameters means that  $R_{0p} = R_M^{(1)}$ ,  $\sigma = R_{1M}^{(0)}/R_M^{(1)}$ ,  $\varphi_{1l} + \varphi_f = \varphi_{00} + m\pi$  and  $R_{0p} \gg R_1$  (i.e.  $\sigma \ll 1$ ); the values of  $R_M^{(1)}$  and  $R_M^{(0)}$  calculated from expressions (3.1.11), (3.3.6), and (4.4.14);  $\sigma \approx [8 \exp(-L)]^2$ .

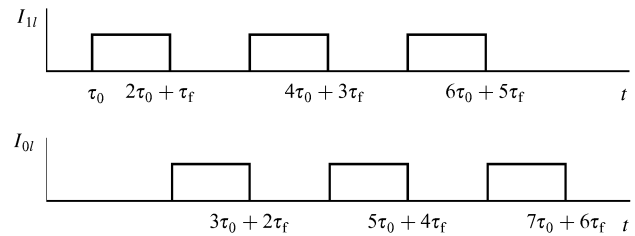


**Figure 18.** Pulses at the output from tunnel-coupled optical waveguides with feedback (see Fig. 17).

For this set of parameters a periodic process appears in the system (Fig. 18). The radiation reaching the input of the zeroth waveguide at the moment  $t = 0$  passes through TCOWs in the time  $\tau_0$  and reaches the output of the first waveguide. Then, after a time  $\tau_f$ , part of this radiation begins to enter the first waveguide and, therefore, after a further time  $\tau_0$ , i.e. at the moment  $t = 2\tau_0 + \tau_f$ , all the radiation begins to emerge now from the zeroth waveguide. Consequently, at the moment  $t = 2\tau_0 + 2\tau_f$  the radiation ceases to enter the first waveguide and, therefore, at the moment  $t = 2\tau_f + 3\tau_0$  all the radiation again emerges from the first waveguide. The process is then repeated with the period  $2(\tau_f + \tau_0)$ .

Similar multivibrators can be constructed in other ways (Fig. 17) and the selection of the parameters is determined by the characteristics of the system.

If the output of the first waveguide is coupled optically to the input of the zeroth waveguide (Fig. 17b), then  $R_{0p} = R_M^{(1)}$  and  $\sigma$  is selected so that for a given value of  $R_{0p}$  after the passage of the signal along the feedback channel we have  $R_0 = R_M^{(1)}$  at the waveguide input.

If the output of the zeroth waveguide is coupled optically to the input of the first waveguide (Fig. 17c), then  $R_{0p} = R_M^{(0)}$ ,  $\sigma = R_{1M}^{(1)}/R_M^{(0)}$ .

If the output of the zeroth waveguide is coupled optically to the input of the zeroth waveguide (Fig. 17d), then  $R_{0p} = R_M^{(0)}$  and  $\sigma$  is selected so that after the passage of the signal along the feedback channel we have  $R_0 = R_M^{(0)}$  at the waveguide input.

In all these cases two antiphase sequences of almost rectangular pulses (Fig. 18) are formed at the waveguide output. The duration of one pulse is  $\tau_f + \tau_0$ . During the time interval  $\tau_f + \tau_0$  all the radiation emerges either from the first or the zeroth waveguide. The system is therefore an optical multivibrator operating in the self-oscillator regime.

## 6.2 Optical multivibrators stable against a signal phase shift

Optical multivibrators have stable output characteristics if these characteristics are independent of the input phase of the signal. Let us consider this in detail. It is obvious that in the course of the passage of a wave (signal) along the feedback channel the change in the wave phase depends strongly on the length of this channel and also on inhomogeneities and fluctuations of the refractive index (which in turn can appear and change under the influence of various factors: temperature changes, deformations, fields, etc.). The output intensities of the optical multivibrators (based on TCOWs) described in Section 6.1 (Figs 17a–17d) depend strongly on the phase of the signal arriving at the input (along the feedback channel) and, consequently, on the phase shift in the feedback loop.

This dependence is described in Sections 3.5 and 4.9 and in Refs [36, 51, 54], and it can be explained—as mentioned already—by the interference between the signal and pump waves at the waveguide input. The parasitic influence of the phase shift in the feedback loop leads to an instability of the wave intensities at the output of an optical vibrator and may stop its operation. Quantitative estimates of the deviation of the signal phase shift in the feedback loop from the calculated value at which an optical multivibrator ceases to operate are given in Ref. [66]. For example, in the case of the calculated (for  $R_{op} = 0.948$ ,  $L = 1.6\pi$ ,  $\Delta = 0$ ) signal phase (for a signal arriving at the input along the feedback channel) equal to  $\varphi_{os} = 0$  it is found that if  $\varphi_{os} > \pi/4$ , the optical multivibrator illustrated in Fig. 17b ceases to operate completely.

In the design of optical multivibrators, unaffected by instabilities of the wave phase in the feedback loop, one can use the results derived in Section 5.4. Examples of such multivibrators are shown in Figs 17e and 17f. Multivibrators can be made sensitive to phase instabilities in one of the following ways [63–66].

(1) One can couple circularly polarised pump radiation into the input of TCOWs and place, in the feedback loop, a device P which transforms one circular polarisation into the opposite circular polarisation [63].

(2) Linearly polarised pump radiation can enter the input of TCOWs and, in the feedback loop, one can place a device P which rotates the plane of polarisation by  $90^\circ$  [64].

(3) One can locate, in the feedback loop, a device P which transforms the radiation frequency ( $\omega \rightarrow \nu$ ), i.e. the pump reaching the input has the frequency  $\omega$  and the signal reaching the input along the feedback channel has the frequency  $\nu$ .

(4) The optical length of the feedback loop can be made greater than the pump coherence length. Then, the signal and pump are incoherent at the input and there is no interference between them. However, this is not always the optical method. In particular, in the case of optical multivibrators one would then need a long feedback loop (longer than the pump coherence length). This would limit the minimum duration of the output pulses.

In cases (1) and (2) the TCOWs should satisfy the requirements set out in Section 5.4 and in Ref. [66].

## 7. Optical self-switching in a system with three unidirectional distributively coupled waves

### 7.1 Equations and integrals

A cubically nonlinear interaction of three UDCWs can be described by the equations

$$\begin{aligned} 2i\beta \frac{c}{\omega} \frac{dA_0}{dz} + K_{01} \exp\left(\frac{i\alpha_{10}z\omega}{c}\right)A_1 + K_{02} \exp\left(\frac{i\alpha_{20}z\omega}{c}\right)A_2 \\ = -\theta_0|A_0|^2A_0 - \theta_{01}|A_1|^2A_0 - \theta_{02}|A_2|^2A_0, \\ 2i\beta \frac{c}{\omega} \frac{dA_1}{dz} + K_{10} \exp\left(-\frac{i\alpha_{10}z\omega}{c}\right)A_0 + K_{12} \exp\left(\frac{i\alpha_{21}z\omega}{c}\right)A_2 \\ = -\theta_1|A_1|^2A_1 - \theta_{10}|A_0|^2A_1 - \theta_{12}|A_2|^2A_1, \\ 2i\beta \frac{c}{\omega} \frac{dA_2}{dz} + K_{20} \exp\left(-\frac{i\alpha_{20}z\omega}{c}\right)A_0 + K_{21} \exp\left(-\frac{i\alpha_{21}z\omega}{c}\right)A_1 \\ = -\theta_2|A_2|^2A_2 - \theta_{20}|A_0|^2A_2 - \theta_{21}|A_1|^2A_2, \end{aligned} \quad (7.1.1)$$

where  $\alpha_{10} = \beta_1 - \beta_0$ ,  $\alpha_{20} = \beta_2 - \beta_0$ ,  $\alpha_{21} = \beta_2 - \beta_1$  are the differences between the refractive indices, and  $K_{10} = K_{01}$ ,  $K_{20} = K_{02}$ ,  $K_{21} = K_{12}$  are the wave coupling coefficients.

We shall now consider the real amplitudes  $\rho_j$  and the phases  $\varphi_j$ . We can easily show that the system of equations (7.1.1) has two integrals when  $K_{02} = K_{20}$ ,  $K_{12} = K_{21}$  and  $K_{01} = K_{10}$  [48, 67]:

$$\begin{aligned} I = \rho_0^2 + \rho_1^2 + \rho_2^2, \\ G = K_{01}\rho_0\rho_1 \cos\psi_0 + \alpha_{10}\beta\rho_1^2 + K_{02}\rho_0\rho_2 \cos\psi_2 + \alpha_{20}\beta\rho_2^2 \\ + K_{12}\rho_1\rho_2 \cos\psi_{21} + \frac{\theta_{01}\rho_0^4}{4} + \frac{\theta_{11}\rho_1^4}{4} + \frac{\theta_{21}\rho_2^4}{4} + \frac{\theta_{01}\rho_0^2\rho_1^2}{2} \\ + \frac{\theta_{02}\rho_0^2\rho_2^2}{2} + \frac{\theta_{12}\rho_1^2\rho_2^2}{2}, \end{aligned} \quad (7.1.2)$$

where  $\psi_0 = \varphi_1 - \varphi_0 + \alpha_{10}z\omega/c$ ,  $\psi_2 = \varphi_2 - \varphi_0 + \alpha_{20}z\omega/c$ ,  $\psi_{21} = \varphi_2 - \varphi_1 + \alpha_{21}z\omega/c$ .

The equations for the wave amplitudes in three tunnel-coupled waveguides are [48]

$$\begin{aligned} 2i\beta \frac{c}{\omega} \frac{dA_0}{dz} + K_{01} \exp\left(\frac{i\alpha_{10}z\omega}{c}\right)A_1 + K_{02} \exp\left(\frac{i\alpha_{20}z\omega}{c}\right)A_2 \\ = -\theta_0|A_0|^2A_0, \\ 2i\beta \frac{c}{\omega} \frac{dA_1}{dz} + K_{10} \exp\left(-\frac{i\alpha_{10}z\omega}{c}\right)A_0 + K_{12} \exp\left(\frac{i\alpha_{21}z\omega}{c}\right)A_2 \\ = -\theta_1|A_1|^2A_1, \\ 2i\beta \frac{c}{\omega} \frac{dA_2}{dz} + K_{20} \exp\left(-\frac{i\alpha_{20}z\omega}{c}\right)A_0 \\ + K_{21} \exp\left(-\frac{i\alpha_{21}z\omega}{c}\right)A_1 = -\theta_2|A_2|^2A_2. \end{aligned} \quad (7.1.3)$$

We shall now consider the case of three TCOWs, which are of interest for several reasons. First, out of all the systems with three UDCWs it is the TCOWs that are of the greatest practical interest. Second, in the symmetric cases the relationships between the ‘cross’ nonlinear coefficients are  $\theta_{01} = \theta_{02} = \theta_{12} = \theta_c$  or  $\theta_{01} = \theta_{02} = \theta_c$ , and because the system of equations (7.1.1) reduces to the system of equations (7.1.3) by a simple replacement of the variables and nonlinearities  $\theta_j - \theta_c \Rightarrow \theta_j$ , which is similar to the substitution (2.5.2).

For the sake of simplicity, we shall consider just the case of identical waveguides characterised by

$$\alpha_1 = \alpha_2 = 0, \quad \theta_0 = \theta_1 = \theta_2 = \theta \quad (7.1.4)$$

and we shall adopt the usual notation:  $R_j = |\theta|I_{j0}/4K$ ,  $I_{j0} \equiv |A_{j0}|^2$ ,  $T_j \equiv I_{j1}/(I_{00} + I_{10} + I_{20})$ ,  $A_{j0} \equiv A_j(z=0)$ ,  $j = 0, 1, 2$ .

### 7.2 Three identical tunnel-coupled optical waveguides distributed in one plane

We shall consider three identical TCOWs located symmetrically in one plane (Fig. 19a):

$$K_{01} = K_{10} = K_{20} = K_{02} = K, \quad K_{12} = 0. \quad (7.2.1)$$

In view of the symmetry of these waveguides, we have  $\rho_1 = \rho_2 = \rho$ ,  $\psi_1 = \psi_2 = \psi = \varphi_1 - \varphi_0$ .

We shall assume that the radiation is coupled only into the central (‘zeroth’) waveguide:

$$R_0 \neq 0, \quad R_1 = R_2 = 0. \quad (7.2.2)$$

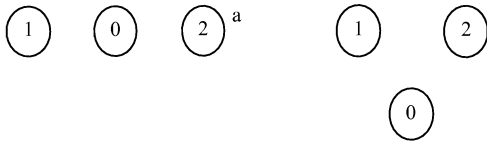


**Figure 19.** Transverse section across three tunnel-coupled optical waveguides: (a)  $K_{10} = K_{20} \gg K_{12}$ ; (b)  $K_{10} = K_{20} = K_{12} = K$ .

It then follows from expressions (7.1.2) that [48]

$$\cos \psi = \frac{2}{I_{0M}} \sqrt{\frac{I_1}{I_0}} \left( I_{00} - \frac{3I_1}{2} \right), \quad (7.2.3)$$

where  $I_{0M} = 4K/|\theta|$  (see Section 3.1).

We shall now turn to the numerical solution of the system of equations (7.1.3) subject to the assumptions

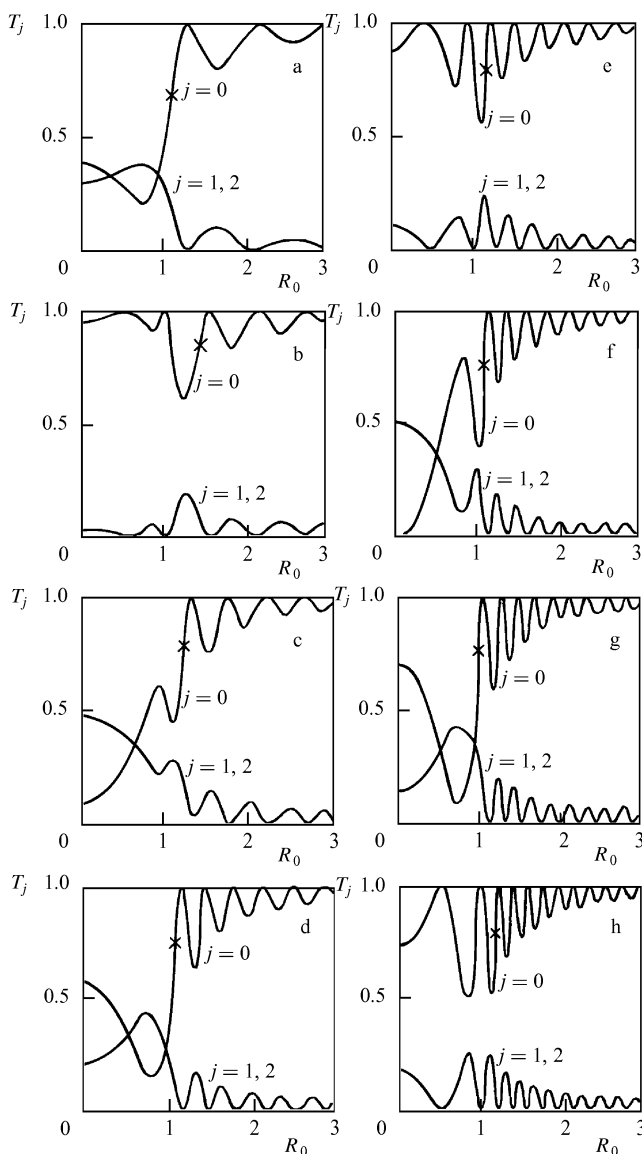


**Figure 20.** Dependences of  $T_j = I_j/I_{00}$  ( $j = 0, 1, \text{ or } 2$ ) on  $R_0 \equiv I_{00}/I_{0M}$ , plotted for  $K_{12} = 0, K_{10} = K_{20} = K; L = \pi$  (a),  $1.5\pi$  (b),  $2\pi$  (c),  $2.5\pi$  (d),  $3\pi$  (e),  $3.5\pi$  (f),  $4\pi$  (g),  $4.5\pi$  (h). The point at which  $\partial T_0/\partial R_0 = \max$  is identified by a cross. Radiation is coupled into the zeroth (central) of three identical tunnel-coupled optical waveguides:  $I_{10} = I_{20} = 0$  (figure taken from Ref. [48]).

described by expressions (7.2.1), (7.2.2), and (7.1.4). This solution is partly presented in Fig. 20, which gives the power transfer coefficients  $T_0$  and  $T_{1,2}$  as functions of  $R_0$ . The numerical solution was obtained for different values of the parameter  $L = 2\pi K l/\lambda\beta$ , introduced by analogy with the case of two UDCWs; the value of this parameter increases by  $\pi/2$  between one part of Fig. 20 and the next.

The nature of the dependence  $T_j(R_0)$  is in this case substantially different than in the case of two UDCWs.

For  $L$  which is a multiple of  $1.5\pi$  there is practically no radiation self-switching (Figs 20b, 20e, and 20h). In these cases the nature of the dependence  $T_j(R_0)$  is the same and energy exchange is considerably less than for other values of  $L$ . An increase in  $L$  increases the frequency of the energy beats caused by a change in  $R_0$  and, consequently, the slope  $\partial I_{0l}/\partial I_{00}$  increases [48].

This cosine of the phase difference reaches its maximum value of unity simultaneously with the attainment of a local maximum value by the coefficients  $T_{1,2}$  and of the corresponding local minimum of  $T_0$ ; it should be noted that  $\cos \psi = 0$  when  $T_{1,2} = 0$  and  $T_0 = 1$  [48].

### 7.3 Coupling between all waveguides

In this section the system of equations (7.1.3) will be investigated in a different case [67] when the coupling between all the waveguides is material:  $K_{12} \neq 0, K_{10} = K_{20} = K \neq 0$ . This case is usually encountered when all three waveguides are separated by the same distance (Fig. 19b). As in Section 7.2, the waveguides are assumed to be identical. The results of numerical calculations [67] are presented partly in Fig. 21 (some of them are also given in a table in Ref. [67]).

It follows from these calculations [67] that, in particular, if  $K_{01} = K_{02} = K_{12} = K$ , the switching slope, i.e. the differential gain  $(\partial I_{0l}/\partial I_{00})_{\max} \equiv (R_0 + R_1 + R_2)(\partial T_0/\partial R_0)_{\max}$ , is higher (for  $L \equiv 2\pi K l/\lambda\beta = 1.6\pi$ , the difference is approximately a factor of 3), but the critical intensity  $I_M$  is also higher (by a factor of 1.5) than in the case of two TCOWs (i.e. when  $K_{02} = K_{12} = 0, K_{01} = K$ ) when we have  $I_M = I_{0M} = 4K/|\theta|$ . As  $K_{12}$  increases, the switching slope at the middle point M rises, but  $I_M$  also rises (Figs 20b and 21). The results of the numerical calculations indicate that the switching slope depends exponentially on the effective parameter  $L_{\text{eff}} = 2\pi K_{\text{eff}} l/\lambda\beta$ , which is proportional to the effective coupling coefficient  $K_{\text{eff}}$ , which increases with increase in  $K_{01}, K_{02}$ , and  $K_{12}$ ; we then have  $I_M \propto K_{\text{eff}}/|\theta|$ .

The self-switching depth increases with increase in  $K_{12}$  (Figs 20b and 21) and for  $K_{12} \approx 1.5K$ , the switching is almost complete.

When radiation is injected into the inputs of two waveguides (a pump into the zeroth waveguide and a small signal into the first waveguide), it is found that in the case of three TCOWs (as in the case of two such waveguides discussed in Section 4.4) the small signal experiences giant amplification and if  $K_{12} = K_{10} = K_{20} = K$ , the slope for three tunnel-coupled waveguides is steeper than for two waveguides, but the amplification appears at a higher pump intensity [67].

Finally, in the case of self-switching of waves with close input intensities (Section 4.6) the configuration of three tunnel-coupled optical waveguides is characterised by higher values of the gain  $\partial I_{0l}/\partial I_{00}$  than in the case of two such waveguides. For example, if  $L = 1.5\pi, R_0 \approx R_1 \approx R_2 \approx 0.8$  and  $K_{01} = K_{02} = K_{12} = K$ , we have

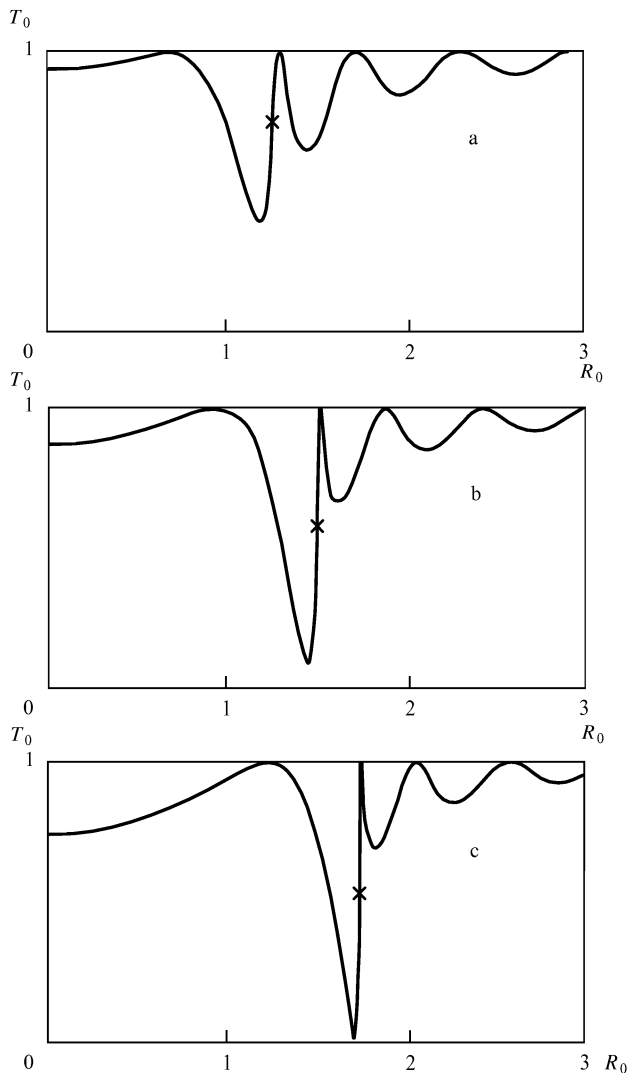


**Figure 21.** Dependences of  $T_0 = I_0/I_{00}$  on  $R_0$ , plotted for  $K_{10} = K_{20} = K$ ;  $K_{12} = K/2$  (a),  $K$  (b),  $3K/2$  (c).  $L = 1.5\pi$ ,  $I_{10} = I_{20} = 0$ . The point at which  $\partial T_0/\partial R_0 = \max$  is identified by a cross (figure taken from Ref. [67]).

$(\partial I_{0l}/\partial I_{00})_{\max} \approx 352.6$  for three waveguides [67], whereas for two waveguides if  $L = 1.5\pi$  and  $R_0 \approx R_1 \approx 0.8$ , we find from expression (4.6.2) that  $(\partial I_{0l}/\partial I_{00})_{\max} \approx 272$ . However, the total power entering three TCOWs is greater than for two waveguides.

Investigations of the self-switching of light in three tunnel-coupled optical waveguides are reported also in Refs [99–103].

## 8. Conclusions

A theory of self-switching of unidirectional distributively coupled waves with a linear coupling coefficient, discovered by the present author, is presented. The results of investigations reviewed above reveal interesting relationships governing such self-switching and demonstrate the possibility of constructing a new class of optical devices on the basis of this effect: these devices include optical transistors, small-signal amplifiers, logic elements, intensity limiters, multivibrators, etc.

The concluding part of this review, which should be published soon, will contain a description of the experi-

mental observations of self-switching of unidirectional distributively coupled waves omitted from this review: self-switching of pulses, self-switching of different-frequency waves with a nonlinear coupling coefficient in a quadratically nonlinear medium, etc.

## References

1. Iogansen L V *Zh. Eksp. Teor. Fiz.* **40** 1838 (1961) [*Sov. Phys. JETP* **13** 1291 (1961)]
2. Zolotov E M, Kiselev V A, Sychugov V A *Usp. Fiz. Nauk* **112** 231 (1974) [*Sov. Phys. Usp.* **17** 64 (1974)]
3. Barnoski M K (Ed.) *Introduction to Integrated Optics* (New York: Plenum Press, 1974)
4. Tamir T (Ed.) *Integrated Optics* (Berlin: Springer, 1975)
5. Hunsperger R G *Integrated Optics Technology* (Berlin: Springer, 1982)
6. Yariv A *Quantum Electronics* 2nd edition (New York: Wiley, 1975)
7. Yariv A *Introduction to Optical Electronics* 2nd edition (New York: Holt, Rinehart and Winston, 1976)
8. Marcuse D *Integrated Optics* (New York: IEEE Press, 1973)
9. Snyder A W, Love J D *Optical Waveguide Theory* (London: Methuen, 1984)
10. Gowar J *Optical Communication Systems* (Englewood Cliffs, NJ: Prentice-Hall, 1984)
11. Akhmanov S A, Khokhlov R V *Nonlinear Optics* (New York: Gordon and Breach, 1972)
12. Bloembergen N *Nonlinear Optics* (New York: Benjamin, 1965)
13. Zernike F, Midwinter J E *Applied Nonlinear Optics: Basics and Applications* (New York: Wiley Interscience, 1973)
14. Akhmanov S A, Vysloukh V A, Chirkin A S *Optics of Femtosecond Laser Pulses* (New York: American Institute of Physics, 1992)
15. Lugovoi V N *Zh. Eksp. Teor. Fiz.* **56** 683 (1969) [*Sov. Phys. JETP* **29** 374 (1969)]
16. Seidel H *Bistable Optical Circuit Using Saturable Absorber Within a Resonant Cavity* US Patent No. 3 610 731 (appl. 19 May 1969, publ. 5 Oct. 1971)
17. Szoke A, Daneu V, Goldhar J, Kurnit N A *Appl. Phys. Lett.* **15** 376 (1969)
18. Duguay M A, Hansen J W *Appl. Phys. Lett.* **15** 192 (1969)
19. McCall S L, Gibbs H M, Venkatesan T N C *J. Opt. Soc. Am.* **65** 1184 (1975)
20. Gibbs H M, McCall S L, Venkatesan T N C *Phys. Rev. Lett.* **36** 1135 (1976)
21. Kaplan A E *Pis'ma Zh. Eksp. Teor. Fiz.* **24** 132 (1976) [*JETP Lett.* **24** 114 (1976)]
22. Askar'yan G A *Pis'ma Zh. Eksp. Teor. Fiz.* **8** 19 (1968) [*JETP Lett.* **8** 10 (1968)]
23. Felber F S, Marburger J H *Appl. Phys. Lett.* **28** 731 (1976)
24. Marburger J H, Felber F S *Phys. Rev. A* **17** 335 (1978)
25. Okuda M, Onaka K *Jpn. J. Appl. Phys.* **16** 769 (1977)
26. Winful H G, Marburger J H, Garmire E *Appl. Phys. Lett.* **35** 379 (1979)
27. Winful H G, Marburger J H *Appl. Phys. Lett.* **36** 613 (1980)
28. Kukhtarev N V, Semenets T I *Kvantovaya Elektron. (Moscow)* **8** 2005 (1981) [*Sov. J. Quantum Electron.* **11** 1216 (1981)]
29. Kukhtarev N V, Semenets T I *Zh. Tekh. Fiz.* **51** 1990 (1981) [*Sov. Phys. Tech. Phys.* **26** 1159 (1981)]
30. Lugovoi V N *Kvantovaya Elektron. (Moscow)* **6** 2053 (1979) [*Sov. J. Quantum Electron.* **9** 1207 (1979)]
31. Gibbs H M *Optical Bistability: Controlling Light with Light* (New York: Academic Press, 1985)
32. Maier A A *Sposob Pereklyucheniya Signala v Tunnel'no-Svyazannykh Opticheskikh Volnovodakh* (Method for Signal Switching in Tunnel-Coupled Optical Waveguides) USSR Patent No. 1 152 397 (appl. 1982, publ. 1988); *Byull. Izobret.* (46) 300 (1988)
33. Maier A A *Kvantovaya Elektron. (Moscow)* **9** 2296 (1982) [*Sov. J. Quantum Electron.* **12** 1490 (1982)]

34. Maier A A *Kvantovaya Elektron. (Moscow)* **11** 157 (1984) [*Sov. J. Quantum Electron.* **14** 101 (1984)]
35. Jensen S M *IEEE J. Quantum Electron.* **QE-18** 1580 (1982)
36. Maier A A *Izv. Akad. Nauk SSSR Ser. Fiz.* **48** 1441 (1984)
37. Maier A A "Self-phase-matching of waves in self-switching of light in nonlinear tunnel-coupled waveguides", Preprint No. 236 (Moscow: Institute of General Physics, Academy of Sciences of the USSR, 1984); *Kvantovaya Elektron. (Moscow)* **12** 1537 (1985) [*Sov. J. Quantum Electron.* **15** 1016 (1985)]
38. Maier A A *Kratk. Soobshch. Fiz.* (12) 20 (1984)
39. Gusovskii D D, Dianov E M, Maier A A, Neustruev V B, Shklovskii E I, Shcherbakov I A "Nonlinear light transfer in tunnel-coupled optical waveguides", Preprint No. 250-13 (Moscow: Institute of General Physics, Academy of Sciences of the USSR, 1984); *Kvantovaya Elektron. (Moscow)* **12** 2312 (1985) [*Sov. J. Quantum Electron.* **15** 1523 (1985)]
40. Maier A A, Preprint No. 122-26 (Moscow: Institute of General Physics, Academy of Sciences of the USSR, 1985); *Kvantovaya Elektron. (Moscow)* **13** 1360 (1986) [*Sov. J. Quantum Electron.* **16** 892 (1986)]
41. Maier A A, Sitariskii K Yu, Preprint No. 311-20 (Moscow: Institute of General Physics, Academy of Sciences of the USSR, 1985); *Kvantovaya Elektron. (Moscow)* **14** 1604 (1987) [*Sov. J. Quantum Electron.* **17** 1018 (1987)]
42. Maier A A, Preprint No. 334-20 (Moscow: Institute of General Physics, Academy of Sciences of the USSR, 1985); *Kvantovaya Elektron. (Moscow)* **14** 1596 (1987) [*Sov. J. Quantum Electron.* **17** 1013 (1987)]
43. Maier A A, Preprint No. 276 (Moscow: Institute of General Physics, Academy of Sciences of the USSR, 1986); *Kratk. Soobshch. Fiz.* (9) 43 (1986)
44. Gusovskii D D, Dianov E M, Maier A A, Neustruev V B, Osiko V V, Prokhorov A M, Sitariskii K Yu, Shcherbakov I A "Experimental observation of the self-switching of radiation in tunnel-coupled optical waveguides", Preprint No. 188 (Moscow: Institute of General Physics, Academy of Sciences of the USSR, 1986); Paper presented at International Seminar "Optical Computing-86", Novosibirsk, 1986 [Reprints of this paper, in English and Russian, were given to all the participants, including Prof. William Rhodes (Editor of *Applied Optics*). In March 1987, Professor Rhodes summarised the results of Refs [33, 34, 44] in a review entitled "Alexander Mayer's paper on nonlinear optical switching in coupled waveguides", which was presented at the OSA Optical Computing Conference held in March 1987, at Lake Tahoe (Incline Village), NV. Prof. Rhodes distributed at this conference and sent out reprints of Ref. [44] in English to many foreign scientists]; *Kvantovaya Elektron. (Moscow)* **14** 1144 (1987) [*Sov. J. Quantum Electron.* **17** 742 (1987)]
45. Maier A A, Serdyuchenko Yu N, Sitariskii K Yu, Shchelev M Ya, Shcherbakov I A "Breakup of an ultrashort pulse in the course of self-switching of light in tunnel-coupled waveguides", Preprint No. 345 (Moscow: Institute of General Physics, Academy of Sciences of the USSR, 1986); Paper presented at International Seminar "Optical Computing-86, Novosibirsk, 1986"; *Kvantovaya Elektron. (Moscow)* **14** 1157 (1987) [*Sov. J. Quantum Electron.* **17** 735 (1987)]
46. Maier A A, Preprint No. 43-20 (Moscow: Institute of General Physics, Academy of Sciences of the USSR, 1987)
47. Maier A A, Preprint No. 62-10 (Moscow: Institute of General Physics, Academy of Sciences of the USSR, 1987); *Kratk. Soobshch. Fiz.* (6) 58 (1987)
48. Maier A A "Self-switching of radiation in three tunnel-coupled optical waveguides", Preprint No. 153-26 (Moscow: Institute of General Physics, Academy of Sciences of the USSR, 1987)
49. Maier A A, Sitariskii K Yu *Sposob Upravleniya Koeffitsientom Preobrazovaniya Moshchnosti Izlucheniya s Odnoi Chastoty na Druguyu* (Method for Control of the Coefficient Representing Power Conversion of Radiation From One Frequency to Another) USSR Author's Certificate No. 1 593 438 (appl. 1987, recorded in the State Register 15 May 1990)
50. Maier A A, Sitariskii K Yu *Kvantovaya Elektron. (Moscow)* **14** 2369 (1987) [*Sov. J. Quantum Electron.* **17** 1507 (1987)]
51. Maier A A, Preprint No. 351-45 (Moscow: Institute of General Physics, Academy of Sciences of the USSR, 1987)
52. Maier A A, Sitariskii K Yu *Dokl. Akad. Nauk SSSR* **299** 1387 (1988) [*Sov. Phys. Dokl.* **33** 293 (1988)]
53. Maier A A, Sitariskii K Yu "Optical transistor and switch based on a quadratically nonlinear interaction of waves", Preprint No. 111-29 (Moscow: Institute of General Physics, Academy of Sciences of the USSR, 1988)
54. Maier A A *Dokl. Akad. Nauk SSSR* **303** 618 (1988) [*Sov. Phys. Dokl.* **33** 852 (1988)]
55. Maier A A "High-gain optical transistor resistant to pump instability", in *Proceedings of Third International Conference Trends in Quantum Electronics '88* Bucharest, 1988, p. 382
56. Maier A A "Light self-switchers and optical transistors based on tunnel-coupled optical waveguides", in *Papers on Optical Communication* (Special Issue) (Bellingham, WA: Society of Photo-Optical Instrumentation Engineers—International Society for Optical Engineering, 1988) p. 27
57. Maier A A, Sitariskii K Yu, Preprint No. 86-23 (Moscow: Institute of General Physics, Academy of Sciences of the USSR, 1989); *Dokl. Akad. Nauk SSSR* **307** 592 (1989) [*Sov. Phys. Dokl.* **34** 644 (1989)]
58. Maier A A, Karataev S G, Preprint No. 73-7 (Moscow: Institute of General Physics, Academy of Sciences of the USSR, 1989); *Dokl. Akad. Nauk SSSR* **309** 619 (1989) [*Sov. Phys. Dokl.* **34** 1025 (1989)]
59. Dianov E M, Kuznetsov A V, Maier A A, Okhotnikov O G, Sitariskii K Yu, Shcherbakov I A *Dokl. Akad. Nauk SSSR* **309** 611 (1989) [*Sov. Phys. Dokl.* **34** 1021 (1989)]
60. Dianov E M, Kuznetsov A V, Maier A A, Okhotnikov O G, Sitariskii K Yu, Shcherbakov I A *Opt. Commun.* **74** 152 (1989)
61. Maier A A "High-gain optical transistor resistant to pump instability" in *Proceedings of OSA Photonic Switching Conference, Salt Lake City, 1989* (Vol. 3 of OSA Proceedings Series) (Washington, DC: Optical Society of America, 1989) p. 85
62. Maier A A, Thesis for Doctorate of Physicomathematical Sciences (Moscow: Institute of General Physics, Academy of Sciences of the USSR, 1990)
63. Maier A A *Opticheskii Mul'tivibrator* (Optical Multivibrator) Russian Federation Patent No. 2 003 150 (1990)
64. Maier A A *Opticheskii Mul'tivibrator* (Optical Multivibrator) USSR Author's Certificate No. 1 805 437 (1990)
65. Maier A A *Dokl. Akad. Nauk SSSR* **315** 95 (1990) [*Sov. Phys. Dokl.* **35** 947 (1990)]
66. Maier A A "Influence, and its elimination, of the phase of a weak alternating signal on its amplification in tunnel-coupled waveguides", Preprint No. 40-30 (Moscow: Institute of General Physics, Academy of Sciences of the USSR, 1991); *Kvantovaya Elektron. (Moscow)* **18** 1447 (1991) [*Sov. J. Quantum Electron.* **21** 1334 (1991)]
67. Maier A A, Preprint No. 42-13 (Moscow: Institute of General Physics, Academy of Sciences of the USSR, 1991); *Kvantovaya Elektron. (Moscow)* **18** 1264 (1991) [*Sov. J. Quantum Electron.* **21** 1148 (1991)]
68. Maier A A, Karataev S G "On the influence of inertia of nonlinearity, nonlinear dispersion of group velocities and dispersion of coupling coefficient on pulse self-switching in tunnel-coupled optical waveguides and on the logical devices based on it", Preprint No. 46 (Moscow: Institute of General Physics, Academy of Sciences of the USSR, 1991)
69. Sitariskii K Yu, Thesis for Candidate of Physicomathematical Sciences (Moscow: Institute of General Physics, Academy of Sciences of the USSR, 1990)
70. Maier A A, Preprint No. 30 (Moscow: Institute of General Physics, Academy of Sciences of the USSR, 1992)
71. Maier A A, Sitariskii K Yu *Dokl. Akad. Nauk SSSR* **337** 596 (1994) [*Phys.-Dokl.* **39** 558 (1994)]
72. Maier A A, Sitariskii K Yu (in press)
73. Kitayama K, Wang S *Appl. Phys. Lett.* **43** 17 (1983)
74. Kitayama K, Kimura Y, Seikai S *Appl. Phys. Lett.* **46** 317 (1985)
75. Li Kam Wa P, Sitch J E, Mason N J, Roberts J S, Robson P N *Electron. Lett.* **21** 26 (1985)

76. Daino B, Gregori G, Wabnitz S *J. Appl. Phys.* **58** 4512 (1985)
77. Daino B, Gregori G, Wabnitz S *Opt. Lett.* **11** 42 (1986)
78. Winful H G *Appl. Phys. Lett.* **47** 213 (1985)
79. Hoffe R, Chrostowski J *Opt. Commun.* **57** 34 (1986)
80. Trillo S, Wabnitz S *Appl. Phys. Lett.* **49** 752 (1986)
81. Snyder A W, Chen Y, Rowland D, Mitchell D J *Opt. Lett.* **15** 357 (1990)
82. Wabnitz S, Wright E M, Seaton C T, Stegeman G I *Appl. Phys. Lett.* **49** 838 (1986)
83. Trillo S, Wabnitz S, Stolen R H, Assanto G, Seaton C T, Stegeman G I *Appl. Phys. Lett.* **49** 1224 (1986)
84. Mecozzi A, Trillo S, Wabnitz S, Daino B *Opt. Lett.* **12** 275 (1987)
85. Caglioti E, Trillo S, Wabnitz S *Opt. Lett.* **12** 1044 (1987)
86. Das U, Chen Y, Bhattacharya P *Appl. Phys. Lett.* **51** 1679 (1987)
87. Trillo S, Wabnitz S *J. Opt. Soc. Am. B* **5** 483 (1988)
88. Chen Y, Snyder A W *Opt. Lett.* **14** 1237 (1989)
89. Trillo S, Wabnitz S, Finlayson N, Banyai W C, Seaton C T, Stegeman G I, Stolen R H *Appl. Phys. Lett.* **53** 837 (1988)
90. Friberg S R, Smith P W *IEEE J. Quantum Electron.* **QE-23** 2089 (1987)
91. Friberg S R, Silberberg Y, Oliver M K, Andrejco M J, Saifi M A, Smith P W *Appl. Phys. Lett.* **51** 1135 (1987)
92. Friberg S R, Weiner A M, Silberberg Y, Sfez B G, Smith P W *Opt. Lett.* **13** 904 (1988)
93. Cada M, Gauthier R C, Paton B E, Chrostowski J *Appl. Phys. Lett.* **49** 755 (1986)
94. Berger P R, Chen Y, Bhattacharya P, Pamulapati J, Vezzoli G C *Appl. Phys. Lett.* **52** 1125 (1988)
95. Jin R, Chuang C L, Gibbs H M, Koch S W, Polky J N, Pubanz G A *Appl. Phys. Lett.* **53** 1791 (1988)
96. Silberberg Y, Smith P W, Miller D A B, et al. *Appl. Phys. Lett.* **46** 701 (1985)
97. Park H G, Huang S Y, Kim B *Opt. Lett.* **14** 877 (1989)
98. Caglioti E, Trillo S, Wabnitz S, Stegeman G I *J. Opt. Soc. Am. B* **5** 472 (1988)
99. Finlayson N, Stegeman G I *Appl. Phys. Lett.* **56** 2276 (1990)
100. Schmidt-Hattenberger C, Trutschel U, Lederer F *Opt. Lett.* **16** 294 (1991)
101. Schmidt-Hattenberger C, Muschall R, Trutschel U, Lederer F *Opt. Quantum Electron.* **24** 691 (1992)
102. Mitchell D J, Snyder A W, Chen Y *Electron. Lett.* **26** 1164 (1990)
103. Soto-Crespo J M, Wright E M *J. Appl. Phys.* **70** 7240 (1991)
104. Trillo S, Wabnitz S, Wright E M, Stegeman G I *Opt. Lett.* **13** 672 (1988)
105. Trillo S, Wabnitz S *Opt. Lett.* **16** 1 (1991)
106. Trillo S, Wabnitz S, Wright E M, Stegeman G I *Opt. Lett.* **13** 871 (1988)
107. Petrov M P, Kuzin E A, Maksyutenko M A *Kvantovaya Elektron. (Moscow)* **18** 1395 (1991) [*Sov. J. Quantum Electron.* **21** 1282 (1991)]
108. Tamir T et al. (Eds) *Guided-Wave Photoelectronics* 2nd edition (Berlin: Springer, 1990)
109. Marcuse D *Theory of Dielectric Optical Waveguides* (New York: Academic Press, 1991)
110. Takagi S *Acta Crystallogr.* **15** 1311 (1962)
111. Pinsker Z G *Dinamicheskoe Rasseyaniye Rentgenovskikh Luchei v Ideal'nykh Kristallakh* (Dynamic Scattering of X Rays in Ideal Crystals) (Moscow: Nauka, 1974)
112. Louisell W H *Coupled Mode and Parametric Electronics* (London: Wiley, 1960) p. 268
113. Akhmanov S A, Zharikov V I *Pis'ma Zh. Eksp. Teor. Fiz.* **6** 644 (1967) [*JETP Lett.* **6** 137 (1967)]
114. Maker P D, Terhune R W, Savage C M *Phys. Rev. Lett.* **12** 507 (1964)
115. Maker P D, Terhune R W *Phys. Rev.* **137** A801 (1965)
116. Stolen R H, Botineau J, Ashkin A *Opt. Lett.* **7** 512 (1982)
117. Jain K, Pratt G W Jr *Appl. Phys. Lett.* **28** 719 (1976)
118. Jeffreys H, Swirls B S *Methods of Mathematical Physics* 3rd edition (Cambridge: Cambridge University Press, 1956)
119. Blow K J, Doran N J, Wood D *Opt. Lett.* **12** 202 (1987)
120. Gradshteyn I S, Ryzhik I M (Eds) *Table of Integrals, Series, and Products* (New York: Academic Press, 1965)
121. Abramowitz M, Stegun I A (Eds) *Handbook of Mathematical Functions with Formulas, Graphs, and Mathematical Tables* (New York: Dover, 1964; reprinted New York: Wiley, 1972)
122. Chen Y J, Carter G M *Appl. Phys. Lett.* **41** 307 (1982)
123. Sen P K *Solid State Commun.* **43** 141 (1982)
124. Kapron F P, Lukowski T I *Appl. Opt.* **16** 1465 (1977)
125. Kaminow I P *IEEE J. Quantum Electron.* **QE-17** 15 (1981)

## Appendix I

It follows from expression (2.4) that the  $m$ th component of a cubically nonlinear polarisation of the medium (at a given frequency) can be expressed in terms of the components of the fields at this frequency:

$$P_{nl,m} = \theta_{mnkl} \{E_n^* E_k E_l + E_n E_k^* E_l + E_n E_k E_l^*\}, \quad (I.1)$$

where the subscripts  $m, n, k,$  and  $l$  can assume the values 1, 2, 3, corresponding to the coordinates  $x, y, z$ .

As a rule, we can use the tensor of an anisotropic medium for  $\hat{\theta}$  because both a linear anisotropy ( $n_e - n_o$ ) and a cubically nonlinear polarisation (proportional to  $I\theta$ ) of a medium are quantities of the first order of smallness. For example,  $|n_e - n_o|$  of fibre waveguides ranges from  $5 \times 10^{-9}$  to  $8 \times 10^{-4}$  [125] and typical values are  $\sim 10^{-6} - 10^{-5}$ . Therefore, the anisotropy of a cubically nonlinear polarisation is a quantity of the second order of smallness even in the case of an anisotropic medium and it can usually be ignored.

The fourth-order cubic nonlinearity tensor of an isotropic medium is [118]

$$\theta_{mnkl} = \tilde{\lambda} \delta_{mn} \delta_{kl} + \tilde{\mu} \delta_{mk} \delta_{nl} + \tilde{\nu} \delta_{ml} \delta_{nk}, \quad (I.2)$$

where  $\delta_{mn} = 1$ , if  $m = n$ , and  $\delta_{mn} = 0$ , if  $m \neq n$ ;  $\tilde{\lambda} = \theta_{1122} = \theta_{2211} = \theta_{2233} = \theta_{3311} = \theta_{1133}$ ,  $\tilde{\mu} = \theta_{2323} = \theta_{1313} = \theta_{3131} = \theta_{2121} = \theta_{3232}$ ,  $\tilde{\nu} = \theta_{1221} = \theta_{2112} = \theta_{2332} = \theta_{3113} = \theta_{1331}$ . Therefore, the nonlinear polarisation vector of an isotropic medium can be expressed in terms of the field vector as follows:

$$P_{nl} = 2\tilde{\kappa} \left[ \frac{1}{2} E^*(E \cdot E) + E(E \cdot E^*) \right], \quad (I.3)$$

where

$$\tilde{\kappa} = \tilde{\lambda} + \tilde{\mu} + \tilde{\nu} = \theta_{1111} \equiv \theta_{xxxx} = \theta_{2222} = \theta_{3333} = \frac{n_0^2 n_2 c}{3\pi},$$

and  $n_2$  is the coefficient in the familiar expression  $n = n_0 + n_2 \tilde{I}$  ( $\tilde{I}$  is the intensity).

The nonlinear coefficient is  $\theta \approx 3\theta_{xxxx} = n_0^2 n_2 c / \pi$ . It is used to estimate  $I_{0M} = 4K/|\theta|$  (Section 3.1). The intensity is  $\tilde{I}_{0M} = (cn_0/2\pi)I_{0M}$ .

## Appendix II

In our analysis of the radiation self-switching and of optical switching in nonlinear systems with UDCWs we have derived and used simple approximations [34, 36, 37] for the elliptic functions when  $|r_1^2| \ll 1$  (where  $r_1^2 = 1 - r^2$ ) and  $\exp L \gg 1$ . These elliptic functions are

$$\text{cn}(L, r) \approx \frac{\text{sech } L - (r_1^2/8) \exp L}{1 + (r_1^4/256) \exp(2L)}, \quad (II.1)$$

$$\operatorname{dn}(L, r) \approx \frac{\operatorname{sech} L + (r_1^2/8) \exp L}{1 + (r_1^4/256) \exp(2L)}, \quad (\text{II.2})$$

$$\operatorname{sn}(L, r) \approx \frac{1 - (r_1^4/256) \exp(2L)}{1 + (r_1^4/256) \exp(2L)} \tanh L. \quad (\text{II.3})$$

We find from expression (II.1) that

$$\left. \frac{\partial \operatorname{cn}(L, r)}{\partial r} \right|_{r=1} \approx \frac{\exp L}{4},$$

where  $\operatorname{cn}(L, 1) \approx \operatorname{sech} L$ ;  $\operatorname{cn}(L, r) \approx 1$  and  $(r_1^2/16) \exp L = -1$  and  $\operatorname{cn}(L, r) \approx -1$  if  $(r_1^2/16) \exp L = 1$ ;  $r_1^2 = 1 - r^2 \approx 2(1 - r)$  and, therefore,  $\operatorname{cn}(L, r) \approx 1$  if  $r \approx 1 + 8 \exp(-L)$  and  $\operatorname{cn}(L, r) \approx -1$  if  $r \approx 1 - 8 \exp(-L)$ .